HABILITATION à DIRIGER des RECHERCHES

Discipline: Sciences Physiques

UNIVERSITE DE LILLE SCIENCES ET TECHNOLOGIES

Laure PILLIER

Chargée de Recherche CNRS
Physicochimie des Processus de Combustion et de l'Atmosphère
PC2A, UMR CNRS 8522 / Université de Lille Sciences et Technologies

EXPERIMENTAL AND MODELLING STUDIES OF COMBUSTION AND ATMOSPHERIC CHEMICAL KINETICS

Soutenue le Vendredi 6 Octobre 2017

Jury

F. BATTIN-LECLERC	**Directrice de Recherche CNRS, LRGP Nancy**	**Rapporteure**
A. CESSOU	**Directrice de Recherche CNRS, CORIA Rouen**	**Rapporteure**
G. TYNDALL	**Directeur de Recherche NCAR, Boulder**	**Rapporteur**
P. DESGROUX	**Directrice de Recherche CNRS, PC2A**	**Examinatrice**
D. PETITPREZ	**Professeur Université Lille, PC2A**	**Examinateur**
A. TOMAS	**Professeur IMT Lille Douai, SAGE**	**Examinateur**
J-F. PAUWELS	**Professeur Emérite Université Lille, PC2A**	**Garant**

Remerciements

Pour commencer, je tiens à remercier Mme Frédérique Battin-Leclerc, Mme Armelle Cessou et Mr Geoffrey Tyndall d'avoir accepté d'être rapporteur(es) de ce manuscrit, ainsi que les examinateurs(trice) de mon jury : Mme Pascale Desgroux, Mr Denis Petitprez et Mr Alexandre Tomas. Merci à Denis d'avoir accepté de présider ce jury.

Je remercie particulièrement les deux personnes qui m'ont donnée envie de faire ce métier ; tout d'abord Mr Jean-François Pauwels, mon co-directeur de thèse et mon garant d'HDR, qui m'a initiée à la cinétique de combustion lors de son cours de DEA, merci pour son soutien pendant toutes ses années et d'avoir facilité mon retour au PC2A, merci de m'avoir coachée pour la préparation de cette HDR, merci pour ses qualités humaines. Et bien sûr un grand merci à Mme Pascale Desgroux, ma directrice de thèse, qui m'a appris tout ce que je sais sur les diagnostics laser, le goût du travail rigoureux et la passion de la recherche. Tous deux font partie des rencontres professionnelles et humaines qui marquent une carrière.

Je remercie chaleureusement Mr Christian Vovelle et Mr Jean-Louis Delfau avec qui j'ai commencé ma carrière CNRS au laboratoire ICARE à Orléans, merci pour leur accueil et merci d'avoir fait en sorte que mon arrivée à ICARE et le montage du brûleur haute pression se déroulent dans les meilleures conditions. Merci pour leur confiance, pour leur savoir.

Un grand merci à Mr Mahmoud Idir pour son aide, son soutien, son enthousiasme, son humour, son amitié… la liste est longue.

Egalement un grand merci à Mme Stéphanie de Persis, qui a accepté de continuer avec moi l'aventure de la combustion haute pression après le départ en retraite de Christian et Jean-Louis. Merci pour sa ténacité dans l'analyse cinétique de nos résultats, son enthousiasme, son soutien, son amitié…

Merci à l'ensemble du personnel technique et administratif d'ICARE, ainsi qu'à Mr Iskender Gökalp, directeur d'ICARE jusqu'en 2016.

Je remercie particulièrement Mr Sébastien Batut qui a largement contribué au montage du nouveau réacteur au PC2A, ainsi que Pascal Demaux, Olivier Hombert, Sébastien Coudert et Christophe Hecquet. Merci pour leur aide, leur disponibilité, leur enthousiasme à monter de nouveaux projets. Merci également à l'ensemble du personnel technique et administratif du PC2A (Valérie V., Sylvie, Béa, Valérie L., S. Germain, Sadio, Christophe S.) qui fait 'tourner la boutique' au quotidien. Merci à l'équipe du Cerla (Bénédicte, Marc, Nathalie, Thierry et Cristian) pour leur accueil et leur aide au quotidien. Merci à mes collègues et non moins amis du PC2A qui se reconnaîtront.

Enfin je remercie les doctorants que j'ai eu la chance d'encadrer : Alexis, Nazim, Nicolas, Julien et le petit dernier Florent, la vie d'un chercheur dépend aussi fortement de la qualité et de la motivation de ses étudiants. Merci à tous les étudiants, doctorants et post-doctorants avec qui j'ai travaillé ou qui ont simplement croisé ma route.

TABLE OF CONTENTS

Part A - Combustion chemical kinetics

Part B - Atmospheric chemical kinetics: Study of the reactivity of radical species in atmospheric chemistry

CURRICULUM VITAE

Laure PILLIER
PC2A – UMR 8522
Bâtiment C11 - Université de Lille 1
59655 Villeneuve d'Ascq - France
Tel : 03-20-33-64-66
Fax : 03-20-43-69-77
e-mail : laure.pillier@univ-lille1.fr

Chargée de Recherche CNRS CR1
42 years old

RESEARCH WORK EXPERIENCE

Since May 2013	Chargée de Recherche CNRS – **PC2A** - Physicochimie des Processus de Combustion et de l'Atmosphère – UMR 8522 – Université de Lille Sciences et Technologies *Research activities:* . Atmospheric and combustion chemistry . Reactivity of radical species in atmospheric chemistry . Flow reactor / Laser diagnostics
2005 - 2013	Chargée de Recherche CNRS – **ICARE** – Institut de Combustion, Aérothermique, Réactivité, Environnement – UPR 3021- Orléans *Research activities :* . Combustion chemical kinetics . NOx formation in combustion . High pressure flame structure / Laser diagnostics . Biomass fuels . Coupling combustion / CO_2 capture
2004 - 2005	Post-Doc - Department of Chemical Engineering, **Cambridge University** (UK) *Research activity*: Laser imaging of combustion instabilities Marie Curie Intra-European Felllowship (European Commission)
2003 - 2004	Attaché Temporaire en Enseignement et Recherche (ATER) – UFR Chimie Temporary lecturer **Université de Lille Sciences et Technologies - PC2A**

CV

EDUCATION

1999-2003	**PhD** Discipline: Spectrochemistry, Molecules, Solides, Reactivity **PC2A** - Physicochimie des Processus de Combustion et de l'Atmosphère – UMR 8522 – Université de Lille Sciences et Technologies *Thesis title* : Formation de monoxyde d'azote dans des flammes prémélangées $CH_4/C_2H_6/C_3H_8/O_2/N_2$: étude expérimentale par diagnostics laser et modélisation (Formation of nitrogen oxide in premixed $CH_4/C_2H_6/C_3H_8/O_2/N_2$ flames : experimental study by laser diagnostics and modelling) Co-financed by Gaz de France, ADEME and CNRS Defended in April 2003 Price for the best PhD of the University of Lille 1 in 2003
1998-1999	**DEA** (Master II) Discipline: Dynamic and structure of reactive systems **LASIR** - Laboratoire de Spectrochimie Infrarouge et Raman – UMR 8516 - Université de Lille Sciences et Technologies *Reseach subject*: Etude de l'effet de la concentration en germanium sur les propriétés structurales des guides d'ondes planaires germano-silicates photosensibles (Spectroscopies Raman et de Luminescence) (Study of the effect of the concentration of germanium on the structural properties of photosensitive germano-silicate planar waveguides)

1997-1998	Maîtrise de Chimie	Université du Littoral (Dunkerque)
1996-1997	Licence de Chimie-Physique	Université du Littoral (Dunkerque)
1994-1996	DEUG Sciences de la Matière	Université du Littoral (Calais)
1994	Bac D	Lycée Mariette (Boulogne sur mer)

PhD students co-SUPERVISION

- **Florent KRAVTCHENKO** (80%) : « Etude de la réactivité d'espèces radicalaires de type peroxyles d'intérêt atmosphérique » (Study of the reactivity of peroxy radical species of atmospheric interest) - 2016-2019 - Université de Lille Sciences et Technologies - Supervisor : Christa Fittschen

- **Nazim MERLO** (20%) : « Caractérisation expérimentale d'une flamme turbulente non prémélangée swirlée : Effet de l'enrichissement en oxygène » (Experimental characterisation of a non premixed swirled turbulent flame: Effect of oxygen enrichment) - Defended 18/12/2014 - Université d'Orléans - Supervisor : Iskender Gökalp

- **Julien MOLET** (60%) : « Formation des oxydes d'azote dans les flammes haute pression : étude expérimentale par Fluorescence Induite par Laser» (Formation of nitrogen oxides in high pressure flames : experimental study by Laser Induced Fluorescence) – Defended 24/01/2014 – Université d'Orléans - Supervisor : Laurent Catoire

- **Alexis MATYNIA** (80%) : « Développement d'un dispositif expérimental pour l'analyse de la structure de flammes de prémélanges à haute pression par diagnostics laser : Application aux flammes méthane/air et biogaz/air » (Development of an experimental setup for the analysis of the structure of high pressure premixed flames by laser diagnostics : Application to methane/air and biogas/air flames) - Defended 06/04/2011 - Université d'Orléans - Supervisor : Philippe Dagaut

- **Nicolas BOUVET** (20%): "Experimental and Numerical Studies of the Fundamental Flame Speeds of Methane/Air and Syngas (H_2/CO)/Air Mixtures" - Defended 17/12/2009 - Université d'Orléans - Supervisor: Iskender Gökalp

MASTER students SUPERVISION

- **Florent KRAVTCHENKO** : « Mesure des radicaux hydroperoxyles HO_2 dans un réacteur à écoulement par cw-CRDS – Validation de la technique » (Measurement of hydroperoxy radicals HO_2 in a flow reactor by cw-CRDS – Validation of the technique) - Master 2 Sciences de l'Environnement Terrestre, spécialité MAEVA / Université Aix-Marseille – February-June 2016

- **Yassine AZEDDINE** : « Effet de l'ajout de l'hydrogène dans des flammes de méthane sur la formation des oxydes d'azote : étude expérimentale et modélisation » (Effect of hydrogen addition in methane flames on the formation of nitrogen oxides : experimental study and modelling) - Master 1 Physique et Sciences pour l'Ingénieur PSPI – Université d'Orléans - April-June 2012

- **Julien MOLET** : « Etude numérique de flammes laminaires prémélangées de méthane à pression atmosphérique et haute pression » (Numerical study of premixed laminar methane flames at atmospheric and high pressure) - Master 2 Physique et Science Pour l'Ingénieur - Spécialité « Energétique, Environnement, Espace » - Université d'Orléans - March-August 2009

- **Vladimiro OSORIO** : « Étude cinétique de la combustion à l'air enrichi en oxygène - Optimisation du couplage des procédés de combustion et de capture du CO_2 par membranes » (Kinetic study of combustion with oxygen enriched air – Optimisation of the coupling between combustion process and CO_2 capture by membrane) - Master 1 Chimie des Pollutions et Risques Environnementaux - Option : Énergie et Environnement – Université d'Orléans - March-August 2008

- **Alexis MATYNIA** : « Cinétique de combustion de combustibles issus de la biomasse » (Combustion kinetic of biomass fuels) - Master 2 Chimie de la Combustion et de l'Atmosphère – Université d'Orléans - February-July 2007

Other students SUPERVISION

- **Florence PIERREPAK** – Licence 3 Sciences Physiques, Université d'Orléans - « Etude expérimentale et modélisation de l'effet de l'ajout d'hydrogène dans une flamme de méthane sur la formation des oxydes d'azote » (Experimental study and modelling of the effect of hydrogen addition in a methane flame on the formation of nitrogen oxides) - 2012 - 2 months

- **Nicolas VENTURINI** - DUT Mesures Physiques, Université de Bourges - Option Techniques Instrumentales - « Gestion des fluides sur des installations expérimentales de combustion par labVIEW » (Fluids control in experimental combustion setup by labVIEW) - 2012 – 2 months

- **Mathieu CHAILLOU** - Licence de Chimie option Chimie Appliquée, Université d'Orléans - « Initiation à la cinétique chimique de combustion et aux techniques laser appliquées à la combustion » (Introduction to combustion chemical kinetics and laser techniques applied to combustion) - 2009 – 2 months

- **Rudy MICHAU** - DUT Mesures Physiques, Université de Tours - « Pilotage et asservissement d'un laser à colorant en vue d'acquisitions de spectres d'excitation de fluorescence induite par laser » (Automatic control of a dye laser for laser induced fluorescence excitation spectra acquisition) - 2009 – 3 months

- **Jérémy VISEUX** - DUT Mesures Physiques, Université de Tours - « Gestion et pilotage des éléments d'une chambre de combustion à haute pression sous LabVIEW » (Automatic control of the components in a high pressure combustion chamber with LabVIEW) - 2007 – 3 months

- **Rémi PASCAL** - Institut Polytechnique des Sciences Avancées, Paris - « Mise en place d'une installation pour l'étude de flammes haute pression » (Implementation of a setup for high pressure flame study) - 2005 – 3 months

- **Jérémie AUGER** - Ingénieur d'Etudes ICARE - « Assistance dans la gestion d'une installation expérimentale de diagnostics optiques dans des flammes sous haute pression » (Technical support on an optical diagnostic experimental setup for high pressure flames study) - 2012 - 6 months

- **Cloe ROCHE** - Ingénieur d'Etudes ICARE - « Assistance dans la gestion d'une installation expérimentale de diagnostics optiques dans des flammes sous haute pression » (Technical support on an optical diagnostic experimental setup for high pressure flames study) - 2011 – 14 months

SCIENTIFIC RESPONSABILITIES – RESEARCH PROJECTS

ANR (Agence Nationale de la Recherche) Projects:

- **Project NO-mecha** : Nouveau mécanisme de formation de NO dans les flammes (New mechanism for NO formation in flames)
2008-2013
Partners: PC2A (Lille), ICARE (Orléans)
Study of NO formation in high pressure flames
Local advisor for ICARE – Involvement: 40%

- **Project CO_2 Energicapt** : Intégration énergétique et démonstrateur de recherche de voies membranaires pour la combinaison de la combustion par air enrichi en oxygène et de la capture CO_2 sur chaudières industrielles existantes (Integration of oxygen-enriched air combustion and CO_2 capture for existing industrial boilers : development of a demonstrator)
2011-2014
Parterns: Leroux & Lotz Technologies (LLT), Polymem, La Compagnie Parisienne de Chauffage Urbain (CPCU), LRGP (Nancy), ICARE (Orléans)
Study of the effect of oxygen enrichment on combustion
Participant - Involvement: 15%

Interdisciplinary Program for Energy (PIE CNRS):

- **Project PHYCAP** : Procédé HYbride de CAPture du dioxyde de carbone (Hybrid process for carbon dioxide capture)
2007-2008
Parterns: LRGP (Nancy), CORIA (Rouen), ICARE (Orléans)
Kinetic of combustion with oxygen enriched air
Participant - Involvement: 30%

- **Project COCASE** : Optimisation du Couplage des Procédés de Combustion et de Capture du CO_2 par Membranes (Optimisation of the coupling between combustion process and CO_2 capture by membrane)
2008-2011
Parterns : LRGP (Nancy), CORIA (Rouen), Pprime (Poitiers), ICARE (Orléans)
Identification of combustion conditions for CO_2 capture
Participant - Involvement: 30%

European projects:

- **INTELLECT D.M.** - Integrated lean low emission combustor design methodology – 6th Framework Program
2004-2005
Post-Doctorate – Marie Curie Intra-European Fellowship

- **2G-CSAFE - ERC Advanced Grant** - Ph. Dagaut (DR ICARE, Orléans)
Combustion of Sustainable Alternative Fuels for Engines used in aeronautics and automotives
WP1- Measurements of stable and labile species for kinetic model validation

2011-2013
Participant

- **PHC Procope** (France – Germany) - Hydroperoxy radical detection by cavity ring-down spectroscopy in the atmosphere simulation chamber SAPHIR
PC2A / Forschungszentrum Jülich
2017-2018
Participant

- **PHC Barrande** (France – Czech Republic) - Hydroperoxy radical detection in ambient atmosphere by cavity ring-down spectroscopy
PC2A/ Academy of Sciences, Praha
2014-2018
Participant

- **GDRE** Energetics and Safety of Hydrogen
2005-2010
Participant

<u>Labex :</u>

- Labex CAPRYSSES - Cinétique chimique et aérothermodynamique pour des propulsions et des systèmes énergétiques propres et sûrs (Chemical kinetics and aerothermodynamics for propulsion and clean systems for energy production)
WP1. Coupled phenomena between chemical kinetics and fluid dynamics for internal combustion engines, gas turbines and gasification
2012-2019
Participant

- Labex CaPPA - Chemical and Physical Properties of the Atmosphere
WP1. From gas phase to aerosols: biogenic VOCs (volatils organic compounds) as precursors for particles
2013-2019
Participant

CPER :

- Climibio - Changement climatique, dynamique de l'atmosphère et impacts sur la biodiversité et la santé humaine (Climate change, dynamics of the atmosphere and impacts on biodiversity and human health)
WP1. Méthodes d'évaluation de la qualité et du changement des milieux (Evaluation methods for quality and change of environment)

CV

WP2. Dynamique de l'atmosphère (Dynamics of the atmosphere)
2014-2020
Participant

TEACHING ACTIVITIES

2010-2012	University of Orléans Temporary teacher (30h) Course: Fundamental aspects of combustion Practical work: Numerical simulation in Combustion 5th year Engineer and Master II
2002-2004	University of Lille Sciences and Technologies Temporary lecturer (18 months, 288h) Tutorials and Practical works in Chemistry 1st year Chemistry
2000-2002	Catholic University of Lille Temporary teacher (72h) Practical work: Organic and analytical chemistry 1st year Chemistry

OTHER RESEARCH ACTIVITIES

Scientific board and committee

- Elected member of the administrative and scientific boards of ICARE laboratory (2007-2012)
- Member of the health and safety committee of ICARE (2011-2013)
- Member of the board of the research federation EPEE (FR776 CNRS EPEE: Energy, Propulsion, Space, Environment)
- Member of the experts committee Section 62, University Pierre et Marie Curie (2009) and University of Rouen (2011, 2014)
- Member of the experts committee Section 31 – University of Orléans (2007-2013)
- Member of the experts committee Section 31 − University of Lille Sciences and Technologies (2013-2017)
- Member of the PhD committee of A. Lo (University of Rouen) (2012)
- Member of the jury Master 2 Atmospheric Environment (Lille1) (2016)

Scientific animation and conference organisation:

- Contribution to the organisation of the 19th International Symposium on Gas Kinetics, Orléans, 22−27 July 2006

- Contribution to the organisation of the “fête de la science”, Campus CNRS Orléans, 2005 and 2010
- Contribution to the organisation of a press visit at ICARE, July 2007
- Contribution to the organisation of the CNRS training workshop "Initiation to laser spectroscopy methods for analysis of reactive environments", Plateforme MéOL, 08-12 September 2014, PC2A Lille - Organisation of practical work on laser polarization
- Contribution to the organisation of the workshop « Interaction Between Indoor and Atmospheric Chemistry”, 15-16 May 2015, Lille
- Contribution to the organisation of the 25th International Symposium on Gas Kinetics, Lille, planned for July 2018

Network member

- French section of the Combustion Institute (GFC : Groupement Français de Combustion)
- OPAL (Optic, Photonic and Laser Application) network

Regular reviewer for scientific journals

Visit in other labs:

- Department of Chemistry of Ions and Clusters - J. Heyrovský Institute of Physical Chemistry - Czech Republic – 2014 – 1 week
- Flame Diagnostics Laboratory - Purdue University (US) - 2005 - 1 week
- Department of Chemistry – University of Bielefeld – 2001 – 2 weeks

CV

SCIENTIFIC PUBLICATIONS AND COMMUNICATIONS

Publications

1. N. Lamoureux, H. El Merhubi, L. Pillier, S. de Persis, P. Desgroux, Modeling of NO formation in low pressure premixed flames, Combustion and Flame 163 (2016) 557-575.

2. L. Pillier, M. Idir, J. Molet, A. Matynia, S. de Persis, Experimental study and modelling of NOx formation in high pressure counter-flow premixed CH_4/air flames, Fuel 150 (2015) 394-407.

3. M. Djehiche, N.L. Le Tan, C.D. Jain, G. Dayma, P. Dagaut, C. Chauveau, M. Idir, L. Pillier and A. Tomas, Quantitative Measurements of HO_2 and Other Products of n-Butane oxidation (H2O2, H2O, CH2O and C2H4) at Elevated Temperatures by Direct Coupling of a Jet-stirred Reactor with Sampling Nozzle and Cavity Ring-Down Spectroscopy (cw-CRDS), Journal of the American Chemical Society, 136, Issue 47 (2014) 16689–16694.

4. G. Cabot, M. Calbry, P. Xavier, A. Vandel, S. de Persis, B. Belaissaoui, E. Favre and L. Pillier, Effect of CO_2 Capture on Combined Cycle Gas Turbine Efficiency Using Membrane Separation, EGR and OEA Effects on Combustion Characteristics, Proceedings of ASME Turbo Expo 2014: Turbine Technical Conference and Exposition GT2014, Volume 4A, Paper N° GT2014-25781, Dusseldorf, Germany, June 16-20 (2014).

5. N. Merlo, T. Boushaki, C. Chauveau, S. de Persis, L. Pillier, B. Sarh, I. Gökalp, Combustion Characteristics of Methane-oxygen Enhanced Air Turbulent Nonpremixed Swirling Flames, Experimental Thermal and Fluid Science 56 (2014) 53–60.

6. N. Bouvet, D. Davidenko, C. Chauveau, L. Pillier, Y. Yoon, On the simulation of laminar strained flames in stagnation flows: 1D and 2D approaches versus experiments, Combustion and Flame 161 (2014) 438-452.

7. N. Merlo, T. Boushaki, C. Chauveau, S. de Persis, L. Pillier, B. Sarh, I. Gökalp, Experimental study of oxygen enrichment effects on turbulent non-premixed swirling flames, Energy and Fuels 27 (2013) 6191-6197.

8. S. de Persis, F. Foucher, L. Pillier, V. Osorio, I. Gökalp , Effect of O_2 enrichment and CO_2 dilution on laminar methane flames, Energy, 55 (2013) 1055-1066.

9. S. de Persis, G. Cabot, L. Pillier, I. Gökalp, A.-M. Boukhalfa, Study of lean premixed methane combustion with CO_2 dilution under gas turbine conditions, Energy and Fuels 27 (2013) 1093–1103.

10. A. Matynia, J. Molet, C. Roche, M. Idir, S. de Persis and L. Pillier, Measurement of OH concentration profiles by laser diagnostics and modelling in high pressure counter-flow premixed methane-air and biogas-air flames, Combustion and Flame 159 (2012) 3300-3311.

11. A. Matynia, M. Idir, J. Molet, C. Roche, S. de Persis and L. Pillier, Absolute OH concentration profiles measurements in high pressure counterflow flames by coupling LIF, PLIF and absorption techniques, Applied Physics B 108 (2012) 393-405 .

CV

12. A. Matynia, J-L. Delfau, L. Pillier, C. Vovelle, Comparative study of the influence of CO_2 and H_2O on the chemical structure of lean and rich methane/air flames at atmospheric pressure, Combustion, Explosion and Shock Waves 45, N°6 (2009) 635-645.

13. C. Vovelle, J-L. Delfau, L. Pillier, Laminar Hydrocarbon Flame Structure, Combustion, Explosion and Shock Waves 45, N°4 (2009) 365-382.

14. J.-L. Delfau, J. Biet, M. Idir, L. Pillier and C. Vovelle, Experimental and numerical study of premixed, lean ethylene flames, Proceedings of the Combustion Institute 31 (2007) 357-365.

15. A. El bakali, L. Pillier, P. Desgroux, B. Lefort, L. Gasnot, J.F. Pauwels and I. da Costa, NO prediction in natural gas flames using GDF-Kin®3.0 mechanism: NCN and HCN contribution to prompt-NO formation, Fuel 85 (2006) 896-909.

16. L. Pillier, A. El Bakali, X. Mercier, A. Rida, J.-F. Pauwels and P. Desgroux, Influence of C_2 and C_3 compounds of natural gas on NO formation: an experimental study based on LIF/CRDS coupling, Proceedings of the Combustion Institute 30 (2005) 1183-1191.

17. A. El Bakali , P. Dagaut , L. Pillier , P. Desgroux , J-F. Pauwels , A. Rida and P. Meunier, Experimental and modeling study of the oxidation of natural gas in a premixed flame, shock tube, and jet-stirred reactor, Combustion and Flame 137 (2004) 109-128.

18. L. Pillier, C. Moreau, X. Mercier, J-F. Pauwels, P. Desgroux, Quantification of Stable Minor Species in Confined Flames by Cavity Ring-Down Spectroscopy : Application to NO, Applied Physics B 74 (2002) 427-434.

19. X. Mercier, L. Pillier, A. El Bakali, M. Carlier, J-F. Pauwels, P. Desgroux, NO Reburning Study Based on Species Quantification Obtained by Coupling LIF and Cavity Ring-Down Spectroscopy, Faraday Discussions, Combustion Chemistry, 119 (2002) 305-319.

20. X. Mercier, L. Pillier, J-F. Pauwels, P. Desgroux, Quantitative Measurement of CN Radical in a Low-pressure Methane/air Flame by Cavity Ring-Down Spectroscopy, Compte Rendu de l'Académie des Sciences, Paris, Tome 2, Série IV (2001) 965-972.

Conference papers

1. M. Blocquet, M. Ward, M. Verriele, S. Dusanter, S. Le Calvé, B. Hanoune, L. Pillier, N. Locoge, C. Fittschen, C. Schoemaecker, Oxidants behaviour in a low energy consumption building with mechanical ventilation, Indoor Air 2016, Gand (Belgium), July 2016.

2. J. Molet, H. El Merhubi, N. Lamoureux, S. de Persis, M. Idir, L. Pillier, P. Desgroux., NO Formation in Premixed CH4/Air Flames, 6th European Combustion Meeting, 25-28 June 2013, Lund, Sweden.

3. M. Djehiche, L. Le Tan, A. Tomas, P. Coddeville, L. Pillier, M. Idir, C. Fittschen, G. Dayma, P. Dagaut, HO2 Measurement by Nozzle Sampling and cw-CRDS, 6th European Combustion Meeting, 25-28 June 2013, Lund, Sweden.

4. N. Merlo, T. Boushaki, C. Chauveau, S. de Persis, L. Pillier, I. Gökalp, B. Sarh, Effects of Oxygen Enrichment on Stability and Pollutant Emissions of Turbulent Non-premixed Swirling Flames, 6th European Combustion Meeting, 25-28 June 2013, Lund, Sweden.

5. J-M. Most, S. Dahikar, S. Pal, A. Claverie, D. Denis, L. Pillier and S. de Persis, Premixed CH4/O2 enriched air combustion: Identification of thermal, chemical and aerodynamic effects, 6th Europen Thermal Sciences Conference (Eurotherm 2012), Journal of Physics Conference Series 11/2012; 395(1):2005-. DOI:10.1088/1742-6596/395/1/012005

6. A. Matynia, J. Molet, , M. Idir, S. de Persis and L. Pillier, Measurements of OH concentration profiles by Laser Induced Fluorescence in high pressure counterflow premixed methane-air and biogas-air flames, Proceedings of the 5th European Combustion Meeting 2011 (ECM2011), Cardiff, Wales, 28th June -1st July 2011.

7. J. Molet, A. Matynia, L. Pillier, M. Idir and S. de Persis, Kinetic study of NOx formation in high-pressure flames, Proceedings of the 5th European Combustion Meeting 2011 (ECM2011), Cardiff, Wales, 28th June -1st July 2011.

8. J-M. Most, S. Dahikar, A. Claverie, D. Denis, O. Kalach, L. Pillier, S. de Persis, Influence of Thermochemical Conditions on the Behavior of Methane/Oxygen Enriched Combustion, Proceedings of the 5th European Combustion Meeting 2011 (ECM2011), Cardiff, Wales, 28th June -1st July 2011.

9. J. Zhou, F. Foucher, S. de Persis, L. Pillier, Effect of oxygen enrichment and CO_2 dilution on laminar methane flame velocities, Proceedings of the 5th European Combustion Meeting 2011 (ECM2011), Cardiff, Wales, 28th June -1st July 2011.

10. L. Pillier, S. De Persis, G. Cabot, R. Bounaceur, Y. Liu, A. Boukhalfa, J-M. Most, I. Gökalp and E. Favre, Coupling of oxygen-enriched combustion and CO_2 capture by membrane processes, 4th European Combustion Meeting (ECM2009), 14-17 April 2009, Vienna, Austria.

11. D. Davidenko, N. Bouvet, L. Pillier, C. Chauveau, Numerical Simulation of a Strained Laminar Flame Burner and Comparison with the Experiment, 4th European Combustion Meeting (ECM2009), 14-17 April 2009, Vienna, Austria.

12. N. Bouvet, L. Pillier, D. Davidenko, C. Chauveau, I. Gökalp, Particle Image Velocimetry for the Determination of Fundamental Flame Velocities: Methodology Validation and Application to Methane-Air Mixtures, 4th European Combustion Meeting (ECM2009), 14-17 April 2009, Vienna, Austria.

13. A. Matynia, L. Pillier, M. Idir, J-L. Delfau, C. Chauveau and C. Vovelle, Study of high pressure counter-flow methane flames, 4th European Combustion Meeting (ECM2009), 14-17 April 2009, Vienna, Austria.

14. A. Matynia, J-L. Delfau, L. Pillier and C. Vovelle, Comparative study of the influence of CO_2 and H_2O on the chemical structure of lean and rich methane/air flames at atmospheric pressure, 6th International Seminar on Flame Structure, Brussels, Sept. 14-18, 2008.

15. J. Biet, J.L. Delfau, L. Pillier, C. Vovelle, Influence of CO_2 and H_2 on the Chemical Structure of a Premixed, Lean Methane-Air Flame, Third European Combustion Meeting (ECM2007), Chania, Crete, April 11-13, 2007.

16. S. Gashi, A.J. Riley, L. Pillier, A.P. Dowling, C.F. Kaminski, Investigation of acoustic instabilities on a lean premixed combustor using time resolved OH PLIF, Second European Combustion Meeting (ECM2005), Louvain la Neuve, Belgium, April 3-6, 2005.

17. S. Gashi, L. Pillier, A.J. Riley, A.P. Dowling, C.F. Kaminski, Flame response to acoustic perturbations using OH PLIF, Seventh World Congress of Chemical Engineering (WCCE2005), Glasgow, July 2005.

18. I. Da Costa, S. Carpentier, L. Pillier, A. El Bakali, J-F. Pauwels, P. Desgroux, GDF-Kin® : A comprehensive chemical mechanism for NOx formation in natural gas combustion, International Gas Research Conference, Vancouver, November 1-4, 2004.

19. L. Pillier, A. El Bakali, X. Mercier, J-F. Pauwels, P. Desgroux, I. Da-Costa, Ph. Meunier, Effect of Ethane and Propane on NO Formation in Low Pressure Premixed $CH_4/O_2/N_2$ Flames, First European Combustion Meeting, Orléans, Oct. 25-28, 2003.

Oral communications

1. C. Schoemaecker, M. Blocquet, M. Rizk, M. Ward, R. Nasreddine, M. Guglielmino, C. Liaud, C. Trocquet, M. Mendez, M. Verriele, S. Dusanter, B. Hanoune, D. Petitprez, L. Pillier, S. Le Calvé, N. Blond, D. Hauglustaine, P. Blondeau, N. Locoge, « Etude de la qualité de l'air dans un bâtiment énergétiquement performant par analyse en temps réel de l'évolution des polluants », Conférence Atmosf'air, Lyon, 2015.

2. J. Molet, A. Matynia, C. Roche, M. Idir, S. de Persis, L. Pillier, « Formation des oxydes d'azote dans les flammes pauvres à contre-courants prémélangées de CH_4/air and CH_4/H_2/air à haute pression », XXXII^{ème} Réunion annuelle du Groupe de Cinétique et Photochimie, Bordeaux, 4-5 Juin 2012.

3. L. Pillier, P. Desgroux, « Mesure de la concentration absolue de NO dans une flamme par Cavity Ring-Down Spectroscopy », Journées des Doctorants en Combustion, Groupement Français de Combustion, Lille, Décembre 2001.

4. M. Blocquet, M. Ward, M. Verriele, S. Dusanter, S. Le Calvé, B. Hanoune, L. Pillier, N. Locoge, C. Fittschen, C. Schoemaecker, "Oxidants behaviour in a low energy consumption building with mechanical ventilation", Conference Indoor Air 2016, Gand, juillet 2016.

5. B. Hanoune, S. Batut, M. Blocquet, S. Coudert, S. Germain, D. Petitprez, L. Pillier, M. Ward, M. Mendez, S. Dusanter, V. Gaudion, T. Leonardis, N. Locoge, M. Rizk, M. Verriele, M. Guglielmino, S. Le Calvé, C. Liaud and C. Schoemaecker, "When Outdoor Air Meets Indoor Air: the Complex Chemistry in Low Energy Buildings", 4th Sino-French Joint Workshop on Atmospheric Environment, Lyon–France, December 10th–13rd, 2014.

6. J. Molet, M. Idir, S. de Persis, L. Pillier, "Effect of hydrogen addition on NOx formation in high pressure counter-flow premixed CH_4/air flames", 2nd Topical workshop: kinetic studies using laminar flames, 25th June 2013, Lund, Sweden.

7. A. Matynia, J-L. Delfau, L. Pillier and C. Vovelle, Comparative study of the influence of CO_2 and H_2O on the chemical structure of lean and rich methane/air flames at atmospheric pressure, 6th International Seminar on Flame Structure, Brussels, Sept. 14-18, 2008.

8. L. Pillier, X. Mercier, P. Desgroux, « Coupling of LIF/CRDS for Flame Structure Studies », 3rd Cavity Ring-Down User Meeting, Villeneuve d'Ascq, Oct. 2003.

Posters

1. F. Kravtchenko, L. Pillier, S. Batut, B. Calimet and C. Fittschen, Etude de la réactivité d'espèces radicalaires de type peroxyles d'intérêt atmosphérique, Journées Interdisciplinaires de la Qualité de l'Air (JIQA 2017), 2-3 Février 2017, Villeneuve d'Ascq.

2. L. Pillier, S. de Persis, M. Idir, N. Lamoureux, P. Desgroux, NO formation in high pressure premixed flames: experimental results and validation of a new revised reaction mechanism, 24th International Symposium on Gas Kinetics and Related Phenomena, York (UK), July 2016.

3. J. Molet, H. El Merhubi, N. Lamoureux, S. de Persis, M. Idir, L. Pillier, P. Desgroux., NO Formation in Premixed CH4/Air Flames, 6th European Combustion Meeting, 25-28 June 2013, Lund, Sweden.

4. M. Djehiche, L. Le Tan, A. Tomas, P. Coddeville, L. Pillier, M. Idir, C. Fittschen, G. Dayma, P. Dagaut, HO2 Measurement by Nozzle Sampling and cw-CRDS, 6th European Combustion Meeting, 25-28 June 2013, Lund, Sweden.

5. N. Merlo, T. Boushaki, C. Chauveau, S. de Persis, L. Pillier, I. Gökalp, B. Sarh, Effects of Oxygen Enrichment on Stability and Pollutant Emissions of Turbulent Non-premixed Swirling Flames, 6th European Combustion Meeting, 25-28 June 2013, Lund, Sweden.

6. A. Matynia, J. Molet, , M. Idir, S. de Persis and L. Pillier, Measurements of OH concentration profiles by Laser Induced Fluorescence in high pressure counterflow premixed methane-air and biogas-air flames, Proceedings of the 5th European Combustion Meeting 2011 (ECM2011), Cardiff, Wales, 28th June -1st July 2011.

7. J. Molet, A. Matynia, L. Pillier, M. Idir and S. de Persis, Kinetic study of NOx formation in high-pressure flames, Proceedings of the 5th European Combustion Meeting 2011 (ECM2011), Cardiff, Wales, 28th June -1st July 2011.

8. J-M. Most, S. Dahikar, A. Claverie, D. Denis, O. Kalach, L. Pillier, S. de Persis, Influence of Thermochemical Conditions on the Behavior of Methane/Oxygen Enriched Combustion, Proceedings of the 5th European Combustion Meeting 2011 (ECM2011), Cardiff, Wales, 28th June -1st July 2011.

9. J. Zhou, F. Foucher, S. de Persis, L. Pillier, Effect of oxygen enrichment and CO_2 dilution on laminar methane flame velocities, Proceedings of the 5th European Combustion Meeting 2011 (ECM2011), Cardiff, Wales, 28th June -1st July 2011.

10. S. de Persis, L. Pillier, I. Gokalp, V. Osorio, G. Cabot, A. Boukhalfa, G. Cabot, J.M. Most, B. Belassaioui, E. Favre, « COCASE : optimisation du couplage des procédés de combustion et de capture du CO2 par membranes », Colloque Energie, Programme Interdisciplinaire Energie du CNRS, Nantes, 16-18 Novembre 2009.

11. A. Matynia, L. Pillier, M. Idir, J-L. Delfau, C. Chauveau and C. Vovelle, Study of high pressure counter-flow methane flames, 6th Mediterranean Combustion Symposium, 7-11 June 2009, Porticcio, Corsica, France.

12. L. Pillier, S. de Persis, G. Cabot, R. Bounaceur, Y. Liu, A. Boukhalfa, J-M. Most, I. Gökalp and E. Favre, Coupling of oxygen-enriched combustion and CO_2 capture by membrane processes, 4th European Combustion Meeting (ECM2009), 14-17 April 2009, Vienna, Austria.

13. D. Davidenko, N. Bouvet, L. Pillier, C. Chauveau, Numerical Simulation of a Strained Laminar Flame Burner and Comparison with the Experiment, 4th European Combustion Meeting (ECM2009), 14-17 April 2009, Vienna, Austria.

14. N. Bouvet, L. Pillier, D. Davidenko, C. Chauveau, I. Gökalp, Particle Image Velocimetry for the Determination of Fundamental Flame Velocities: Methodology Validation and Application to Methane-Air Mixtures, 4th European Combustion Meeting (ECM2009), 14-17 April 2009, Vienna, Austria.

15. A. Matynia, L. Pillier, M. Idir, J-L. Delfau, C. Chauveau and C. Vovelle, Study of high pressure counter-flow methane flames, 4th European Combustion Meeting (ECM2009), 14-17 April 2009, Vienna, Austria.

16. N. Bouvet, L. Pillier, D. Davidenko, C. Chauveau, I. Gökalp, Laminar Flame Velocity Determination Using Particle Image Velocimetry And The Counterflow Flame Burner : Application To Syngas Combustion, Work in Progress Poster, 32nd International Symposium on Combustion, McGill University, Montreal, Canada, August 3-8, 2008.

17. A. Boukhalfa, G. Cabot, E. Favre, I. Gökalp, L. Pillier, PHYCAP: Procédé HYbride de CAPture du dioxyde de carbone, Projet Exploratoire P.E. 1-8, Colloque Energie, Programme Interdisciplinaire Energie du CNRS, Futuroscope, Poitiers, 6-8 Février 2008.

18. A. Matynia, J-L. Delfau, L. Pillier, C. Vovelle, Analyse de l'influence des ajouts de CO_2 et H_2 sur les structures de flamme prémélangées Méthane/Air riches, Journées des Doctorants en Combustion, Groupement Français de Combustion, Orléans, Novembre 2007.

19. J. Biet, J-L. Delfau, L. Pillier, C. Vovelle, Influence of CO_2 and H_2 on the Chemical Structure of a Premixed, Lean Methane-Air Flame, ECM2007, Chania, Crete, 11-13 April, 2007.

20. J. Biet, J.L. Delfau, M. Idir, L. Pillier, C. Vovelle, « Structure of Premixed, Laminar, Lean Ethylene Flames at Atmospheric Pressure and Modelling", 19th International Symposium on Gas Kinetics, Orléans, July 22−27, 2006.

21. L. Pillier, X. Mercier, P. Desgroux, « Effect of Ethane and Propane on NO Formation in Low Pressure Premixed $CH_4/O_2/N_2$ Flames », Gordon Research Conference: Laser Diagnostics in Combustion, Oxford (UK), August 19-25, 2003.

22. L. Pillier, X. Mercier, A. Rida, J-F. Pauwels, P. Desgroux, « Mesure de la Concentration Absolue de NO dans une Flamme par Cavity Ring-Down Spectroscopy », Colloque Combustion Propre, Orléans, Juin 2001.

23. L. Pillier, P. Desgroux, « Quantitative Measurement of NO in Flames by Cavity Ring-Down Spectroscopy », Gordon Research Conference: Laser Diagnostics in Combustion, Mount Holyoke College, South Hadley, MA (USA), July 2001.

Invited seminars

1. C. Vovelle, J-L. Delfau, L. Pillier, Laminar Flame Structure, Plenary Lecture of the 6th International Symposium on Flame Structure, Brussels, 14-17 September 2008.

2. L. Pillier, B. Ayoola, R. Balachandran, S. Gashi, A. Riley, Cl. Kaminski, E. Mastorakos, « Etude par PLIF des instabilités de combustion en flammes prémélangées pauvres », Journée d'étude « Diagnostics Laser : principes et adaptation à l'étude de processus de combustion », Section française du Combustion Institute, Ecole Centrale Paris, 13 Oct. 2005.

Activity reports for industrial contract

L. Pillier
Formation de monoxyde d'azote dans des flammes prémélangées $CH_4/C_2H_6/C_3H_8/O_2/N_2$: étude expérimentale par diagnostics laser et modélisation
Contract CNRS/ADEME/GDF
6 reports between 2000 and 2003

Introduction

Today, most of the energy is produced from fossil fuels resources (oil, natural gas, coal), and it will be the case for several decades. Faced with the current energy challenge, it is essential to make the energy production systems less harmful for the environment. Two problems have to be addressed urgently: the reduction of greenhouse gas emissions and shortage of fossil energy reserves. The development and optimisation of new combustion modes and the use of cleaner alternative energy sources require a precise knowledge of the combustion chemical processes in order to improve the energy efficiency and to reduce pollutants formation.

Since my PhD (2003), my research activities come within the scope of this problematic, and concern essentially the study of combustion chemical kinetics in flames, and more recently atmospheric chemical kinetics. The development and validation of complex chemical mechanisms require comparisons of their predictions with precise experimental data. During my career, I have developed different innovative experimental devices for the study of reactive gas phase environments involving mainly laser diagnostic techniques.

My first experience in this field was during my PhD (1999-2003) in PC2A laboratory (PhysicoChimie des Processus de Combustion et de l'Atmosphère, UMR 8522, CNRS et Université de Lille Sciences et Technologies) under the supervision of Pascale Desgroux et Jean François Pauwels. The aim of my PhD was the development of a detailed chemical kinetic mechanism for the formation of nitrogen oxide (NO) in natural gas flames. It was co-financed by Gaz de France, ADEME (Agence De l'Environnement et de la Maîtrise de l'Energie) and the CNRS (Centre National de la Recherche Scientifique). During this work, an extensive experimental study of low pressure premixed flames structures was performed using Laser Induced Fluorescence (LIF), laser absorption and Cavity RingDown Spectroscpy (CRDS) for the measurements of species like OH, CH or NO and a new combustion chemical mechanism was then proposed: GDFkin®3.0. This mechanism was a basis for numerous following research studies on NOx formation in flames at PC2A and it is still a topical subject in the Combustion research group.

After my PhD, I have obtained a Marie Curie Intra-European Fellowship (European Commission) for a postdoc position (2004-2005) in the Chemical Engineering Department of the University of Cambridge (UK), in the group of Clemens Kaminski. I worked on laser based imaging (LIF) in a low emission, lean premixed gas turbine combustor to elucidate the role of acoustically excited instabilities that can damage the combustor.

I have then obtained my CNRS research position (Chargée de Recherche) in 2005 at the ICARE laboratory (Institut de Combustion, Aérothermique, Réactivité, Environnement, UPR CNRS 3021, Orléans). I have started my career at ICARE in the “Flame Structure” group with Christian Vovelle and Jean-Louis Delfau. After their retirement, I have formed a new research team with Stéphanie de Persis (lecturer at ICARE/University of Orléans) with the help of Mahmoud Idir (Research Engineer at ICARE). We were involved in several research projects (ANR, PIE) with other french laboratories (PC2A-Lille, LRGP-Nancy, CORIA-Rouen, Pprime-Poitiers) and industrial partners (Leroux & Lotz Technologies, Polymem, Compagnie Parisienne de Chauffage Urbain). My activities at ICARE were divided in three main topics:

- The development of new combustion modes for energy production
- The combustion kinetics of biomass fuels: biogas and syngas
- The NOx formation in combustion

During my position at ICARE (2005-2013), I have developed a new experimental device dedicated to the study of flame structure at high pressure using laser based techniques.

Following my transfer request in 2012, I have joined the PC2A laboratory in May 2013, in the ‘Atmospheric Physical Chemistry – Homogeneous reactivity in the atmosphere’ group with Christa Fittschen and Coralie Schoemaecker. The research project that I develop concerns the study of the reactivity of radical species in atmospheric chemistry (HOx and RO_2 radicals). I am developing a new experimental setup to study reactions between RO_2, HO_2 and OH radicals, with measurements of rate constants and branching ratios. The new setup consists of a fast flow tube (several $m.s^{-1}$) coupled to two laser diagnostic techniques: Laser Induced Fluorescence for OH radicals measurements, continuous wave-Cavity RingDown Spectroscopy (cw-CRDS) for HO_2 radicals measurements; and Mass Spectrometry with Molecular Beam (MB/MS) for products measurements.

In PC2A, I am still involved in the combustion kinetics with recent writing of papers on NOx formation in flames with Nathalie Lamoureux, Pascale Desgroux (PC2A) and my former colleagues at ICARE (Stéphanie de Persis and Mahmoud Idir). Furthermore, I’m currently working with my colleague

Guillaume Vanhove (lecturer PC2A / University of Lille / Combustion Chemistry Group / Rapid Compression Machine team) to develop a new research project on plasma assisted Low Temperature Combustion (LTC).

This manuscript relates most of my research activities since my recruitment at the CNRS (2005), it is divided into two main parts: part A - Combustion chemical kinetics, part B - Atmospheric chemical kinetics.

In part A, I will first describe my works on the development of new combustion modes for energy production, with two main topics: the study of combustion kinetics in lean flames and the effect of oxygen-enrichment of air in combustion for CO_2 capture. The latter topic was a part of two main collaborative projects with academic laboratories and industrial partners (PIE project COCASE and ANR project CO_2 Energicapt). Next, I will present my activities related to the combustion kinetics of biomass fuels: biogas and syngas; the high pressure flame burner that I have developed at ICARE will be detailed in this part. The last part will be devoted to the study of the formation of NOx in high pressure flames (ANR project NO-mecha). For the whole of this research projects, I had the opportunity to co-supervise four PhD students (Nicolas Bouvet, Alexis Matynia, Julien Molet and Nazim Merlo) and four Master students (Alexis Matynia, Vladimiro Osorio, Julien Molet and Yassine Azeddine).

In part B, I will present my new research project on the study of the reactivity of radical species in atmospheric chemistry. The new flow tube and its coupling with LIF, cw-CRDS and MB/MS will be described. Validation of the experimental setup will then be presented with HO_2 radical measurements by cw-CRDS and OH radicals measurements by LIF, as well as the first measurements we have obtained with the mass spectrometer. I am currently co-supervising a PhD student (Florent Kravtchenko, 2016-2019) on this topic.

Part A - Combustion chemical kinetics

A1. New combustion modes for energy production

In this first part, I have compiled my research activities concerning the development of new combustion modes for cleaner energy production. The first topic concerns the combustion in lean flame conditions for reduction of pollutants and fuel consumption. The second topic concerns the combustion in oxygen enriched air conditions for CO_2 capture application.

1.1. Combustion kinetics in lean mixtures

Burning lean hydrocarbon–air mixtures offers the potential of fuel economy and reduced pollutants formation (CO, CO_2, soot, NOx,…). However, very lean flame conditions are subject to instabilities, eventually leading to flame extinction, and can produce intermediate oxygenated products, particularly aldehydes. A better knowledge of the combustion chemistry of lean fuel–air mixtures was needed to overcome these limitations. The study undertaken in this objective in the group of C. Vovelle at ICARE, during the PhD of J. Biet [Biet, 2004; Biet et al., 2005; Delfau et al., 2007] concerned different small hydrocarbons (methane, propane, propene and ethylene), in order to obtain detailed data on the formation of intermediate species with 1 to 3 carbon atoms which control the combustion kinetics of heavier hydrocarbons. Upon my arrival in C. Vovelle's group at ICARE, I was involved in the study of ethylene lean flames [Delfau et al., 2007]. The objective was to extend the experimental database on lean mixtures and validate existing detailed chemical mechanisms in these conditions.

In this work, the chemical structure of lean (equivalence ratio ϕ = 0.5 and 0.7) premixed ethylene–oxygen–nitrogen flames stabilized on a flat-flame burner at atmospheric pressure was studied experimentally and compared with modelling. The species mole fraction profiles were measured by Gas Chromatography (GC for CH_4, C_2H_4, C_2H_2, C_2H_6, C_3H_6, C_3H_8, CO, CO_2, CH_3CHO, H_2, O_2 and N_2) and by Fourier Transform Infrared spectroscopy (FTIR for CH_2O and H_2O). These data were used to check the ability of four detailed reaction mechanisms to correctly predict the species mole fraction profiles: the UDEL [Davis et al., 1999], Konnov [Konnov, 2000], UCSD (University of California, San Diego, available at http://web.eng.ucsd.edu/mae/groups/combustion/mechanism.html, 2005) and Dagaut [Dagaut et al. 2005] mechanisms. The UDEL mechanism is based on addition of reactions for C_3–C_6 species to the GRImech3.0 mechanism [Smith et al., 1999], it includes 70 species and 455 reversible reactions. The mechanism developed by Konnov is more detailed, in its original version it contains 127 species:

$C_xH_yO_z$ from C_0 to C_6 and nitrogenous intermediates. In this work, the N-species subsystem was removed so that the number of species was reduced to 93 involved into 730 reversible and 47 non-reversible reactions. The third mechanism has been developed at the University of California San Diego (UCSD) to describe phenomena relevant to flame conditions with the number of reactions and species kept to a minimum. The 2005 version with 40 species (up to C_3) and 175 reversible reactions was used in this work. The fourth mechanism, developed by Dagaut, contains 54 species involved into 281 reactions.

A detailed comparison between experimental and modelling results is presented in [Delfau et al., 2007]. A very good agreement was observed for the main species: reactants consumption, final products (CO_2, H_2O) and the main intermediates (CO, H_2). However, marked differences between the four mechanisms were observed in the prediction of intermediate species present in small concentrations, such as CH_2O, CH_3CHO. Pathways analyses were performed to identify the origins of these discrepancies. It was shown that the same reactions were involved in the four mechanisms to describe the consumption of ethylene, but with differences in their relative importance, as illustrated in Figure 1 for the leanest (ϕ=0.5) C_2H_4-O_2-N_2 flame. C_2H_3 and CH_2HCO are the main radicals formed in this first step and their consumption differs between the mechanisms either by the use of different kinetic data for common reactions or by differences in the nature of the consumption reactions.

Publication linked to this work:
Delfau J-L., Biet J., Idir M., Pillier L. and Vovelle C., Experimental and numerical study of premixed, lean ethylene flames, Proc. Combust. Inst. 31 (2007) 357-365.

Part A1: New combustion modes for energy production

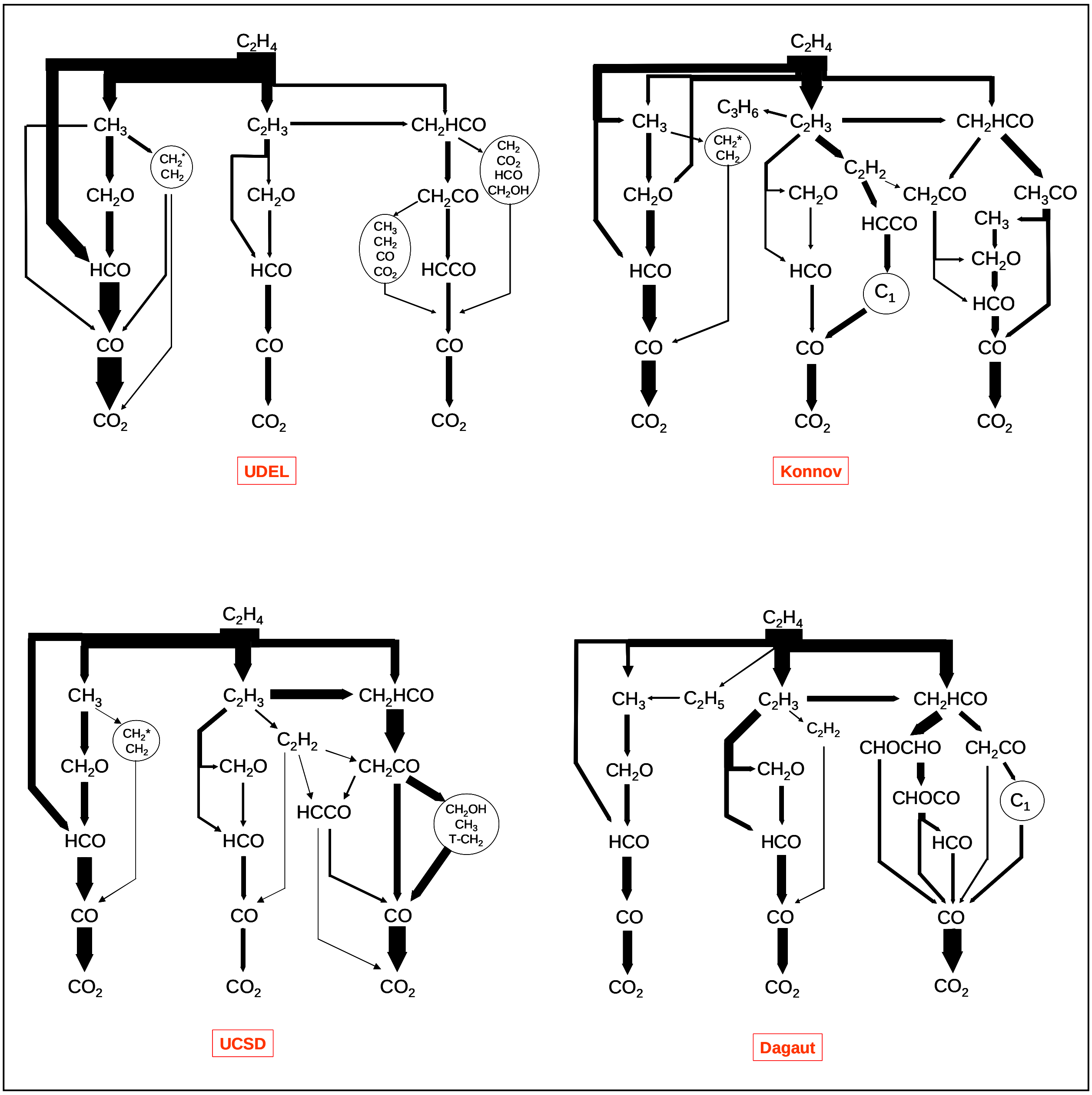

Figure 1: *Pathways analyses in the lean C_2H_4-O_2-N_2 (ϕ=0.5) flame*

1.2. Oxygen-enriched air combustion for CO_2 capture

In the context of greenhouse gas emissions mitigation, Carbon dioxide Capture and Storage (CCS) is a promising option for fossil-fuel power plants [Herzog, 2001]. Most of the research in this area focuses on minimizing the energy required for CO_2 capture [Dechamps et al., 2004; Wall, 2007]. While CO_2 pre-combustion capture offers the most promising alternative for integrated coal or natural gas combined cycle power plants, post-combustion capture is usually the only option for other industrial plants (cement, steel, glass, refineries, chemical plants, etc.). In post-combustion processes, the capture step dominates and typically accounts for 60−80% of the overall cost of the capture−transportation−injection−storage chain [Davidson et al., 2005]. A reduction of the energy cost (in GJ per ton of CO_2 captured) associated to the capture step is considered as the main goal to achieve a concrete application. The choice of the capture technology and the composition of gas mixtures to be processed play obviously a major role with regard to this cost. To optimize the CO_2 capture cost, thermodynamic cycles of power plants have to be modified, and resulting new designs inevitably lead to new combustion modes.

From a practical point of view, CO_2 capture in post-combustion processes is currently envisaged within two possibilities [Figueroa et al., 2008]:

i) Oxycombustion, i.e. with a high purity oxygen supply to avoid dilution with nitrogen, leading to an “easy” capture of concentrated CO_2 (> 90%) after water vapour condensation;

ii) Conventional post-combustion capture, i.e. CO_2 capture in the exhaust gas of a conventional process with air supply (in this case, CO_2 concentration is usually between 4 and 15% depending on the fuel type and the combustion process). Absorption in liquids (amine washing), adsorption, cryogenic fractionation or membrane separation processes can be used. Among these processes, post-combustion membrane separation affords a greatly reduced energy cost [Bounaceur et al., 2006; Favre, 2007; Favre et al., 2009] if a relatively high content of CO_2 is produced in the exhaust gas (>30% at atmospheric pressure). However, this capture process cannot be directly applied to the most competitive power plant technique (combined cycle), which combines gas and steam turbines. In gas turbines, high air dilution is used in order to keep the turbine inlet temperature below the metallurgical temperature limit. Unfortunately, this dilution leads to a lower CO_2 concentration of close to 5% in the exhaust gases. One solution to increase the CO_2 concentration, called EGR (Exhaust Gas Recirculation), is to replace (totally or partially) air dilution by cooled exhaust gases. Moreover, EGR can be used to decrease NOx emissions by controlling the flame temperature, a process already used in car engines, and to decrease the compression work by lowering the compressed air mass flow rate.

An intermediate solution between oxycombustion and conventional post-combustion is to use enriched oxygen combustion. O_2 enrichment allows to reduce nitrogen quantity, which plays a heat sink role via its specific heat capacity, flame temperature is then higher and the thermal transfers are improved [Charles, 2013; Wu et al., 2010; Ditaranto et al., 2011; Baukal et al., 1997; Bisio et al., 2002]. Moreover the exhaust gas volume is reduced, which allows a reduction of the size of the power plant and its associated capture process unit. The energy required to heat nitrogen is then lowered. Consequently, for a given heat power, O_2 enrichment permits to consume less fuel, Wu et al. (2010) have observed a reduction of 26% of the fuel (natural gas) consumption when O_2 concentration changes from 21 to 30% vol., while maintaining the combustor temperature at 1493 K. However, O_2 enriched combustion can lead to an increase of NOx through the thermal-NO pathway as temperature will increase and EGR will then be essential to control the flame temperature [Zhang et al., 2013]. O_2 enrichment has also an effect on flame velocity, increasing substantially the flame stability [Dyakov et al., 2001; Dirrenberger et al., 2011]. When O_2 enriched combustion is adopted, CO_2 capture technologies using membrane permeation can be considered as they are sensitive to CO_2 partial pressure [Bounaceur et al., 2006; Favre, 2007; Favre et al., 2009].

During my research work at ICARE laboratory, I was involved in three projects related to the study of oxygen-enriched air combustion for CO_2 capture application, which I will describe hereafter.

1.2.1 Optimisation of the coupling between combustion process and CO_2 capture by membrane (COCASE project)

1.2.1.1 Context and objectives

The COCASE project (Optimisation du Couplage des Procédés de Combustion et de Capture du CO_2 par Membranes) was a research project funded by the “Programme Interdisciplinaire Energie du CNRS” (2008-2011). Four research institutes were involved: LRGP-Nancy (coordinator: E. Favre), ICARE-Orléans, CORIA-Rouen and Pprime-Poitiers. The global objective of the COCASE project was to investigate a technological solution for post-combustion CO_2 capture by membrane separation with minimal energy consumption and combustion efficiency with limiting pollutants emissions.

The approach starts from the principle that the energy required for the capture of a specific component in a mixture is proportional to the dilution rate of the component to extract and to the level of enrichment required. The COCASE project aimed to investigate the potentialities of a hybrid process associating two technologies for lower energy consumption:

i) Oxygen-enriched air production (typically 30 to 80% of oxygen) for combustion process supply, using a flexible and energetically interesting process (cryogeny for large units, membrane permeation for other units), which could present an alternative solution between oxycombustion (i.e. combustion with pure oxygen) and the conventional post-combustion capture;

ii) CO_2 capture in the flue gas using a membrane process particularly well suited for high CO_2 concentrated mixtures [Bounaceur et al., 2006].

A diagram of principle is given in Figure 2.

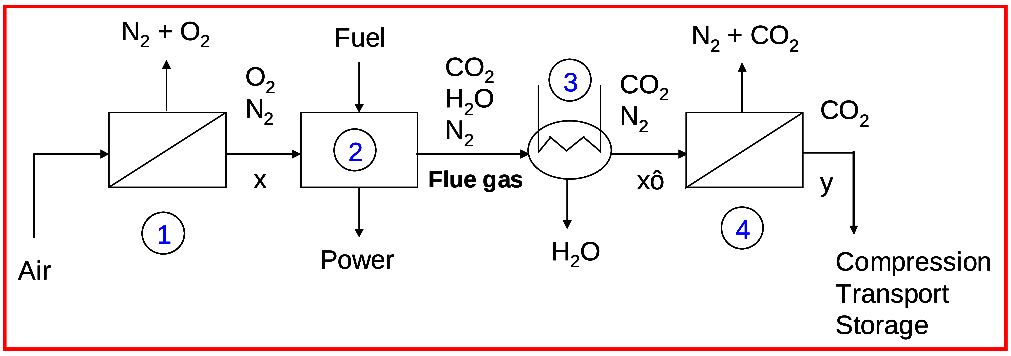

***Figure 2**: Synoptic of the hybrid process including an oxygen-enriched combustion section (oxygen production unit: 1, combustion unit: 2) and a CO_2 capture section (drying process: 3, capture process: 4).*
x: mole fraction of O_2; x': mole fraction of CO_2; y: mole fraction of CO_2 after the separation unit
[Favre et al., 2009]

The scientific objective of the COCASE project was to identify, using modelling and experimental tools, the optimal operating conditions of the hybrid process. Five aspects were addressed:

1) Identification of the combustion conditions allowing a correct operation of the entire system: oxygen production-combustion-capture (ICARE) and delivery of a numerical database for the CO_2 capture tests (LRGP)
2) Experimental study of the effect of O_2 enrichment and gas recirculation on combustion in a model gas turbine chamber (CORIA) and comparison between experiments and modelling (CORIA/ICARE)
3) Experimental study of the effect of O_2 enrichment and gas recirculation on combustion in a diffusion counterflow flame (Pprime) and comparison between experiments and modelling (Pprime/ICARE)
4) Study of the performances of the membrane separation unit for different gas mixtures (LRGP)
5) Energetic analysis of the coupling gas turbine/CO_2 capture by membrane (LRGP/CORIA)

The research activities that I have carried out at ICARE with my colleagues S. de Persis and I. Gökalp, during the COCASE project, focused on the chemical kinetic modelling of methane combustion with oxygen enriched air and dilution by CO_2 or EGR.

This part of the work aimed to identify the combustion conditions (initial gas mixtures composition, oxygen content, equivalence ratio, exhaust gas composition) allowing a correct operation of the entire process in terms of flame velocity, temperature, pollutants emission (NOx, CO, unburnt compounds), CO_2 content in the exhaust gas and oxygen consumption. Methane was chosen as the fuel as it is the main component of natural gas, which generates the minimum of CO_2 per kWh. Comparison with experimental results obtained in a model gas turbine chamber (CORIA) and a diffusion counterflow flame (Pprime) was also undertaken.

1.2.1.2 Main results

1.2.1.2.1. Effect of oxygen enrichment on methane combustion

Modelling was performed for laminar CH_4-O_2-N_2 premixed flames in conditions close to gas turbine operation conditions: initial temperature 600 K, pressure from 0.1 to 0.8 MPa and equivalence ratio from lean (ϕ=0.7) to slightly rich (ϕ=1.1). Flame modelling was performed with the PREMIX code [Kee et al., 1985] and the GRImech3.0 mechanism [Smith et al., 1999]. This study was performed during the training of V. Osorio (Master I student, 2008) who I co-supervised.

First, the influence of increasing oxygen enrichment (from 21 to 100% O_2) was studied. As an example, Figure 3 shows the variations of the laminar flame velocity S_L and the adiabatic temperature T when the O_2 content increases from air (21%) to oxycombustion (100%) conditions in the slightly rich CH_4-O_2-N_2 flame (ϕ= 1.1). Figure 4 shows the calculated NOx (X_{NO} + X_{NO2}) emission (in ppm@15% O_2 in the exhaust gas) and the CO_2 mole fraction in the burnt gases for the same conditions. The results show, as expected, an increase of the adiabatic flame temperature and the flame velocity when the O_2 content in air increases. For the same O_2 content, the adiabatic flame temperature increases with pressure while the flame velocity decreases. The plot of NOx emissions versus the percentage of O_2 (Figure 4) gives a bell-shape profile with a maximum for 60-70% of O_2. NOx emissions increase drastically as the pressure increases due to an increase in temperature (the thermal-NO mechanism predominates for the present temperatures). As expected, NOx are not formed for oxycombustion (100% O_2) condition, however the adiabatic flame temperature is very high (more than 3000K). For a real industrial application, this would require a thermal protection of the combustion chamber walls and of the turbine blades. CO_2 mole fraction slightly increases with O_2 content and pressure but remains too low (about 10%) for an economically favourable application of CO_2 capture by membrane processes. Same trends are observed for the other equivalence ratios.

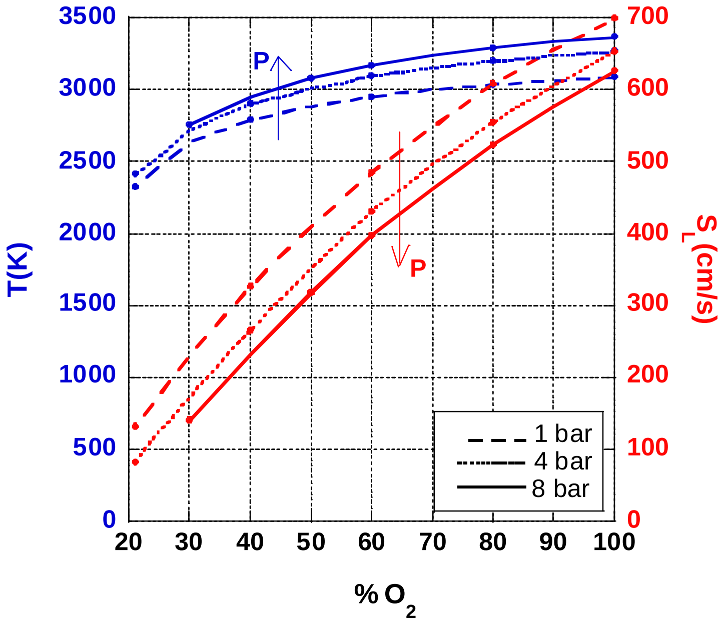

***Figure 3**: Adiabatic flame temperature T (K) and laminar flame velocity S_L ($cm.s^{-1}$) versus the percentage of O_2 in "air" for three different pressures (1, 4 and 8 bar) for a slightly rich CH_4-O_2-N_2 flame (ϕ= 1.1)*
[Pillier et al., 2009]

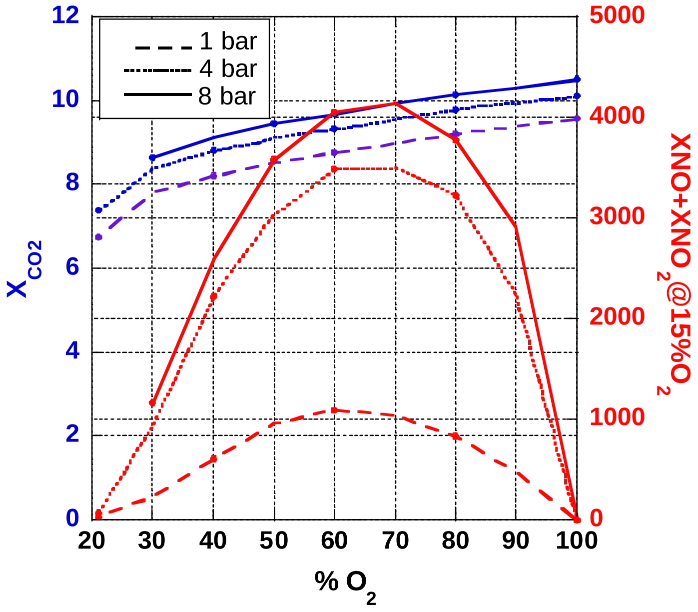

***Figure 4**: CO_2 mole fraction XCO_2 (%) and NOx emissions (X_{NO}+X_{NO2} in ppm@15% O_2 in the exhaust gas) in the burnt gases of a slightly rich CH_4-O_2-N_2 flame (ϕ= 1.1) versus the percentage of O_2 in 'air' for three different pressures (1, 4 and 8 bar) [Pillier et al., 2009]*

1.2.1.2.2. Effect of CO_2 dilution on methane combustion

A possible solution consists in diluting the initial mixture by CO_2 (the captured CO_2 for example or EGR) in order to decrease the combustion temperature and then NOx emissions, as well as to increase the final CO_2 content for capture. The aim is to obtain low NOx emissions that meet current environmental legislations for gas turbines (i.e. ~15 ppm @15% O_2). Figure 5 shows the variations of the laminar flame velocity and the adiabatic flame temperature when the O_2 (from 50 to 100%) and CO_2 (from 0 to 60%) initial contents increase at a pressure of 0.4 MPa and for the slightly rich CH_4-O_2-N_2 flame (ϕ= 1.1). Figure 6 shows the NOx emissions and CO_2 mole fraction in the burnt gases for the same conditions.

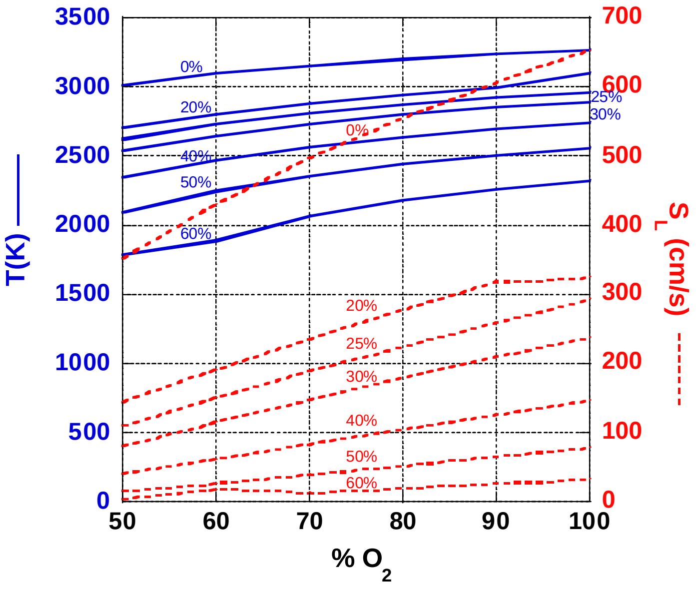

Figure 5*: Adiabatic flame temperature T (K) and laminar flame velocity S_L (cm.s^{-1}) versus the percentage of O_2 in "air" and the CO_2 content in the initial mixture at P= 4 bar for a slightly rich CH_4-O_2-N_2-CO_2 flame (ϕ= 1.1)*
[Pillier et al., 2009]

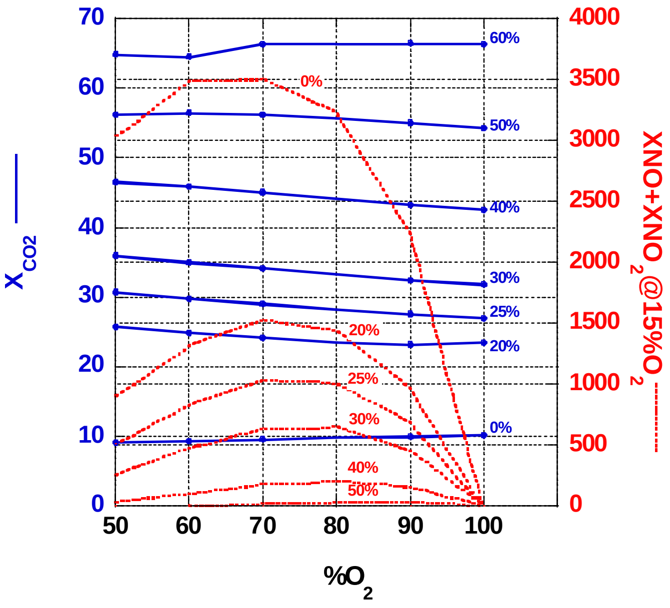

Figure 6*:* CO_2 mole fraction XCO_2 (%) *and NOx emissions (X_{NO}+X_{NO2}) in the burnt gases of a slightly rich CH_4-O_2-N_2-CO_2 flame (ϕ= 1.1) versus the percentage of O_2 in "air" and the CO_2 content in the initial mixture at P= 4 bar.*
[Pillier et al., 2009]

CO_2 dilution plays its expected role: it decreases the adiabatic flame temperature (due to its high heat capacity) and increases the CO_2 content in the burnt gases, which is advantageous for the membrane capture process. However, a high CO_2 dilution (60% CO_2) is necessary to reach the NOx emissions critical value (~15 ppm @15%O_2). In this case, the laminar flame velocity becomes very low (< 20 cm.s^{-1} for 50 to 80% O_2).

This numerical study shows therefore that oxygen-enriched combustion (60-80 % O_2) allows to obtain a high CO_2 content in the exhaust gas while maintaining low NOx emissions if the initial gas is diluted by high quantities of CO_2 (or EGR).

This work allows to build a numerical database with conditions that meet the initial specifications in terms of flame velocity (>10 cm.s^{-1}) and flame temperature (T<1273 K), NOx levels (<15 ppm @ 15% O_2) and CO_2 content in the exhaust gases (> 30% at 0.1 MPa for membrane process). This database was used by LRGP for their CO_2 capture tests.

Publication linked to this work:
Pillier L., de Persis S., Cabot G., Bounaceur R., Liu Y., Boukhalfa A., Most J-M., Gökalp I. and Favre E., Coupling of oxygen-enriched combustion and CO2 capture by membrane processes, 4th European Combustion Meeting (ECM2009) (2009) Vienna, Austria.

1.2.1.2.3. Study of the effect of O_2 enrichment and gas recirculation in a model gas turbine chamber

In this study, our modelling results were compared to experimental results obtained in the model gas turbine chamber, by Gilles Cabot at CORIA.

The experimental setup presented in Figure 7 is an atmospheric scale gas turbine combustion chamber. It is composed of an air−fuel mixture supply line, an axial swirl injector and a transparent combustion chamber to perform optical diagnostics. Detailed information concerning the CORIA burner arrangements is provided in [de Persis et al., 2013; Cabot et al., 2014]. Measurements of O_2, CO_2, NO and CO mole fractions in the burnt gases were performed using gas analysers. The flame structure was characterized by imaging of CH* chemiluminescence and OH Planar Induced Laser Fluorescence (OH-PLIF).

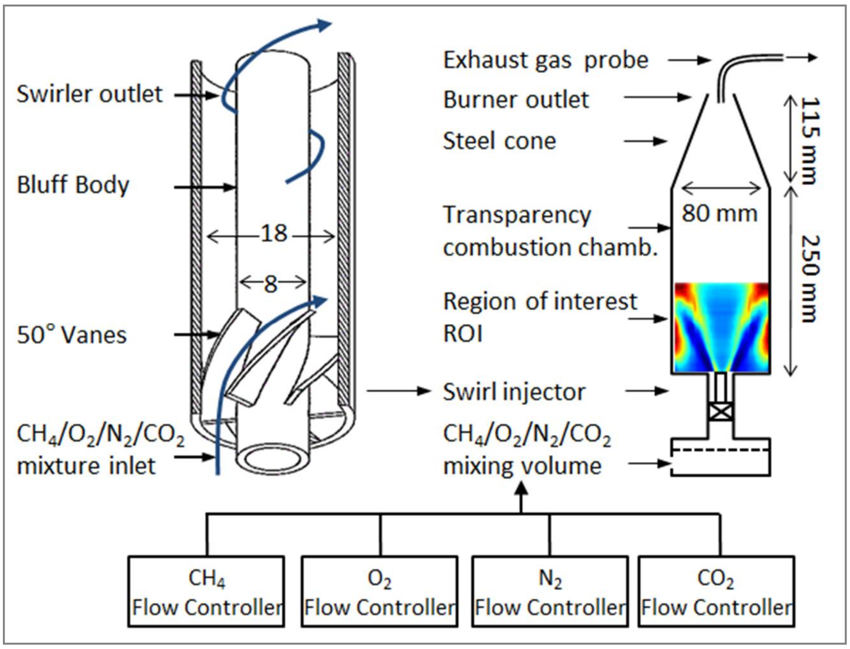

***Figure 7**: Scheme of the burner*
[Cabot et al., 2014]

In this work, measurements and modelling were carried out for exhaust gas recirculation (EGR) conditions, in a first approximation, only composed of CO_2. The Fuel/Oxidant/EGR reactive mixture can be written as follow:

$$1\ CH_4 + 2\ (1+e)\times(1\ O_2 + a\ N_2 + b\ CO_2) \qquad \textit{Equation 1}$$

where a and b are respectively the numbers of moles of N_2 and CO_2 for each mole of O_2 and e is the excess of oxygen.

First, oxygen excess and CO_2 ratio (e and b coefficients of the equation 1) were varied from 0 up to the blow off limit for a=3.78 (air), the inlet pressure and temperature being respectively 0.1 MPa and 300 K and the air mass flow rate was kept constant to 4 $g.s^{-1}$. An example of the evolution of the flame shape as the CO_2 dilution (b) or as the air dilution (e) increases is given in Figure 8. In the two cases, as the dilution increases, the flame structure passes progressively by the four following states: stable anchored flame, stable lifted flame, stable stretched flame and finally extinguished flame. The operability domain of the burner is reported in Figure 9 as a matrix of CH* emission as a function of e and b dilution parameters. On this figure, lines separating the four observed flame structures are drawn; the flame structure transitions were examined by simulations of the laminar flame velocity and adiabatic flame temperature. It was observed that those both flame parameters remain constant on each transition line. For instance, the line separating anchored and lifted flames is located at S_L =11 ±1 cm.s^{-1} and T=1700 ±50 K and the line separating lifted and stretched flames is located at S_L =7 ±0.7 cm.s^{-1} and T=1600 ±50 K.

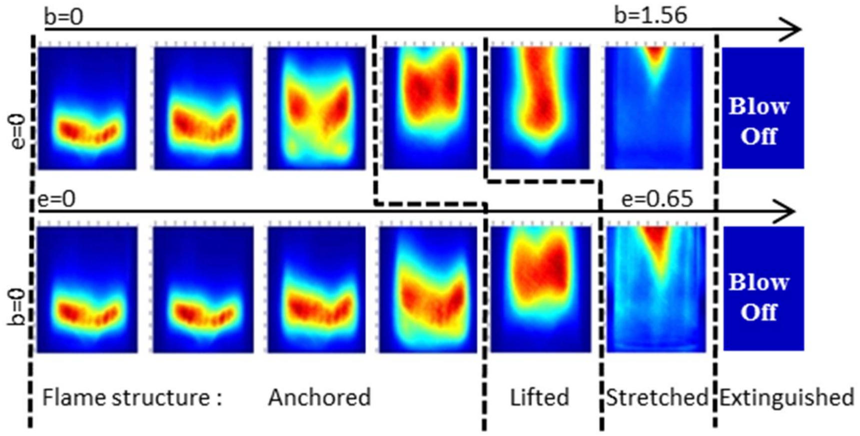

Figure 8: *Example of the evolution of the flame structure as b and e increase from 0 to blow-off limit (inlet condition 0.1 MPa, 300K) [Cabot et al., 2014]*

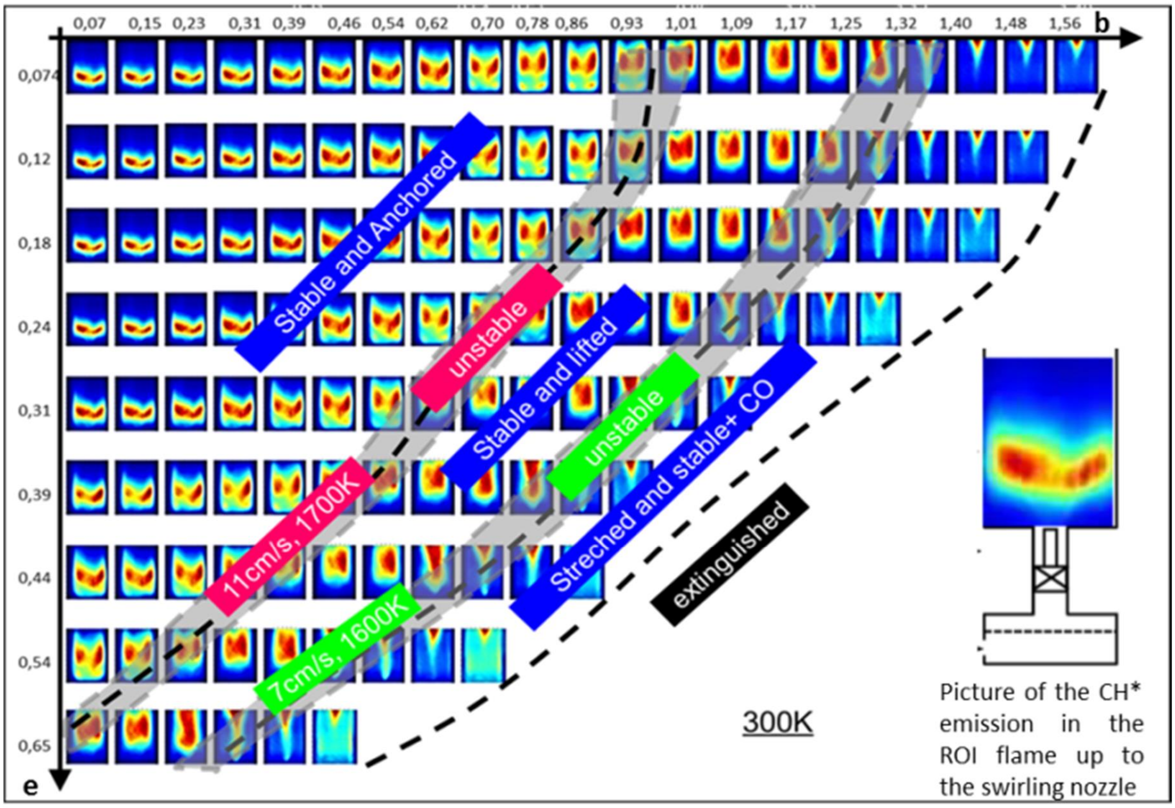

Figure 9 *: Operability domain of the swirl burner (inlet condition 0.1 MPa, 300K) - Evolution of the flame structure (CH* emission, ROI: Region Of Interest) as a function of oxygen excess (e) and CO_2 dilution (b) - Flame structure transition lines [Cabot et al., 2014]*

In Figure 10, NO emissions are reported as a function of the oxygen excess (e) and the CO_2 dilution (b). As expected, the higher dilution with air or CO_2 is, the less NO emissions are. As an example, comparisons between measurements and modelling of NO emissions are shown in Figure 11 for e= 0.244. The level of calculated NO is only 2 times higher than the measured NO and the evolution of NO emission as the CO_2 dilution (b) increases is very well predicted.

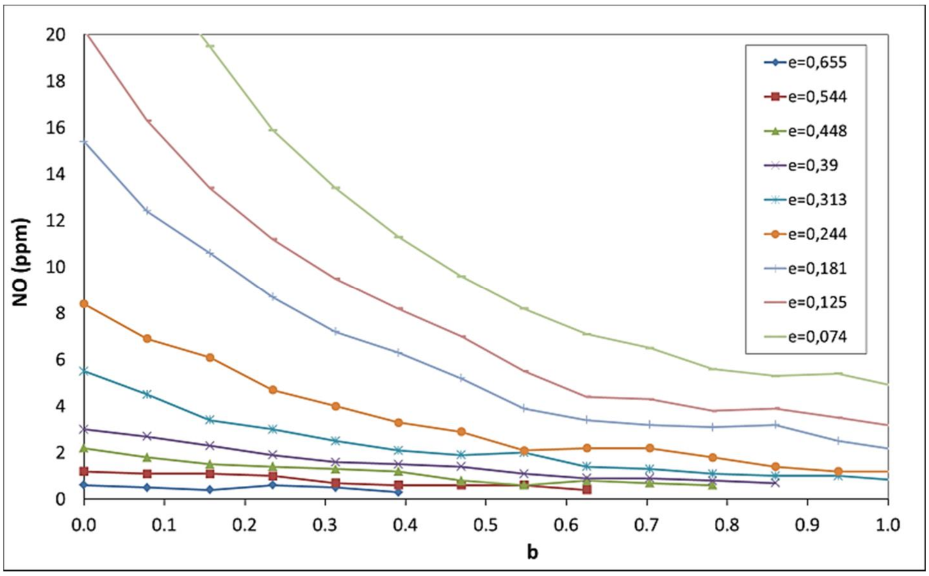

Figure 10 *: NO emissions as a function of CO_2 dilution (b) and oxygen excess (e) [Cabot et al., 2014]*

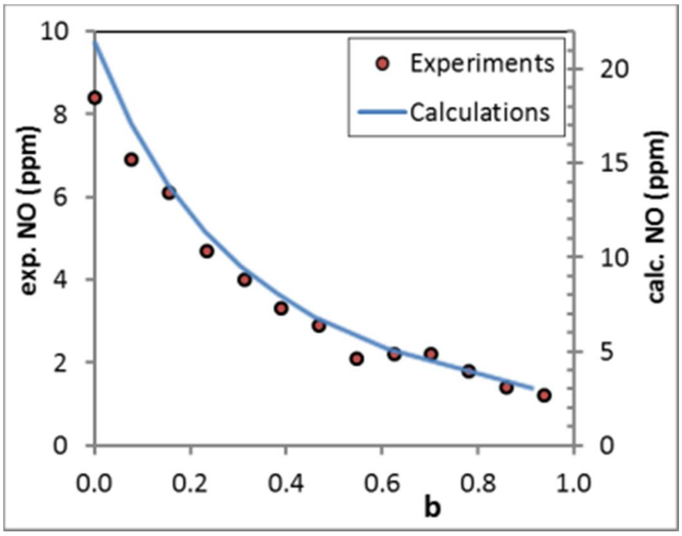

Figure 11 *: Experimental and modeling results of NO emissions (e= 0.244, T=300K) [Cabot et al., 2014]*

Secondly, the experiments for Oxygen Enriched Air (OEA) and CO_2 dilution were performed at constant adiabatic flame temperature. The excess of oxygen e was limited to the smallest acceptable value to ensure a sufficient combustion quality, e was kept constant and equal to 0.1. The O_2, N_2 and CO_2 mass flow rates were appropriately changed in order to keep adiabatic flame temperature at a constant value. To keep flame temperature constant, N_2 was replaced by CO_2. The mole fraction of N_2 (X_{N2}) being an important term in the NO_X production, the results are plotted as a function of X_{N2}:

$$X_{N_2} = \frac{a}{\frac{1}{2(1+e)} + 1 + a + b} \qquad \text{Equation 2}$$

As an example, Figure 12 shows a comparison between measured and calculated NO emissions for the case : e=0.1 and T=1800K, presenting again good predictions of the evolution of NO emissions as CO_2 dilution increases (X_{N2} decreases).

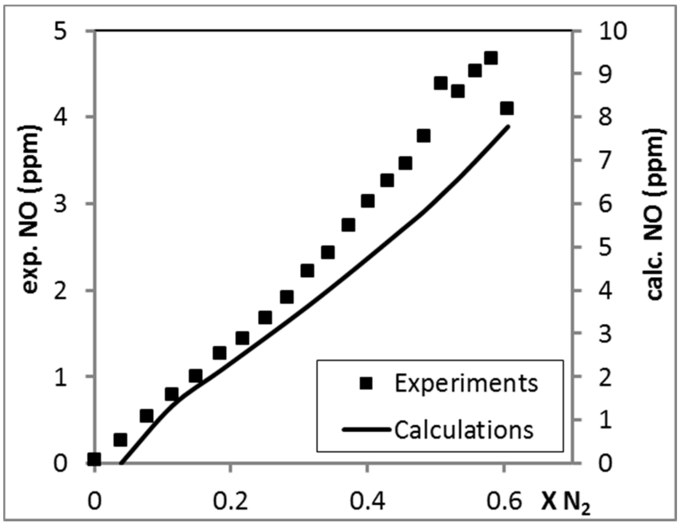

***Figure 12** : Experimental and modeling results of NO emissions as a function of CO_2 dilution (e=0.1, T=1800K) [Cabot et al., 2014]*

This study shows that the combustion with Oxygen Enriched Air (OEA) and Exhaust Gas Recirculation (EGR) can lead to a stable flame without change of actual burners developed for fuel/air combustion (injector and combustion chamber). Moreover, for a constant flame temperature, a decrease of pollutant emissions (NO and CO) was observed when the EGR (CO_2) dilution is increased.

The interesting results obtained during the COCASE project allow starting a larger scale research project involving industrial partners: the ANR project CO_2 Energicapt. This project is presented hereafter.

Publications linked to this work:

Cabot G., Calbry M., Xavier P., Vandel A., de Persis S., Belaissaoui B., Favre E., Pillier L., Effect of CO_2 Capture on Combined Cycle Gas Turbine Efficiency Using Membrane Separation, EGR and OEA Effects on Combustion Characteristics, Proceedings of ASME Turbo Expo 2014: Turbine Technical Conference and Exposition GT2014, Volume 4A, Paper N° GT2014-25781, Dusseldorf, Germany, June 16-20, 2014.

de Persis S., Cabot G., Pillier L., Gökalp I., Boukhalfa A.M., Study of lean premixed methane combustion with CO_2 dilution under gas turbine conditions, Energy and Fuels 27 (2) (2013) 1093–1103.

1.2.2 Coupling combustion-capture applied to an industrial boiler (CO_2 Energicapt project)

1.2.2.1 Context and objectives

The CO_2 Energicapt project (Integration of oxygen-enriched air combustion and CO_2 capture for existing industrial boilers: development of a demonstrator) was a research project funded by the ANR EESI « Efficacité Energétique des Systèmes Industriels » program (2011-2014). The objective was to investigate the technical and energetic integration and the development of a research demonstrator for CO_2 capture by membrane processes in existing industrial boilers, converted to oxygen enriched combustion.

This project included five industrial and academic partners:

Industrial partners

- Leroux & Lotz Technologies LLT (project coordinator): boilers manufacturer
- Compagnie Parisienne de Chauffage Urbain CPCU: district heating company
- Polymem : membranes manufacturer for water treatment

Academic partners

- Laboratoire Réactions et Génie des Procédés LRGP, Nancy
- Institut de Combustion, Aérothermique, Réactivité, Environnement ICARE, Orléans

This project was articulated around five mains tasks :

- The first task concerned the feasibility study of oxygen enriched air combustion in medium power industrial boilers which generate between 25 000 and 100 000 t/year of CO_2, including three aspects:
  - Study of the oxygen enrichment of air by membrane separation (Polymem)
  - Study of the natural gas combustion with oxygen enriched air (ICARE)
  - Thermodynamic study of the effects of oxygen enrichment in natural gas industrial boilers (LLT)

  This work constitutes a database for the sizing step of the boiler demonstrator.

- The second task concerned the CO_2 capture process development (PTFE hollow membranes with Mono Ethanol Amine MEA solvent) and validation in laboratory tests (LRGP)
- The three other tasks concerned mainly the sizing and assembly of the CO_2 capture demonstrator and its integration and validation on the existing boiler in the CPCU site (LLT, CPCU).

In this project, I was involved in the tasks assigned to ICARE, which were:

- The kinetic study of natural gas combustion with oxygen enriched air
- The study of the effect of oxygen enrichment on the dynamics of turbulent diffusion flames with the characterization of the exhaust gas composition

To meet these objectives, the methodology was to consider firstly the combustion of only methane (main component of natural gas) in the laminar regime before studying the turbulent (swirled) regime, which is closer to the existing burner configuration operated at CPCU.

This work [Merlo et al., 2013, 2014] was performed during the PhD of N. Merlo (defended in December 2014) who I co-supervised. The objective of his thesis was the study of the impact of oxygen enrichment on the dynamics and chemistry of methane-oxidant diffusion flames.

1.2.2.2 Main results

A new turbulent flame burner was developed, consisting of two concentric tubes with a swirler placed in an annular part for the oxidant flow (air or oxygen-air) as shown in Figure 13. The central tube delivers the methane through eight holes symmetrically distributed on the periphery of the pipe, just below the burner exit plane. The radial injection of fuel is used to enhance mixing at the near field of the burner exit.

The burner was placed in a square cross-section 25 kW chamber of 48 x 48 cm^2 and 1 m in height (Figure 14) operating at atmospheric pressure. The walls of the combustion chamber are water cooled on the outside and refractory-lined inside. The chamber ends with a convergent section of 20 cm height and a final circular section of 10 cm diameter in order to limit the air intake from the top. Six windows are placed in each face of the chamber, allowing optical access. An oxygen-air mixture is employed as the oxygen-enriched oxidizer flow.

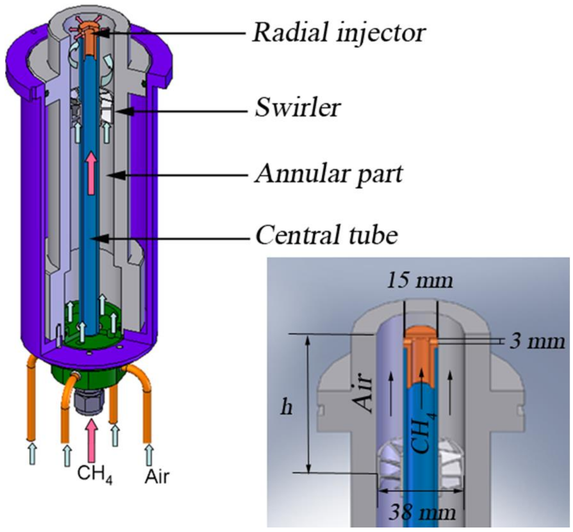

***Figure 13**: Coaxial swirl burner*
[Merlo et al., 2014]

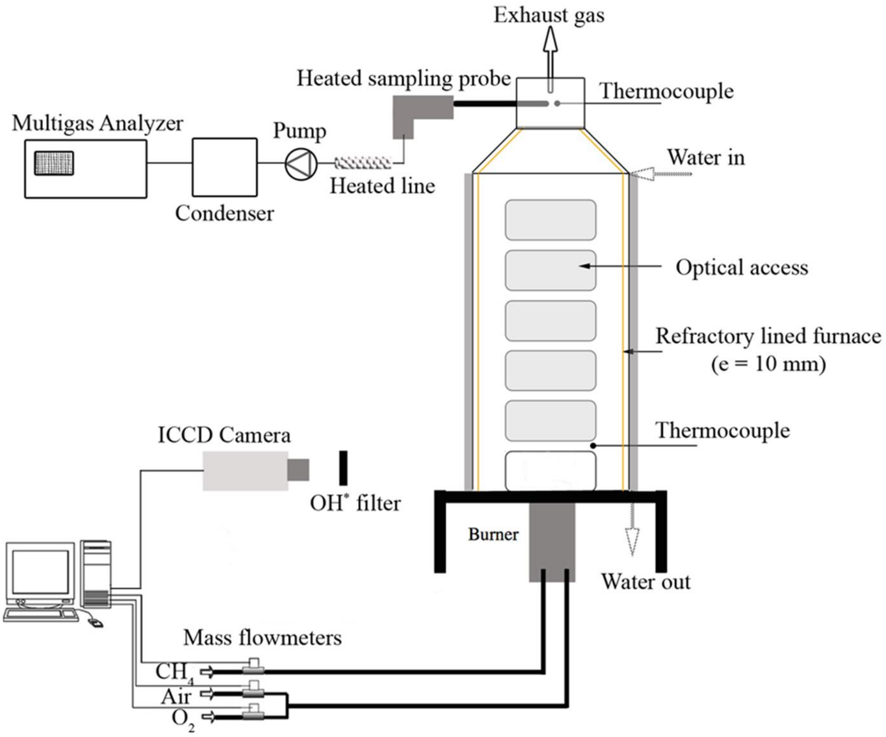

Figure 14: *Schematic view of the experimental set-up*
[Merlo et al., 2014]

The measurements were done for oxygen concentrations ranging from 21 to 30 % in volume, with swirl numbers S_n (ratio between tangential velocity and axial velocity) of 0.8 and 1.4, and for global equivalence ratios of 0.8, 0.9 and 1. Combustion products were sampled using a heated sampling probe and transported with a heated transfer line to prevent condensation of water vapour. Before operating gas measurements, a condenser removes the water vapour contained in the combustion gases; all measurements correspond therefore to dry exhaust gas conditions. Mole fractions of NO_x, CO, CO_2, O_2 and SO_2 were measured by a multi-gas analyzer. OH* chemiluminescence technique was used to visualize the reaction zone and to measure the lift-off heights and flame lengths, and Particle Image Velocimetry (PIV) was used to measure the flow field structures.

To illustrate the effect of O_2 enrichment on flame stability, Figure 15 presents the measured lift-off heights for the two swirl numbers S_n =0.8 and 1.4 (at h=60 mm, distance between the swirler and the burner exit), for a range of oxygen volume fractions from 21 to 30 % and global equivalence ratios ϕ ranging from 0.8 to 1. For all cases, an increase in oxygen enrichment leads to a decrease in lift-off heights, showing that oxygen enrichment extends the flammability limits.

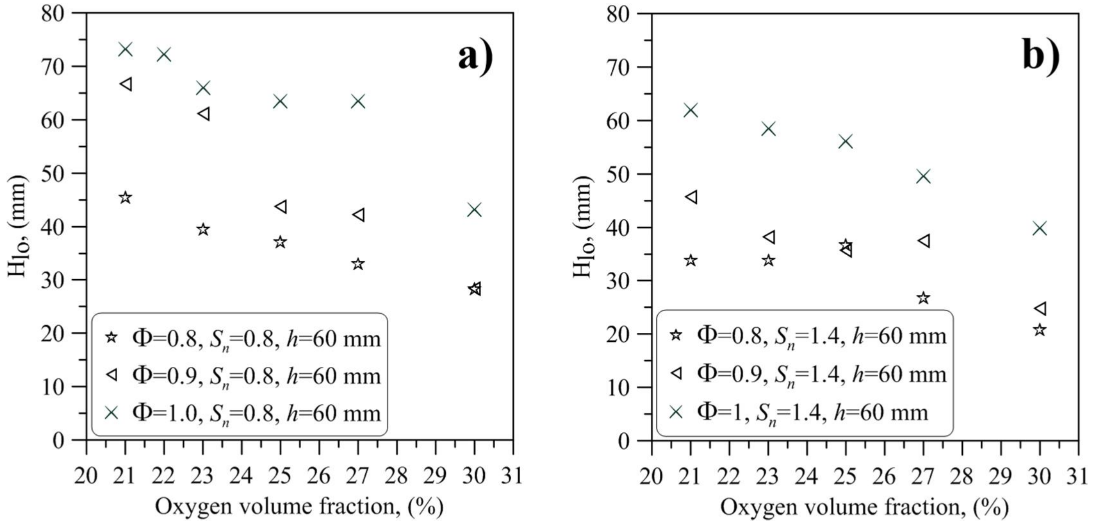

Figure 15*: (a) Lift-off height with oxygen addition for 3 global equivalence ratios 0.8, 0.9 and 1*
(a) S_n = 0.8 at h= 60 mm and (b) S_n = 1.4 at h= 60 mm
[Merlo et al., 2014]

Concerning pollutants emission, Figures 16 to 18 show CO, CO_2 and NOx emissions respectively, as a function of oxygen enrichment from 21 to 30 %, for the three global equivalence ratios (ϕ=0.8, 0.9, 1) and the two swirl numbers (0.8 and 1.4). Figures 16 (a) and (b) illustrate that CO emissions decrease drastically with oxygen enrichment. Oxygen enrichment enhances CO conversion to CO_2. In the case of a swirl number of 1.4, CO emissions are slightly lower than for 0.8 mainly for oxygen addition lower than 25 %. Swirl intensity tends to improve the mixing and to increase the residence time inside the reaction zone promoting the CO conversion to CO_2.

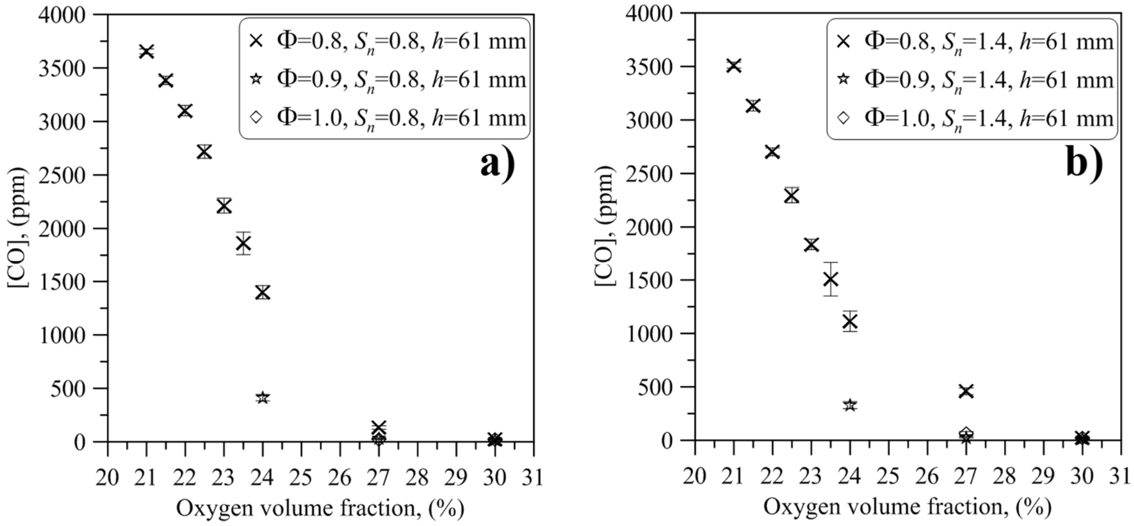

Figure 16*: CO emission with oxygen enrichment for ϕ = 0.8, 0.9 and 1*
(a) S_n = 0.8 at h = 61 mm and (b) S_n = 1.4 at h = 61 mm [Merlo et al., 2014]

The latter trends are coherent with CO_2 emissions shown in Figure 17. CO_2 increases quasi-linearly with oxygen enrichment. For a global equivalence ratio of 0.8, CO_2 concentration increases by a factor of 1.5 between 21 % and 30 % of oxygen. Increasing the global equivalence ratio tends to promote the CO_2 formation. These linear CO_2 evolutions can be explained considering complete methane combustion in air and in oxygen-enriched air as shown in equation 3:

$$[CO_2]_{Complete} = \frac{\phi.[O_2]}{2-\phi[O_2]} \qquad \textit{Equation 3}$$

CO_2 predictions for a complete combustion are also represented in Figure 17, they are always slightly higher than the measurements since the CO conversion to CO_2 is never completed. With the increase of swirl intensity, CO_2 emissions are closer to complete combustion predictions which support the idea that increasing swirl intensity leads to improve the mixing.

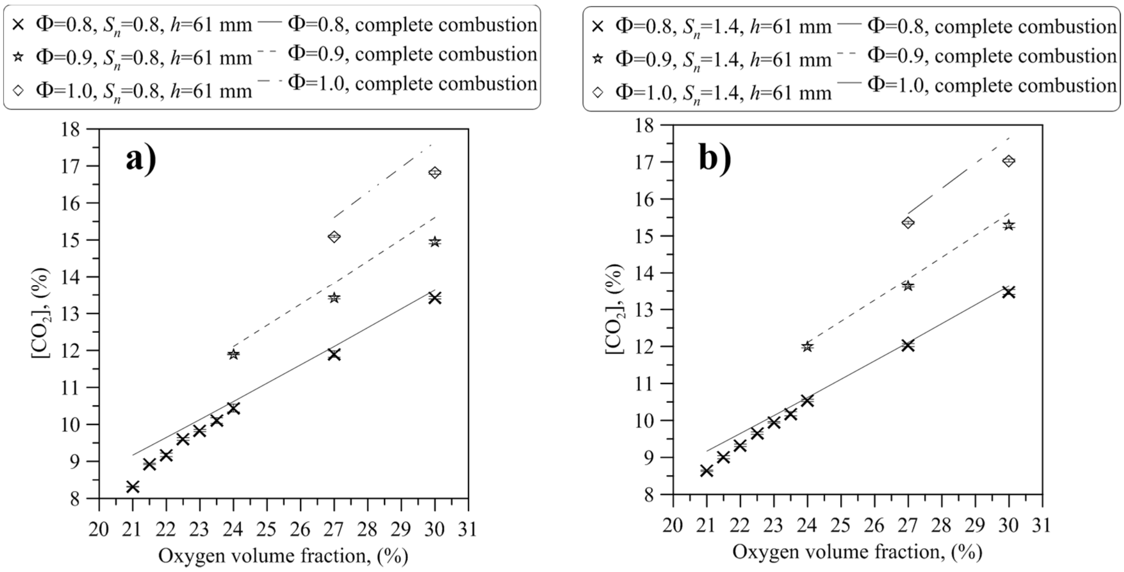

***Figure 17**: CO_2 emission with oxygen enrichment for ϕ = 0.8, 0.9 and 1*
(a) S_n = 0.8 at h = 61 mm and (b) S_n = 1.4 at h = 61 mm.
[Merlo et al., 2014]

NO_x emissions, shown in Figure 18, largely increase when oxygen enrichment increases. Indeed, when the oxygen enrichment rate increases from 21 to 30 %, NO_x emissions increases from 10 to 170 ppm with a global equivalence ratio of 0.8 and a swirl number of 0.8. Increasing the swirl number tends to reduce the NO_x production in particular for oxygen content greater than 27 %. Assuming that

NO_x production is mainly described by the formation of NO via the thermal-NO mechanism, the temperature of the NO_x formation zone in flames decreases with increasing the swirl intensity.

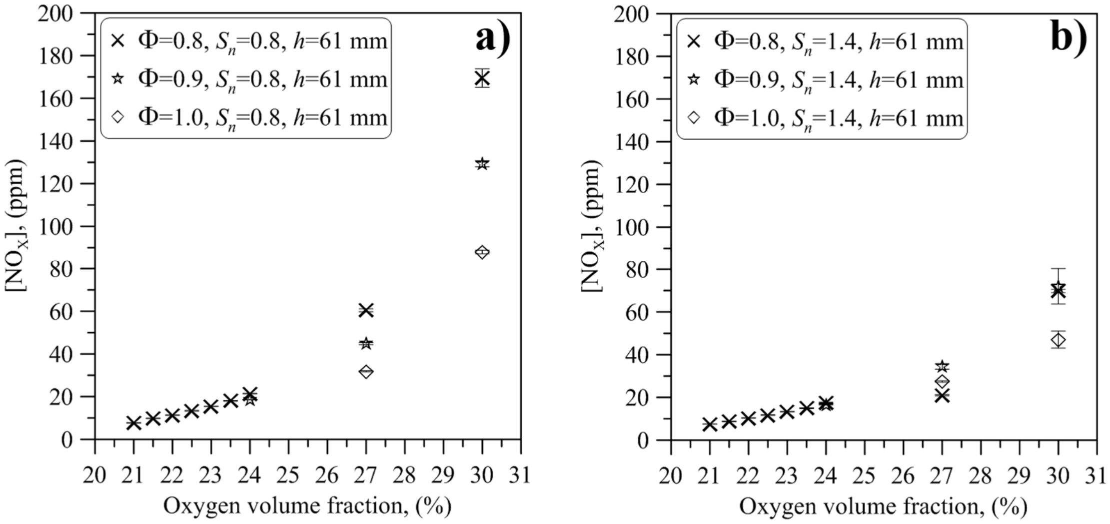

***Figure 18**: NO_x emission with oxygen enrichment for ϕ = 0.8, 0.9 and 1*
(a) S_n = 0.8 at h = 61 mm and (b) S_n = 1.4 at h = 61 mm.
[Merlo et al., 2014]

To resume, the main results obtained in this work can be summarized as follows:

1. Oxygen enrichment promotes higher CO conversion into CO_2; CO_2 concentrations increase linearly with oxygen addition.
2. NO_x emissions increase strongly with oxygen addition mainly due to the increase of the flame temperature (Thermal-NO formation).
3. Flame stability is enhanced with oxygen addition even for low oxygen enrichment rates.
4. Flame lift-off heights and its fluctuations largely decrease with oxygen addition.
5. Increasing the degree of swirl promotes flame stabilization.

More generally, the project CO_2 Energicapt was successful as the demonstrator was integrated on the existing boiler at CPCU and tests showed that it effectively captures CO_2, with a rate of 85% of CO_2 captured for an exhaust gas flow rate of 12 $Nm^3.h^{-1}$.

This project won the **« *Trophée de la recherche publique Energie-Environnement-Climat* » in 2015.**

Publications linked to this work:

Merlo N., Boushaki T., Chauveau C., de Persis S., Pillier L., Sarh B., Gökalp I., Experimental study of oxygen enrichment effects on turbulent non-premixed swirling flames, Energy and Fuels 27 (10) (2013) 6191-6197.

Merlo N., Boushaki T., Chauveau C., de Persis S., Pillier L., Sarh B., Gökalp I., Combustion Characteristics of Methane-oxygen Enhanced Air Turbulent Nonpremixed Swirling Flames, Experimental Thermal and Fluid Science 56 (2014) 53–60.

1.2.3. Effect of O_2 enrichment and CO_2 dilution on laminar methane flames velocities

In the framework of my research activities on oxygen enriched air combustion, I undertook a collaboration project with F. Foucher from the Prisme laboratory (Laboratoire Pluridisciplinaire de Recherche en Ingénierie des Systèmes et Mécanique Energétique) in Orléans, focused on the study of the effects of O_2 enrichment and CO_2 dilution on laminar methane flames velocities.

In this work, laminar flame velocities of CH_4-O_2-N_2-CO_2 mixtures were measured using the shadowgraphy technique in a spherical combustion chamber at atmospheric pressure at Prisme laboratory. The ratio $X(O_2)/(X(O_2)+X(N_2))$ was varied from 0.21 to 1.0 and the mole fraction of CO_2 in the mixture was varied from 0 to 0.4, for an equivalence ratio of 0.7 and an initial temperature of 300K. Experimental uncertainty for laminar flame velocity was about ± 3 cm/s. Laminar flame velocities were calculated using the PREMIX code [Kee et al., 1985] and the GRImech3.0 mechanism [Smith et al., 1999]. The procedure proposed by Liu et al. [Liu et al., 2003] was adopted to compare the thermal or chemical effect of CO_2 addition by introducing a fictitious additive "FCO_2" which has the same thermochemical and transport properties as the normal CO_2 but it is not consumed or produced in the reaction mechanism. It is included in the list of third-body species with the same collision efficiencies as CO_2.

Figure 19 shows the comparison between experimental and calculated laminar flame velocities for CH_4-O_2-N_2-CO_2 mixtures as a function of the ratio $O_2/(O_2+N_2)$ for three different volume fractions of CO_2 in the mixture: 0% (in black), 29% (in red) and 40% (in green). For comparison, experimental results from the literature [Mazas, 2010; Han et al., 2007; Jahn, 1934; Oh and Noh, 2012] are also plotted.

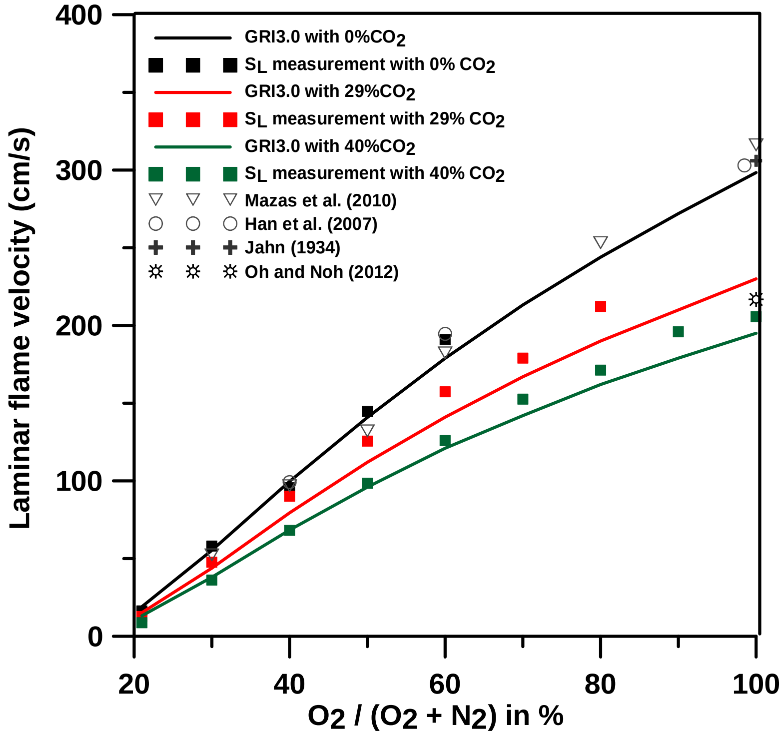

***Figure 19**: Comparison between experimental (symbols) and calculated (lines) laminar methane flame velocities as a function of the ratio $O_2/(O_2+N_2)$ for three volume fractions of CO_2 in the mixture: 0% (in black), 29% (in red) and 40% (in green) for an equivalence ratio of 0.7, a temperature of 300K and a pressure of 0.1MPa.*

Experimental uncertainty for S_L= ± 3 cm/s

[de Persis et al., 2013]

As expected, the laminar flame velocity increases when the ratio $O_2/(O_2+N_2)$ increases and it decreases with increasing CO_2 dilution. The results presented here show a very good agreement between our experiments, experiments from the literature and modelling in CH_4-O_2-N_2 mixtures without CO_2 dilution (black symbols and lines in Fig. 19). However, laminar flame velocities are underestimated by modelling using the GRImech3.0 mechanism when the mixture is diluted with CO_2 (29 % and 40 % of CO_2) and the differences between experiments and modelling increase as the ratio $O_2/(O_2+N_2)$ increases. Those results are in agreement with Han et al. (2007) and Mazas (2010) who found that the GRImech3.0 mechanism underestimates the laminar flame velocities of oxygen enriched methane flames with or without CO_2 dilution.

In order to determine if CO_2 has a simple thermal effect or a chemical effect, calculations with fictitious CO_2 ("FCO_2") were performed using the methodology proposed by Liu et al. [2003] for the CH_4-O_2-N_2-CO_2 flames with CO_2 volume fractions of 29% and 40%. The results are shown in Figure 20. It shows differences between calculated laminar flame velocities with and without FCO_2 and those differences increase when the ratio $O_2/(O_2+N_2)$ increases. It demonstrates that CO_2 has a chemical effect, which increases with the ratio $O_2/(O_2+N_2)$ and CO_2 addition. The reaction responsible for the chemical effect of CO_2 is $CO_2+H=CO+OH$ which competes for H atoms consumption with O_2 ($H+O_2=O+OH$) which is the main branching reaction in high temperature combustion [Glarborg and Bentzen, 2008].

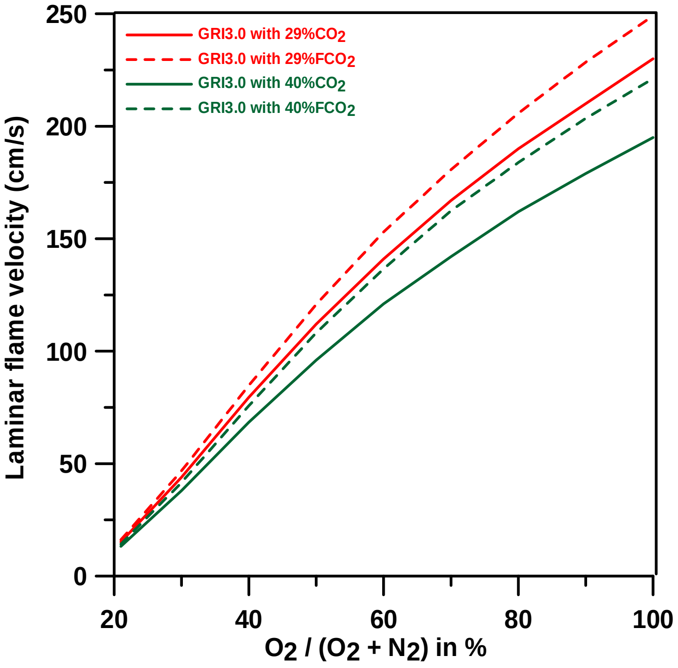

***Figure 20**: Comparison between calculated laminar flame velocities obtained using the GRI3.0 mechanism with CO_2 (line) and with FCO_2 (dashed line) for an equivalence ratio of 0.7, for 29% and 40 % of CO_2 in the mixture, as a function of the ratio $O_2/(O_2+N_2)$ [de Persis et al., 2013]*

Publication linked to this work:
de Persis S., Foucher F., Pillier L., Osorio V., Gökalp I. , Effect of O_2 enrichment and CO_2 dilution on laminar methane flames, Energy 55 (2013) 1055-1066.

A2. Combustion kinetics of biomass fuels: biogas and syngas

In this second part, my research activities concerning the combustion in biogas/air and syngas/air flames at atmospheric and high pressure are presented.

2.1. Context and objectives

The depletion of fossil resources, along with growing awareness regarding the impacts of human activities on climate, has motivated the intensification of research on cleaner alternative energy sources. In this context, renewable biomass fuels represent an interesting solution as they allow the reduction of pollutants emissions in the atmosphere.

Syngas (or synthesis gas) is a mixture composed mainly of hydrogen and carbon monoxide, it can be used for hydrogen production, electricity production or for chemical products synthesis. Syngas sources are very varied and omnipresent in nature: syngas can be produced from gasification of natural gas, coal, gasoline, biomass or organic wastes [Lee et al., 1996; Kwak et al., 2006; Richards et al., 2009]. In Integrated Gasification Combined Cycle (IGCC) power plants, syngas is mainly produced from gasification of coal or biomass [Brdar and Jones, 2000] and it is then burnt in a gas turbine. Syngas composition can be very variable (Table 1) as it will depend on the production mode and syngas sources, CO_2 concentration can reach 30%.

Syngas	PSI	Tampa	El Dorado	Pernis	Sierra Pacific	ILVA	IBIL	Schwarze Pumpe	Sarlux	Fife	Exxon Singapore
H_2	24.8	27.0	35.4	34.4	14.5	8.6	12.7	61.9	22.7	34.4	44.5
CO	39.5	35.6	45.0	35.1	23.6	26.2	15.3	26.2	30.6	55.4	35.4
CH_4	1.5	0.1	0.0	0.3	1.3	8.2	3.4	6.9	0.2	5.1	.5
CO_2	9.3	12.6	17.1	30.0	5.6	14.0	11.1	2.8	5.6	1.6	17.9
N_2 + AR	2.3	6.8	2.1	0.2	49.3	42.5	46.0	1.8	1.1	3.1	1.4
H_2O	22.7	18.7	0.4	–	5.7	--	11.5	–	39.8	--	.1
LHV, - Btu/ft^3	212	202	242	209	127	193	115	318	163	322	242
- kJ/m^3	8350	7960	9535	8235	5000	7600	4530	12,520	6420	12,690	9,530
T_{fuel}, F/ C	570/300	700/371	250/121	200/98	1000/538	400/204	1020/549	100/38	392/200	100/38	350/177
H_2/CO Ratio	.63	.75	.79	.98	.62	.33	.83	2.36	.74	.62	1.25
Diluent	Steam	N_2/H_2O	N_2/Steam	Steam	Steam	--	--	Steam	Moisture	Water	N_2/Steam
Equivalent LHV											
- Btu/ft^3	150	118	113*	198	110**	--	115	200	--	*	116
- kJ/m^3	5910	4650	4450	7800	4334	--	4500	7880	--	--	4600

* Always co-fired with 50% natural gas
** Minimum range

GT25217B

***Table 1**: Example of Syngas composition variability for General Electric gas turbines operating on refinery residues [*Brdar and Jones, 2000*]*

Biogas is a mixture composed mainly of methane and carbon dioxide. Depending of its sources, it can contain variable quantities of water, nitrogen, oxygen, hydrogen sulphide, aromatic traces or organohalogen compounds (Table 2). Biogas is produced by anaerobic fermentation of animal or vegetal organic matter under the action of some bacteria. Due to its high concentration of CO_2, biogas combustion is different from natural gas combustion. Indeed, the presence of CO_2 leads to the decrease of flame parameters like temperature, flame velocity and flame stability domain.

Biogas	CH_4 (%)	CO_2 (%)	O_2 (%)	N_2 (%)	H_2S (ppm)	Benzene (mg m^{-3})	Toluene (mg m^{-3})
Landfill	47–57	37–41	<1	<1–17	36–115	0.6–2.3	1.7–5.1
Sewage digester	61–65	36–38	<1	<2	b.d.	0.1–0.3	2.8–11.8
Farm biogas plant	55–58	37–38	<1	<1–2	32–169	0.7–1.3	0.2–0.7
Landfill	59.4–67.9	29.9–38.6	n.a.	n.a.	15.1–427.5	21.7–35.6	83.3–171.6
Landfill	37–62	24–29	<1	n.a.	n.a.	<0.1–7	10–287
Landfill	55.6	37.14	0.99	n.a.	n.a.	3.0	55.7
Landfill	44	40.1	2.6	13.2	250	n.a.	65.9
Sewage digester	57.8	38.6	0	3.7	62.9	n.a.	n.a.
Sewage digester	62.6	37.4	n.a.	n.a.	n.a.	n.a.	n.a.
Sewage digester	58	33.9	0	8.1	24.1	n.a.	n.a.

b.d.—Below detection limit 0.1 ppm. n.a.—not analysed.

***Table 2**: Composition of biogas from different biogas production plants [Rasi et al., 2007]*

Part A2: Combustion kinetics of biomass fuels: biogas and syngas

A precise understanding of the combustion kinetics of syngas and biogas, in conditions close to industrial applications; i.e. at atmospheric and high pressure, is essential to control energy production and pollutants emission.

In this context, my scientific approach was as follow:

- First, my work has consisted in the study of flame structure of mixtures representative of syngas: H_2-CO-air and biogas: CH_4-CO_2-air. The experimental study was dedicated to the chemical species analysis in flames stabilised on a flat flame burner at atmospheric pressure using GC and FTIR, as well as Laser Induced Fluorescence measurements. The experimental species profiles were then compared to flame modelling with different mechanisms using the PREMIX code [Kee et al., 1985].
- Meanwhile, an experimental setup allowing measurements of laminar flame velocity (methane and syngas) in a counterflow burner using the PIV technique at atmospheric pressure, was developed during the PhD of N. Bouvet (defended in December 2009), in collaboration with C. Chauveau and I. Gökalp at ICARE.
- The final aim was to widen the experimental database at higher pressure. In that purpose, I have developed an experimental device for stabilisation of counterflow laminar flames at high pressure (0.1-1MPa), during the PhD of A. Matynia (defended in April 2011).

2.2. Syngas and biogas flames structure at atmospheric pressure

2.2.1. Experimental setup

The flames were stabilized on a flat-flame burner at atmospheric pressure (Figure 21). The upper part of the burner was made of a brass disc with small holes (0.7 mm diameter) drilled on a 4.1 cm diameter circular area. A stabilisation grid (perforated plate) was located 1 cm above the burner surface to reduce heat exchanges between the flame and the burner and move the flame downstream.

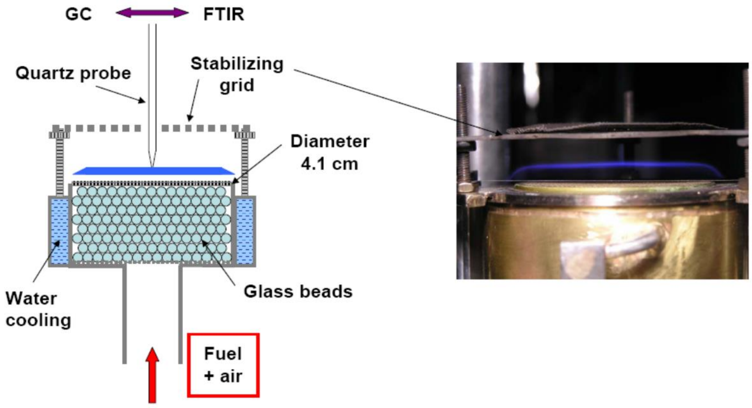

Figure 21*: Experimental setup for flame structure measurements at atmospheric pressure*

Gas samples were withdrawn along the symmetry axis of the flame by a quartz-microprobe (500 μm diameter quartz tube drawn to a cone at the end). A hole (100 μm diameter) was drilled at the tip of this cone. Gaseous samples withdrawn from the flame were analysed either by GC or by FTIR. For GC analyses, the gaseous samples were stored in Pyrex flasks at low pressure (2.0 kPa maximum) and compressed by a home-made piston up to 53 kPa prior to injection into the chromatograph. Gaseous samples were collected directly in the FTIR cell up to 3.3 kPa. Stable species analysed by GC were CH_4, C_2H_4, C_2H_2, C_2H_6, CO, CO_2, CH_3CHO, H_2, O_2 and N_2. CH_2O and H_2O were measured by FTIR. Species calibration was performed by using gaseous mixtures of known compositions. The accuracy was estimated to be ± 5% for CO_2, CO, H_2, O_2 and N_2 and C_1 and C_2 hydrocarbons, ± 10% for H_2O and ± 20% for CH_2O and CH_3CHO. These deviations correspond to the inaccuracies resulting from sampling pressure measurements and GC or FTIR reproducibility.

The temperature of the burnt gases was measured in each flame by a Pt/Pt-10%Rh thermocouple constructed with thin wires (50 µm diameter) tightened parallel to the burner surface and coated with a BeO-Y_2O_3 deposit to reduce catalytic effects [Kent, 1970]. The measured temperatures were increased by 12% to compensate radiative heat losses. This factor was determined in previous experiments [Biet et al., 2005] where heat losses were measured by means of the electrical compensation technique [Bonne et al., 1960]. To measure the temperature through the flame zone, the sampling probe was used as a pneumatic temperature-measuring device (choked flow) by determining the rate of gas flow into a known volume as a function of the probe position in the flame. This technique has been previously used by Kaiser et al. (2000).

2.2.2. Main results

2.2.2.1. Syngas flames

In this work, two flames were studied (Table 3): a CO-H_2-air flame and a CO-H_2-CO_2-air flame in lean conditions (ϕ=0.6), CO_2 was added to the syngas flame to investigate its influence on flame structure as CO_2 concentration can be important in syngas.

Syngas flames		
	CO-H_2-air	**CO-H_2-CO_2-air**
ϕ	0.6	0.6
α	0.15	0.15
β	0	0.5
X_{CO}	0.171	0.146
X_{H_2}	0.030	0.026
X_{CO_2}	/	0.146
X_{Air}	0.799	0.682

***Table 3**: Syngas flames conditions (X: mole fraction)*

$$\alpha = \frac{X_{H_2}}{X_{CO} + X_{H_2}} \quad \text{and} \quad \beta = \frac{X_{CO_2}}{X_{CO} + X_{CO_2}}$$

By comparing the experimental profiles of the major species in the CO-H_2-air and CO-H_2-CO_2-air flames (Figure 22), we can notice that the gradient of concentration is less important in the flame diluted with CO_2 and the flame is shifted forward. This difference attests to a decrease of the reactivity (and flame velocity) which can be attributed to thermal, transport, radiative or chemical effects of CO_2 in the flame [Liu et al., 2003]. The temperature of the burnt gases in both flames were also measured with T= 1910 ± 70 K in the CO-H_2-air flame and T= 1610 ±70 K in the flame diluted with CO_2.

The experimental results were compared with simulated species profiles using the PREMIX code and the mechanism developed by Li et al. (2007) for syngas combustion (also shown in Fig.22). A kinetic analysis was then performed (pathways analysis), showing that the chemical effect of CO_2 is limited in our flame conditions, the decrease of reactivity was mainly attributed to thermal effect due to the higher heat capacity of CO_2.

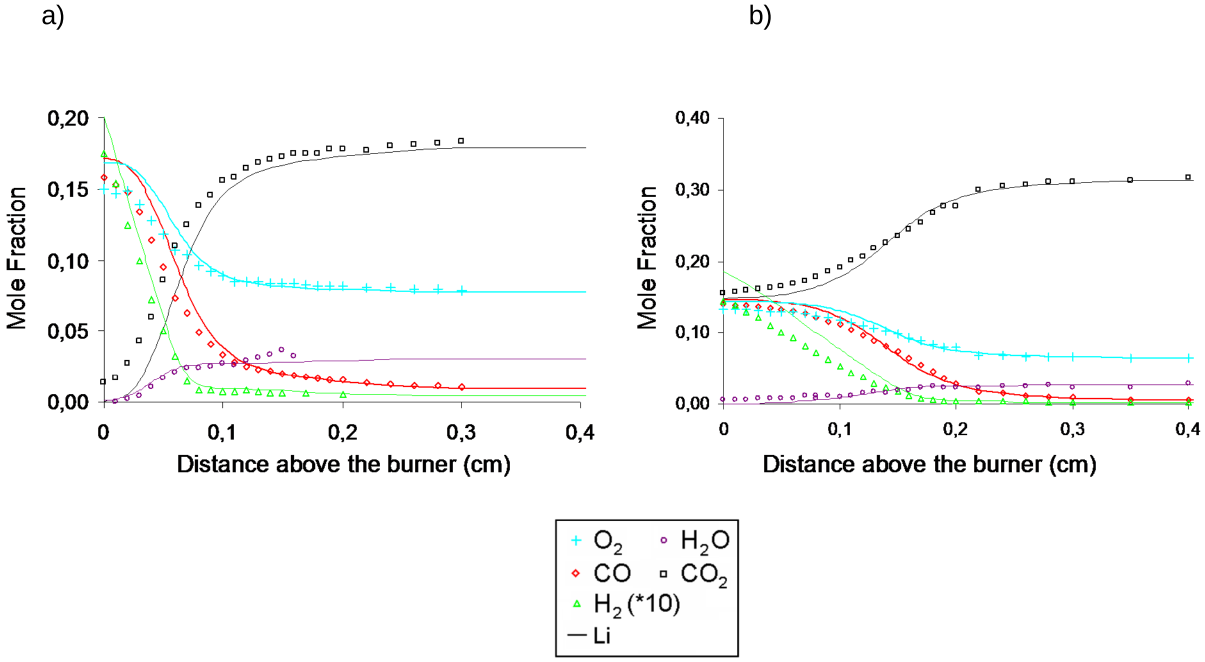

Figure 22*: Experimental and simulated major species profiles in the flames (a) CO-H2-Air, ϕ=0.6, α=0.15, β=0 and (b) CO-H2-CO2-Air, ϕ=0.6, α=0.15, β=0.5*

2.2.2.2. Biogas flames

In this case, we have studied the effect of CO_2 addition to methane flames as well as water addition. Six premixed flames were stabilized on the flat flame burner described above, at atmospheric pressure, and were studied experimentally and by modelling: three lean flames with equivalence ratio maintained constant at ϕ= 0.7: CH_4-air (flame 1a), CH_4-CO_2-air (flame 2a) and CH_4-H_2O-air (flame 3a), and three rich flames with equivalence ratio maintained at ϕ= 1.4: CH_4-air (flame 1b), CH_4-CO_2-air (flame 2b) and CH_4-H_2O-air (flame 3b). The ratios $[CO_2]/[CH_4]$ and $[H_2O]/[CH_4]$ were kept equal to 0.4 for both flames series. Table 4 lists the initial conditions for these flames.

Mole Fractions	Flame 1a CH_4-air	Flame 2a CH_4-CO_2-air	Flame 3a CH_4-H_2O-air	Flame 1b CH_4-air	Flame 2b CH_4-CO_2-air	Flame 3b CH_4-H_2O-air
CH_4	0.0683	0.0665	0.0665	0.1279	0.1217	0.1217
CO_2	/	0.0266	/	/	0.0487	/
H_2O	/	/	0.0266	/	/	0.0487
Air	0.9317	0.9069	0.9069	0.8721	0.8296	0.8296
ϕ	0.7	0.7	0.7	1.4	1.4	1.4

***Table 4**: Initial conditions of the lean and rich CH_4-air, CH_4-CO_2-air and CH_4-H_2O-air flames. P = 0.1 MPa, T_0= 298 K*

The flames structures were simulated using the PREMIX code and four detailed combustion mechanisms were used to simulate the laminar flame velocity, temperature and species mole fraction profiles: the GRImech3.0 mechanism [Smith et al., 1999], the mechanism developed by Dagaut et al. (2005), the 2005 version of the mechanism developed at the University of California, San Diego (UCSD) and the GDFkin®3.0 mechanism [El Bakali et al., 2006]. Detailed results are presented in [Matynia et al., 2009].

The comparison between experiments and modelling showed that the four mechanisms are able to reproduce the major species profiles (CH_4, O_2, CO_2, H_2O, CO and H_2) at both equivalence ratios and the evolution when CO_2 or H_2O are added to the flame, however discrepancies are noticed for the C_2 minor intermediates (C_2H_2, C_2H_4, C_2H_6).

In the lean flames, dilution by CO_2 or H_2O decreases the maximum mole fractions of CO, H_2 and C_2 intermediates (Table 5). In the rich flames, the CO_2 addition slightly increases the CO mole fraction in the burnt gases but decreases the H_2 and C_2 species mole fractions. However, H_2O addition produces only weak variations of the CO, H_2 and C_2 species mole fractions. NO mole fractions were also calculated showing that the addition of CO_2 and H_2O reduces the NO mole fraction by respectively 28% and 23% for the lean flame, and 58% and 54% for the rich flames.

The influence of CO_2 and H_2O on laminar flame velocity and temperature was also investigated in this work, results are presented in [Matynia et al., 2009].

Publication linked to this work:
Matynia A., Delfau J.L., Pillier L., Vovelle C., Comparative study of the influence of CO_2 and H_2O on the chemical structure of lean and rich methane/air flames at atmospheric pressure" , Combustion, Explosion and Shock Waves, 45 (6) (2009) 635-645.

Maximum Mole Fractions	Flame 1a CH_4-air	Flame 2a CH_4-CO_2-air	Flame 3a CH_4-H_2O-air	Flame 1b CH_4-air	Flame 2b CH_4-CO_2-air	Flame 3b CH_4-H_2O-air
CO	$1.8x10^{-2}$	$1.6x10^{-2}$	$1.3x10^{-2}$	$7.2x10^{-2}$	$7.6x10^{-2}$	$6.4x10^{-2}$
H_2	$5.1x10^{-3}$	$2.8x10^{-3}$	$3.4x10^{-3}$	$6.1x10^{-2}$	$4.4x10^{-2}$	$7.1x10^{-2}$
C_2H_6	$4.2x10^{-4}$	$3.2x10^{-4}$	$2.6x10^{-4}$	$1.3x10^{-3}$	$1.2x10^{-3}$	$1.1x10^{-3}$
C_2H_4	$2.3x10^{-4}$	$1.8x10^{-4}$	$1.5x10^{-4}$	$1.6x10^{-3}$	$1.5x10^{-3}$	$1.5x10^{-3}$
C_2H_2	$3.5x10^{-5}$	$2.5x10^{-5}$	$2.0x10^{-5}$	$2.4x10^{-3}$	$1.8x10^{-3}$	$2.3x10^{-3}$

***Table 5**: Experimental maximum mole fractions in the lean and rich CH_4-air, CH_4-CO_2-air and CH_4-H_2O-air flames*

2.3. Methane and biogas flames structure at high pressure

The laminar flame structure study is a powerful tool for the analysis and the development of kinetic combustion mechanisms. However, such studies are generally carried out on circular flat flame burner (McKenna burner) at sub-atmospheric and atmospheric pressures. Indeed, at high pressure, the flamefront sits extremely close to the burner and it becomes impossible to obtain experimental profiles of temperature and species concentration through the flamefront. Furthermore, the important reduction of the flamefront thickness when pressure increases almost prevents the use of intrusive techniques such as probe sampling and it becomes necessary to resort to non-intrusive optical diagnostics. Counterflow burners constitute an ideal configuration to overcome those problems. This alternative configuration allows the drifting of the flames away from the burner while keeping a 1D structure along the symmetrical axis of the burner (Figure 23). Moreover, this experimental device permits to obtain nearly adiabatic flames as those ones are stabilized far from the burner nozzles (reducing heat losses to the burner) by aerodynamic strain along a stagnation plane. In the case of twin premixed flames, both flamefronts are stabilized far from the burner nozzles, which allows species and temperature profiles measurements along the flame axis.

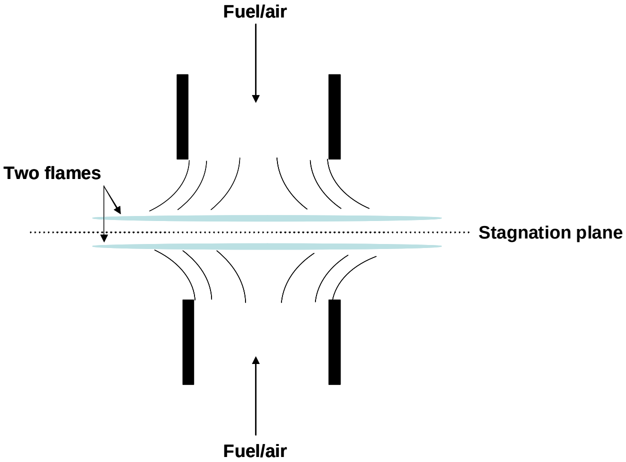

***Figure 23**: Schematic representation of a counterflow burner (premixed flames)*

An important part of my work at ICARE was devoted to the implementation and optimisation of the experimental device for stabilisation of premixed laminar flames at high pressure, during the PhD of A. Matynia (defended in April 2011).

2.3.1. High pressure facility

The high pressure facility (Figure 24) implemented at ICARE consists in a cylindrical stainless steel combustion chamber of 80 cm height and 25 cm diameter. This chamber is certified to withstand static pressures as high as 6.0 MPa and a maximum temperature at the inner wall of 473 K. It is equipped with four optical windows of 40 mm diameter for flame visualisation and laser diagnostics. In order to avoid condensation on the windows, a weak flow of nitrogen is injected on the inner face of each window. The chamber is cooled with a water circulation in a doubled-wall cylinder and in the top cover.

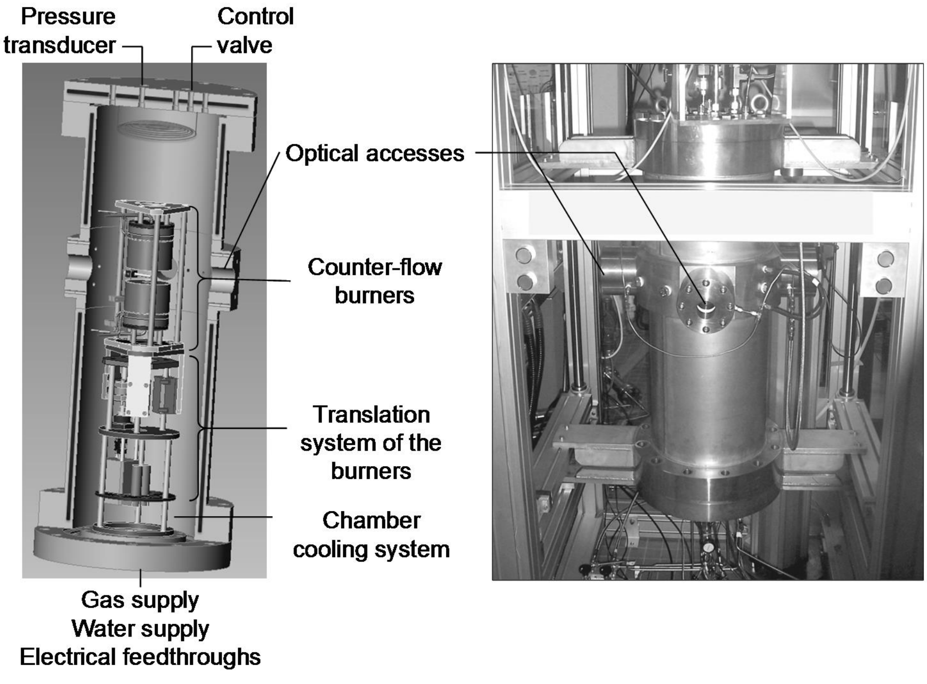

***Figure 24**: Diagram and picture of the high pressure facility*

The flames inside the chamber are stabilised between two twin counterflow burners (Figure 25). Each burner has an outer diameter of 90 mm and a height of 90 mm. Each burner is composed of two co-annular nozzles of 7 mm inner (D) and 13 mm outer diameters, which were aerodynamically shaped according to a modified empirical calculation from Rolon (1988), resulting in a nearly uniform velocity profile on their exit, which enhances the flame stability range [Bouvet, 2009]. The outer nozzle is used for a nitrogen co-flow around the burner, which permits to isolate the flame from the surrounding gases. The distance between the nozzles of the burners can be manually adjusted by moving the top burner compared with the bottom one. In the present study, the distance between the burners (L) is fixed at 10 mm, leading to a L/D ratio equal to 1.4. Moreover, the lower burner can be laterally shifted in order to superimpose the axis of the burners. The burners are cooled using a closed loop water circulation at a fixed temperature between 30 and 45°C, depending on the flame conditions, to avoid water condensation at the burner surfaces.

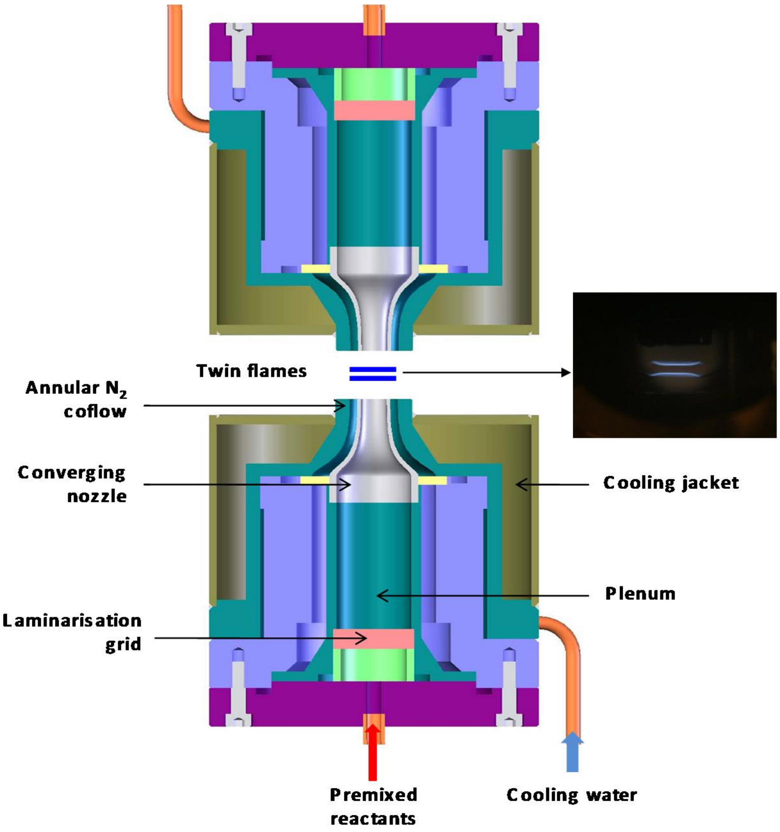

***Figure 25**: Diagram of the twin counterflow burners*

Both burners are mounted on a vertical translation system located inside the chamber below the burners. This translation system is composed of a planetary roller screw driven by a stepper motor. Due to mechanical hysteresis, the precision of the positioning of the burners is about ± 50 µm. Gas flows (premixed gases and co-flows), as well as cooling water and electrical wirings, are introduced through the bottom cover of the chamber. Burnt gases are evacuated through the top cover. The pressure within the vessel is controlled with a pressure transducer coupled with a control valve.

Different active and passive safety systems are installed in different places of the chamber. The passive ones include a safety valve and a rupture disk. The active ones include thermal (thermocouples J and K types) and pressure sensors which are connected to a programmable controller. The latter controls different safety electro-pneumatic valves. Gas flows are monitored with mass-flow controllers (Brooks), for each burner and for each gas, through a laboratory made Labview program. Each gas flow-meter is regularly and independently calibrated. Gases are premixed in a first cylindrical chamber filled with millimetric glass balls. A second downstream chamber serves as a buffer in order to attenuate the eventual flow fluctuations. Each chamber has an internal volume of 330 mL and can support 30 MPa. For safety reasons, flames are ignited at atmospheric pressure with a retractable hot kanthal wire placed between the burners.

The burner was characterized in terms of flame stability domain, temperature, pressure, safety. The influence of different parameters like nitrogen coflow, premixed gas temperature, etc… was deeply investigated during the PhD of A. Matynia. With this system, we have managed to stabilise CH_4-air and CH_4-CO_2-air ($XCO_2/[XCH_4+XCO_2]=0.4$) flames (Figure 26) at pressures up to 0.7 MPa and at different equivalence ratios (ϕ= 0.7 to 1.3) and these flames were studied using laser diagnostic techniques as described hereafter.

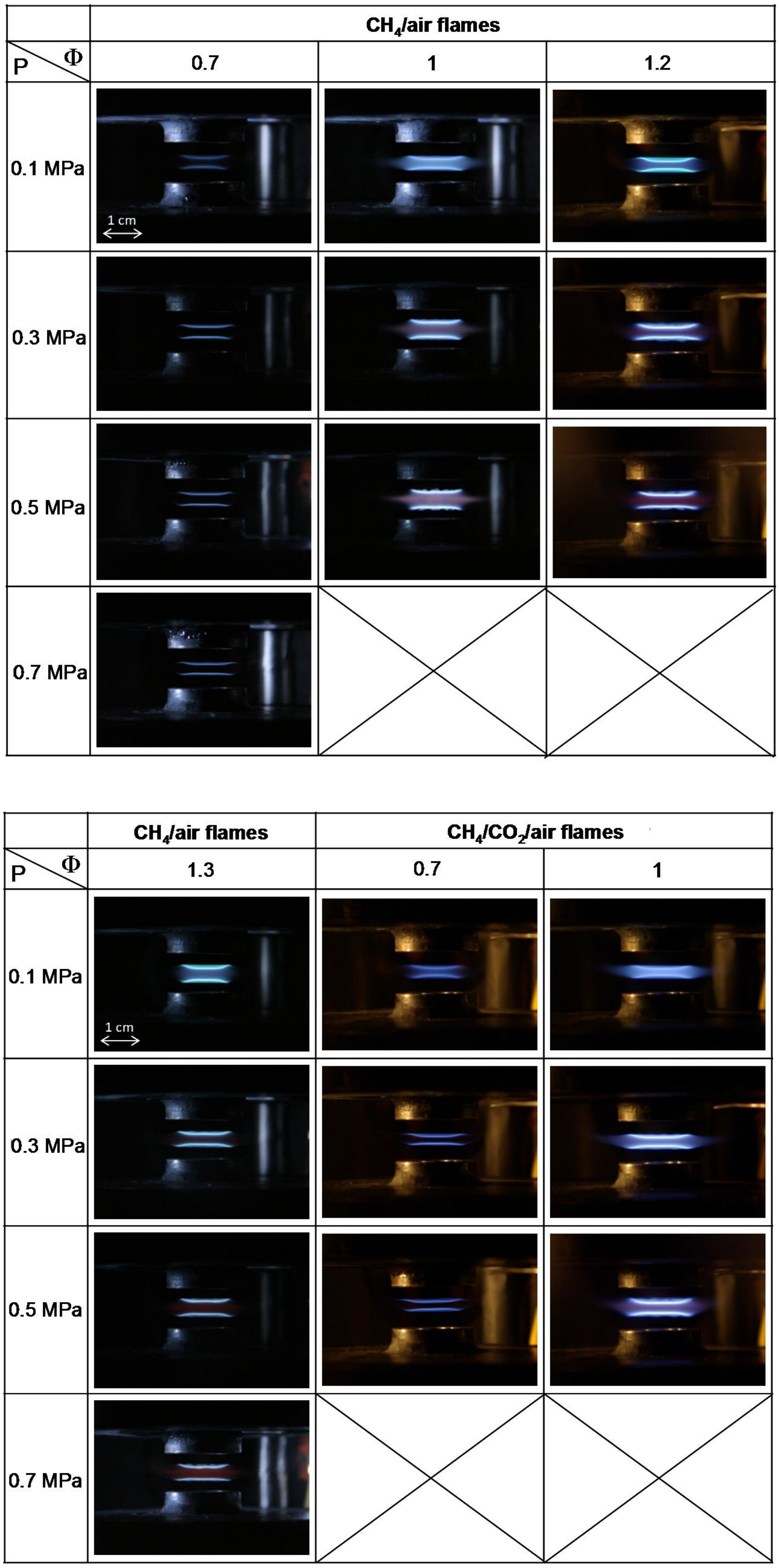

Figure 26: *Pictures of the twin premixed CH_4-air and CH_4-CO_2-air flames at different equivalence ratios ϕ and pressures P*

2.3.2. OH LIF measurements

To start, we chose to validate the system with OH LIF measurements as OH radical is present in flames in relatively high concentration and its spectroscopy is well known. LIF measurements in high pressure environment become very complex because of important variations of pressure and temperature dependent parameters such as the fluorescence quantum yield (and quenching), the Boltzmann fraction, the spectral overlap; variations which modify locally the ratio between the fluorescence signal and OH concentration. Therefore an important work was done on the analysis of the fluorescence signals at high pressure with a particular attention to the calculation of quenching variations and spectral broadening effects. This work, detailed in our publication [Matynia et al., 2012a], shows that, in our flame conditions, the variation of the parameters mentioned above along the flame axis could be neglected at a given pressure. A thorough calibration of the fluorescence signal, in each flame, allows overcoming the complex calculation of these parameters. Calibration of LIF signals was performed using laser absorption measurements of OH and the PLIF (Planar Laser Induced Fluorescence) technique to determine the absorption length.

2.3.3. Flame Modelling

The second step of this work was to compare our experimental results with modelling to test predictions of OH concentration profiles at high pressure using different kinetic mechanisms. Modelling was performed with the OPPDIF code [Lutz et al., 1997] and three detailed mechanisms: GRImech 2.11 [Bowman et al., 1995], GRImech 3.0 [Smith et al., 1999] and GDFkin®3.0_NCN [Lamoureux et al., 2010]. The GRImech 3.0 mechanism [Smith et al., 1999], containing 53 species involved in 325 reversible reactions, was used as it is a reference mechanism widely employed in the literature concerning methane and natural gas combustion. The previous version of this mechanism, GRImech2.11 [Bowman et al., 1995] (49 species, 277 reactions), was also tested. The GDFkin®3.0_NCN mechanism [Lamoureux et al., 2010] is an updated version of GDFkin®3.0 [El Bakali et al., 2006] including the NCN pathway for prompt-NO formation (see Part A3), it is composed of 883 reactions and 119 species. The thermodynamic and transport properties files provided with each mechanism were employed.

The effects of radiation heat losses in the CH_4-air and CH_4-CO_2-air counterflow flames were studied by including a radiation subroutine, developed by Gore et al. (1999), into the energy equation within the OPPDIF code. This routine assumes optically thin radiation originating from the major species within the flame. The calculation is based on the Planck mean absorption coefficients calculations as a function of temperature for the major species CO_2, H_2O, CO, and CH_4 using the RADCAL program of Grosshandler (1993). According to Gore et al. (1999), the optically thin limit assumption, for which only the loss by emission is considered, is adequate for stable flames with moderately high strain rates away from the radiative extinction limits, which is our case.

2.3.4. Main results

2.3.4.1. CH_4-air flames

Figure 27 compares the experimental and calculated OH mole fraction profiles in the CH_4-air flames. It can be observed that the OH profiles are characterised by strong gradients, which mark the location of the flamefronts. The OH profiles tend to present a “U” shape due to OH consumption in the burnt gases, which is more pronounced at high pressure. Calculated OH profiles obtained with the GDFkin®3.0_NCN and both GRImech (2.11 and 3.0) mechanisms reproduce very well the experimental profile shape for all the flames. Flamefront positions are in good agreement with the experiments for ϕ =0.7 and 1 in the CH_4-air flames. However, it is more difficult to draw any conclusions concerning the rich flames as, in this case, differences between the position of the three calculated profiles are quite significant. This is due to differences in the predictions of laminar flame velocity between the three mechanisms in rich conditions. Laminar flame velocity calculations were performed and show that GDFkin®3.0_NCN predicts slightly higher laminar flame velocities in rich conditions at atmospheric pressure (S_L = 36.5 cm.s^{-1} at ϕ = 1.2) compared to GRImech 2.11 (S_L = 36 cm.s^{-1} at ϕ = 1.2) and GRImech 3.0 (S_L = 35 cm.s^{-1} at ϕ = 1.2) which present results that are closer to the experimental values available in the literature. At 0.3 MPa (ϕ = 1.2), differences between the three mechanisms predictions of the flamefront positions are even more important, linked to higher discrepancies in flame velocity predictions; at 0.3 MPa S_L = 27.2 cm.s^{-1} with GDFkin®3.0_NCN, 20.8 cm.s^{-1} with GRImech 3.0 and 22.8 cm.s^{-1} with GRImech 2.11. Sensitivity analysis on flame velocity shows that these differences can be attributed to the reaction: $CH_3 + H = CH_4$ [or $CH_3 + H (+M) = CH_4 (+M)$], for which the GRImech mechanisms adopt a pressure-dependent rate constant while the GDFkin®3.0_NCN mechanism uses a pressure-independent rate constant.

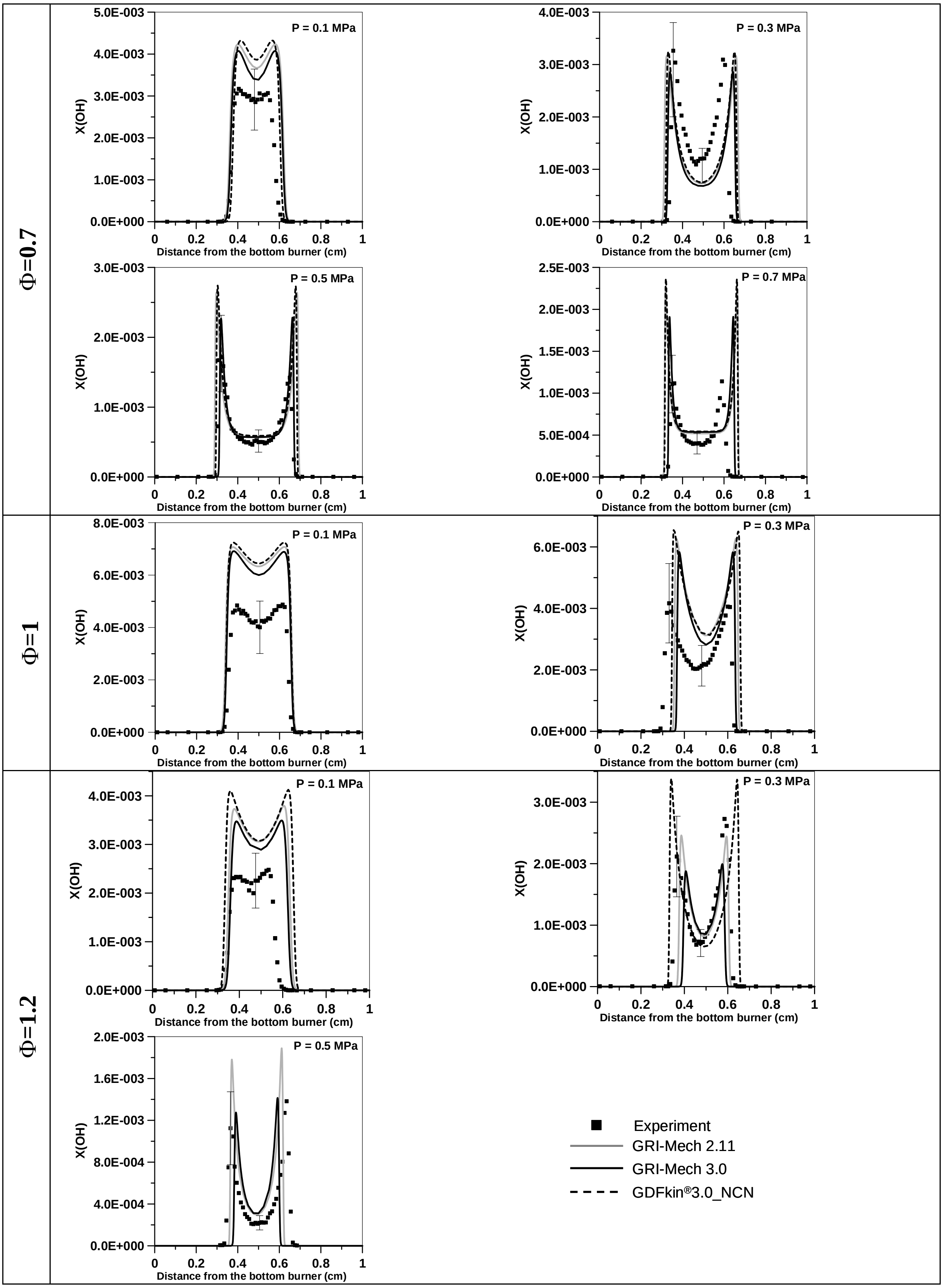

***Figure 27**: Comparison between experimental and calculated OH mole fraction profiles for the CH_4-air flames at different equivalence ratios ϕ = 0.7, 1.0 and 1.2 and different pressures P= 0.1 to 0.7 MPa [Matynia et al., 2012b]*

As shown in Figure 27, calculated OH mole fractions are quantitatively in good agreement with experiments for the lean flames. A slight overestimation is observed for the stoichiometric CH_4-air flames at 0.1 and 0.3 MPa. For the rich flames, simulations with the GDFkin®3.0_NCN and the GRImech mechanisms slightly overestimate OH concentration at atmospheric pressure, while the agreement is fairly good at higher pressure (0.3 and 0.5 MPa). Concerning the influence of pressure on the OH mole fraction, results show that the OH mole fraction in the burnt gases decreases when the pressure increases. Calculated values obtained with the GDFkin®3.0_NCN and both GRImech mechanisms reproduce this evolution quite well.

2.3.4.2. CH_4-CO_2-air flames

The comparison between experimental and calculated OH mole fraction profiles in the CH_4-CO_2-air flames is presented in Figure 28. Results show that, as for the CH_4-air flames, the maximum OH mole fraction decreases as the pressure increases. Similarly, OH profiles widen in the burnt gases at high pressure. These features are well reproduced by modelling for all the three mechanisms.

However, in the lean CH_4-CO_2-air flames, the distance between the two flamefronts is not well predicted by modelling at all pressures. The maximum OH mole fraction is overestimated by all mechanisms at atmospheric pressure but a good agreement is observed at higher pressure. For stoichiometric flames, the agreement between experiments and modelling is good at high pressure, but the OH mole fraction is also overestimated at atmospheric pressure for the three mechanisms.

Finally, comparison between CH_4-air and CH_4-CO_2-air flames shows a slight decrease in the OH mole fraction in the burnt gases when CO_2 is added at atmospheric pressure. For higher pressures, the differences observed are within the error bars.

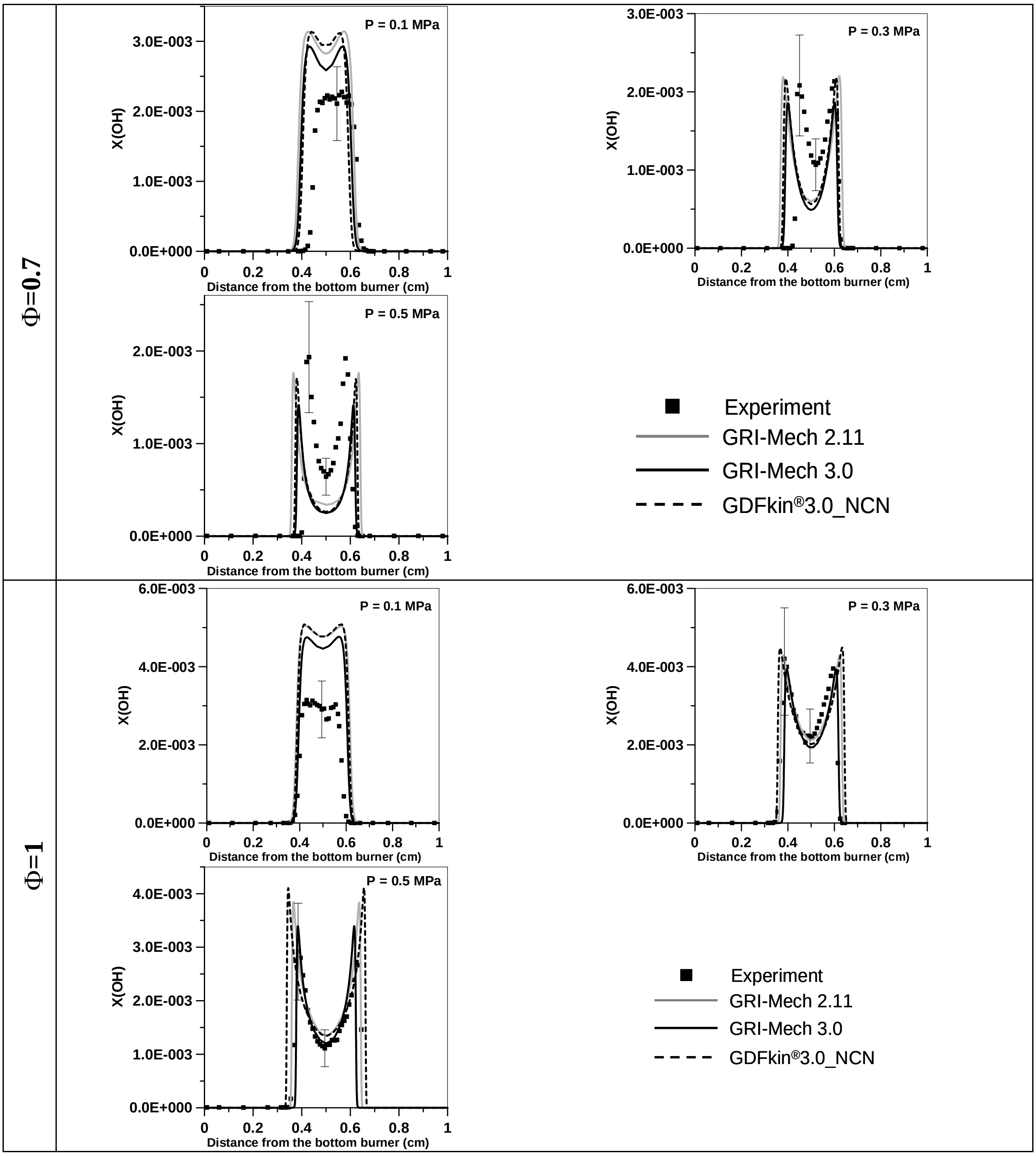

***Figure 28**: Comparison between experimental and calculated OH mole fraction profiles for the CH_4-CO_2-air flames at different equivalence ratios ϕ = 0.7 and 1.0 and different pressures P = 0.1 to 0.5 MPa.*

[Matynia et al., 2012b]

2.3.4.3. Reaction pathways analysis

Net elementary reaction rates, involving the OH radical, were calculated and their relative contributions to the total formation or consumption of OH were determined (expressed as a percentage of production or consumption of OH). This analysis was performed in the lean flames using the GDFkin®3.0_NCN mechanism. Figure 29 shows the main elementary reactions which contribute to the formation and consumption of OH for the lean CH_4-air flame (Figure 29a) and CH_4-CO_2-air flame (Figure 29b) as a function of pressure, at the peak OH location.

The hydroxyl radical is mainly produced by reactions:

$H_2O + O \rightarrow 2\,OH$ (R10)
$H + O_2 \rightarrow OH + O$ (R6)

And to a lesser extent by: $H + HO_2 \rightarrow 2\,OH$ (R14)
$O + H_2 \rightarrow OH + H$ (R5)

In the lean CH_4-air flames, the contribution of R10 to the formation of OH increases with pressure, while the contributions of R14 and R5 decrease when pressure increases. The contribution of R6 decreases when pressure increases from 0.1 MPa to 0.3 MPa and slightly increases when pressure is further increased to 0.7 MPa.

OH is consumed through the reactions:

$CO + OH \rightarrow CO_2 + H$ (R23)
$HO_2 + OH \rightarrow H_2O + O_2$ (R11)
$H_2 + OH \rightarrow H_2O + H$ (R9)

And to a lesser extent through: $2\,OH \rightarrow H_2O_2$ (R17)

In the lean CH_4-air flame, the contribution of R23 decreases as pressure increases, while the contribution of R11 increases. The contribution of R9 decreases when pressure increases from 0.1 MPa to 0.3 MPa and slightly increases when pressure is further increased.

These trends can be explained by a decrease in H and O radical mole fractions as pressure increases, as well as CO and H_2 mole fractions. However, H_2O, CO_2 and HO_2 mole fractions slightly increase with pressure. The same trends are observed for the CH_4-CO_2-air flames (Figure 29b).

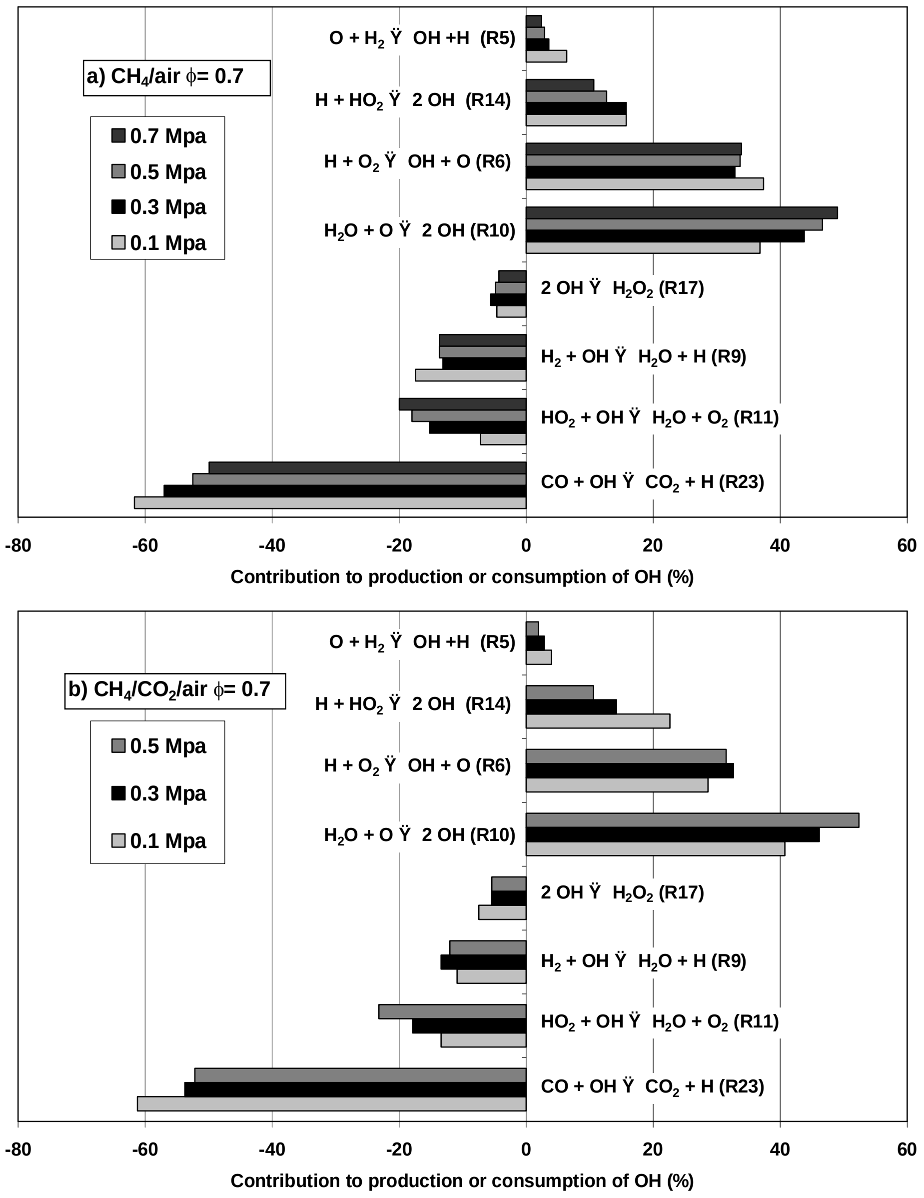

Figure 29*: Contributions (%) to OH production or consumption of elementary reactions as a function of pressure in a) the lean CH_4-air flames and b) the lean CH_4-CO_2-air flames. GDFkin®3.0_NCN mechanism. [Matynia et al., 2012b]*

To conclude, the results obtained during the PhD of A. Matynia (defended in April 2011) have demonstrated the performance of the developed experimental device to perform species profiles measurements in high pressure premixed counterflow flames. This system was later used to investigate NOx formation in high pressure combustion (see part A3).

Part A2: Combustion kinetics of biomass fuels: biogas and syngas

---

Publications linked to this work:
Matynia A., Idir M., Molet J., Roche C., de Persis S. and Pillier L., Absolute OH concentration profiles measurements in high pressure counterflow flames by coupling LIF, PLIF and absorption techniques, Appl. Phys. B 108 (2012a) 393-405 .

Matynia A., Molet J., Roche C., Idir M., de Persis S. and Pillier L., Measurement of OH concentration profiles by laser diagnostics and modelling in high pressure counterflow premixed methane-air and biogas-air flames, Combust. Flame, 159 (2012b) 3300-3311.

2.4. Measurements of methane-air and syngas-air laminar flame velocities

This study, initiated in collaboration with C. Chauveau and I. Gökalp at ICARE, during the PhD of N. Bouvet (defended in December 2009), was devoted to the measurements of laminar flame velocities, using the Particle Image Velocimetry (PIV) in the counterflow configuration or the stagnation plate (flame impacting a metal disk) configuration. The methodology developed was first applied to the well-characterized methane-air mixtures for validation. An extensive comparison with the literature database was provided. Both 1D (PREMIX, OPPDIF) as well as 2D (Fluent©) numerical tools were used to confirm the reliability and accuracy of the developed approach [Bouvet et al., 2014]. This method was then applied for the measurements of laminar flame velocities of various syngas (H_2+CO) mixtures. The results were compared to other experimental approaches including spherical and conical flame configurations for a wide range of equivalence ratios (ϕ =0.4 to 5.0) and mixture compositions (5/95 % to 50/50 % of H_2/CO). A comparison with modelling was also performed using the mechanism of Li et al. (2007). An example of the results obtained is presented in Figure 30 for a 50/50% H_2/CO + air mixtures.

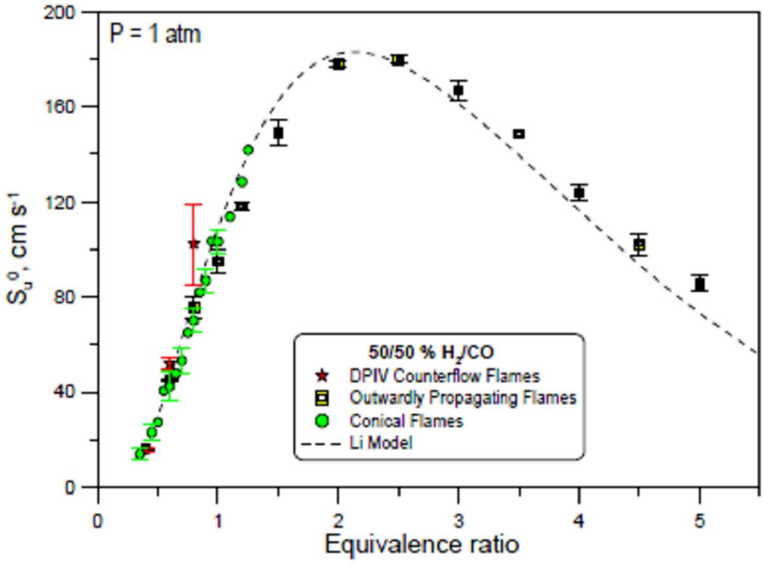

***Figure 30**: Laminar flame velocities comparison of 50/50% H$_2$/CO + air mixtures measured with the counterflow, outwardly propagating and conical flame techniques, comparison with modelling*

Publication linked to this work:

Bouvet N., Davidenko D., Chauveau C., Pillier L., Yoon Y., On the simulation of laminar strained flames in stagnation flows: 1D and 2D approaches versus experiments, Combust. Flame 161 (2014) 438-452.

A3. NO formation in high pressure flames

3.1. Context and objectives

The combustion of fossil fuels (natural gas, coal, oil) leads to a number of pollutant emissions in the atmosphere: carbon oxides COx (CO, CO_2), sulphur oxides SOx (SO_2), nitrogen oxides NOx (NO, NO_2), unburned hydrocarbons and soot particles. Among them, NOx emissions are more and more regulated because of their damaging effect on human health and environment. The necessity to control NOx emissions while optimising the use of fossil energy resources needs a better understanding of the combustion processes, and particularly the chemical kinetic of NOx formation during combustion. The study of the NOx formation/consumption chemistry in high pressure flames is of great interest in terms of application as most of the power generation and propulsion engines operate at high pressure.

This work comes within the scope of the ANR project: NO-mecha (BLAN08-0130-01, 2008-2013), initiated by Pascale Desgroux (coordinator) from PC2A, in collaboration with ICARE laboratory in Orléans where I was the local scientific advisor. It follows years of effort to understand NOx formation in flames in PC2A laboratory since the PhD of L. Gasnot [Gasnot, 1995] and my PhD (2003).

The aim of the project NO-mecha was to revisit and validate a kinetic mechanism for NO formation in a large range of experimental conditions, based on experimental data obtained in sub-atmospheric (at PC2A) and high pressure (at ICARE) flames.

The main NO formation pathways in flames are identified:

- The thermal-NO [Zeldovich, 1946] $N_2+O = NO+N$

  $N+O_2 = NO+O$

  $N+OH = NO+H$

- The prompt-NO [Fenimore, 1971] $CH+N_2 = HCN +N$

- The NNH route [Bozzelli and Dean, 1995] $N_2+H = NNH$

  $NNH+O = NH+NO$

- The N_2O route [Malte and Pratt, 1974]

N_2+O (+M) = N_2O (+M)

N_2O+H = NO+NH

N_2O+O = 2 NO

In the last decade, a special attention was given on prompt-NO formation as it was demonstrated, by theoretical and experimental studies, that the initiation reaction CH + N_2 = HCN + N (known to be spin forbidden) has to be replaced by the reaction CH + N_2 = NCN + H [Moskaleva and Lin, 2000; Vasudevan et al., 2007; Harding et al. ,2008]. In 2006, we were the first [El Bakali et al., 2006] to implement the new initiation reaction in the GDFkin®3.0_NCN (hydrocarbon oxidation mechanism GDFkin®3.0 developed at PC2A, associated to the N-species sub-mechanism developed during my PhD at PC2A). Since then, N. Lamoureux and P. Desgroux from PC2A have performed an extensive experimental and numerical study on the role of NCN in the prompt-NO mechanism in low pressure flames with the measurements of species like CH, NO, NCN, HCN or NCO [Lamoureux et al., 2009, 2010, 2011, 2013a, 2013b, 2015, 2016] combining LIF and CRDS techniques in low pressure flames. In 2010, Lamoureux et al. [Lamoureux et al., 2010] reported an experimental and modelling study in low pressure (5.3 kPa) CH_4–O_2–N_2 and C_2H_2–O_2–N_2 premixed flames where they propose a revision of the GDFkin®3.0_NCN mechanism by varying the rate constants of sensitive reactions over their range of accuracy to obtain the best compromise between experiments and simulations. This new mechanism and its associated thermokinetic database were then further updated by [Lamoureux et al., 2015]: the NCN thermodynamic data were updated by considering the heat capacity (Cp) values reported by Goos et al. [Goos et al., 2013], while the heat of formation (450.2 $kJ.mol^{-1}$) was conserved. Finally, Lamoureux et al. [Lamoureux et al., 2016] validated a new detailed sub-mechanism: NOmecha2.0, for NO chemistry at high temperature on a large database obtained in laminar premixed flames, jet-stirred and plug-flow reactors under sub-atmospheric and atmospheric conditions.

The objective of my work at ICARE, within the ANR project NO-mecha, was to validate this mechanism in high pressure flames during the PhD of J. Molet (defended in January 2014) by performing measurements of NO by Laser Induced Fluorescence (LIF) in CH_4-air flames and CH_4-H_2-air flames to investigate the role of hydrogen addition in NO formation.

3.2. Experimental part

The high pressure CH_4-air and CH_4-H_2-air flames were stabilised using the high pressure burner that I have developed at ICARE and detailed previously in section (2.3.1.). I will develop in this section the methodology employed to measure NO concentration profiles by LIF in the high pressure flames.

3.2.1. LIF experimental setup

The LIF experimental setup is presented in Figure 31. The laser system consists of a frequency-doubled Nd-YAG pulsed laser (Quantel Brillant B, repetition rate 10 Hz, 6 ns pulses) pumping a dye laser (Quantel TDL+). For NO excitation, a wavelength around 226 nm was obtained by mixing the frequency-doubled output of the dye laser (mixture of Rhodamine 590 and 610) with the residual infrared radiation from the Nd-YAG laser. The resulting laser beam near 226 nm has a diameter of 6 mm, and delivers a few mJ per pulse. The beam linewidth is 0.06 cm^{-1} (Quantel specifications). Measurements in the linear fluorescence regime were made by reducing the beam energy per pulse to 100 µJ with a variable attenuator composed of a half-wave plate and a Glan-Taylor prism. Part of the laser beam is collected by a fast photodiode in order to monitor the laser beam energy fluctuations. The beam is focused with a f = 350 mm lens inside the high pressure chamber, on the centre axis between the counterflow burners. The fluorescence signal is collected at right angle through a f = 500 mm lens and focused with a f = 300 mm lens on the entrance slit of a 500 mm focal spectrometer equipped with a photomultiplier (PM) tube. A 90° rotating periscope rotates the image of the probe volume and sets it parallel to the entrance slit of the spectrometer. The entrance slit is 100 µm in width and 4 mm in height, giving a probe volume of 160 µm by 6.4 mm in the flame, according to the magnification ratio of the optical collection system. The exit slit is adjusted to select the suitable fluorescence signal collection bandpass. Detected signals are sampled with a 1 GHz bandwidth oscilloscope.

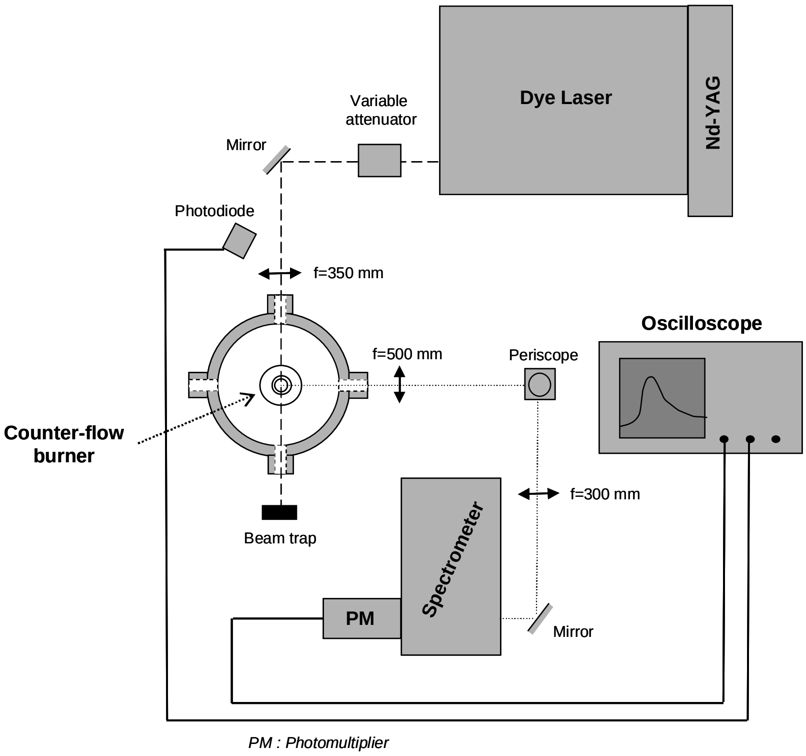

***Figure 31**: NO-LIF experimental setup*

[Pillier et al., 2015]

3.2.2. Spectroscopic considerations and analysis of the NO LIF signal

NO LIF measurements in high pressure environments are disturbed by various spectral features: interferences with O_2 fluorescence bands (Schumann Runge $B^3\Sigma^-$-$X^3\Sigma^-$bands), collisional broadening and shifting, and absorption by CO_2 and H_2O (laser attenuation and trapping) [Bessler et al., 2002, 2003a, 2003b]. The excitation/detection scheme was carefully chosen, based on excitation and fluorescence spectra analysis, to limit interferences on NO LIF signals and a theoretical correction procedure was proposed to take into account the influence of spectral broadening and quenching on LIF signals when pressure increases. This methodology is presented hereafter.

3.2.2.1. Choice of the excitation line

Firstly, the chosen excitation line must be well isolated to limit the overlap with neighbouring NO absorption lines when pressure increases, as collisional broadening increases with pressure. The absorption coefficient must be sufficiently high to obtain a good signal to noise ratio, whereas laser absorption and trapping need to be limited. Interferences from the Schumann-Runge bands of O_2 and absorption from combustion products (CO_2 and H_2O) need to be minimised. Finally, the variations of the Boltzmann fraction with temperature must be weak.

In most studies relating to NO measurements by LIF in high pressure flames within the A-X (0,0) band, two excitation lines are recommended: the $Q_2(26.5)$ line at 225.58 nm [Klassen et al., 1995] or the $P_1(23.5)$, $Q_1+P_{21}(14.5)$, $Q_2+R_{12}(20.5)$ feature at 226.03 nm [Battles et al., 1995]. Figure 32 represents an excitation spectrum measured in the burnt gases of the stoichiometric CH_4-air counterflow flame at atmospheric pressure (the signal is collected over the A-X(0,1) band). The O_2 absorption spectrum was calculated using the Lifsim code [Bessler et al., 2003c] and superposed on the NO experimental spectrum.

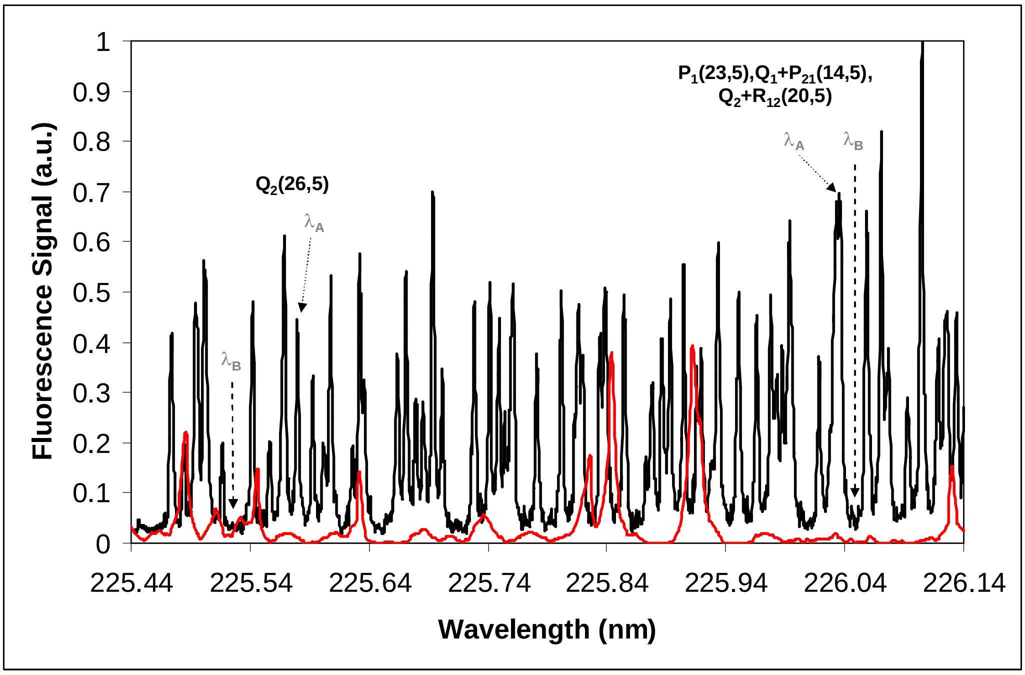

***Figure 32**: Experimental NO excitation spectrum (black line) measured in the burnt gases of a stoichiometric CH_4-air counterflow flame at 0.1 MPa and calculated O_2 excitation spectrum (red line) using the Lifsim code [Bessler et al., 2003c] (T= 2000 K, resolution = 0.001 nm)*
[Pillier et al., 2015]

For each excitation feature ($Q_2(26.5)$ and $P_1(23.5)$, $Q_1+P_{21}(14.5)$, $Q_2+R_{12}(20.5)$), the wavelength positions corresponding to maximum and minimum NO signals are shown (λ_A for excitation line peak, λ_B for minimum NO signal). The “background” wavelengths λ_B were chosen following the recommendations of [Klassen et al., 1995] and [Battles et al., 1995] and yield to a comparable intensity of O_2-LIF signal, compared to the excitation line peak position. In our flame conditions, the $P_1(23.5)$, $Q_1+P_{21}(14.5)$, $Q_2+R_{12}(20.5)$ candidate presents the highest signal to noise ratio and the lowest O_2 interferences compared to the $Q_2(26.5)$ line. The same conclusion was reached by [Bessler et al., 2003b] in high pressure flat flames, as [Naik et al., 2004] found no particular improvement using the $P_1(23.5)$, $Q_1+P_{21}(14.5)$, $Q_2+R_{12}(20.5)$ feature compared to the $Q_2(26.5)$ line in their high pressure counterflow diffusion flames.

3.2.2.2. Choice of the detection band

Fluorescence spectra were measured in the burnt gases of the lean (ϕ=0.7) CH_4-air counterflow flame for both excitation features: Figure 33a for the $Q_2(26.5)$ line at 0.1 MPa and Figures 33b and 33c for the $P_1(23.5)$, $Q_1+P_{21}(14.5)$, $Q_2+R_{12}(20.5)$ feature, at 0.1 MPa and 0.7 MPa respectively. The lean flame was chosen to maximise the interferences from O_2. The black spectrum is the fluorescence spectrum with laser excitation “on resonance” (λ_A) with the absorption line and the grey spectrum represents the fluorescence spectrum with laser excitation “off resonance” (λ_B) with a minimum contribution of NO fluorescence. The fluorescence spectra clearly show the contributions of interference sources (emission bands centred at 233, 238, 241, 245 and 249 nm). To identify the nature of these contributions (shown in Figure 33), fluorescence spectra were also measured in a CH_4-O_2-Ar flame (not shown here) without any nitrogen source. Spectra in Figures 33a and 33b clearly show that, at atmospheric pressure, an excitation via the $P_1(23.5)$, $Q_1+P_{21}(14.5)$, $Q_2+R_{12}(20.5)$ line in the A-X(0,0) band with fluorescence signal collection through the A-X(0,1) band (centred at 236 nm with a 2.8 nm bandpass) is the best compromise to maximise the NO LIF signal and minimise interferences in our flame conditions. Figure 33c shows that O_2 LIF interferences and background signal contribution to the A-X(0,1) NO band increase with increasing pressure, therefore the NO LIF profiles measurements and their calibration need to be systematically performed on resonance (λ_A) and “off resonance” (λ_B).

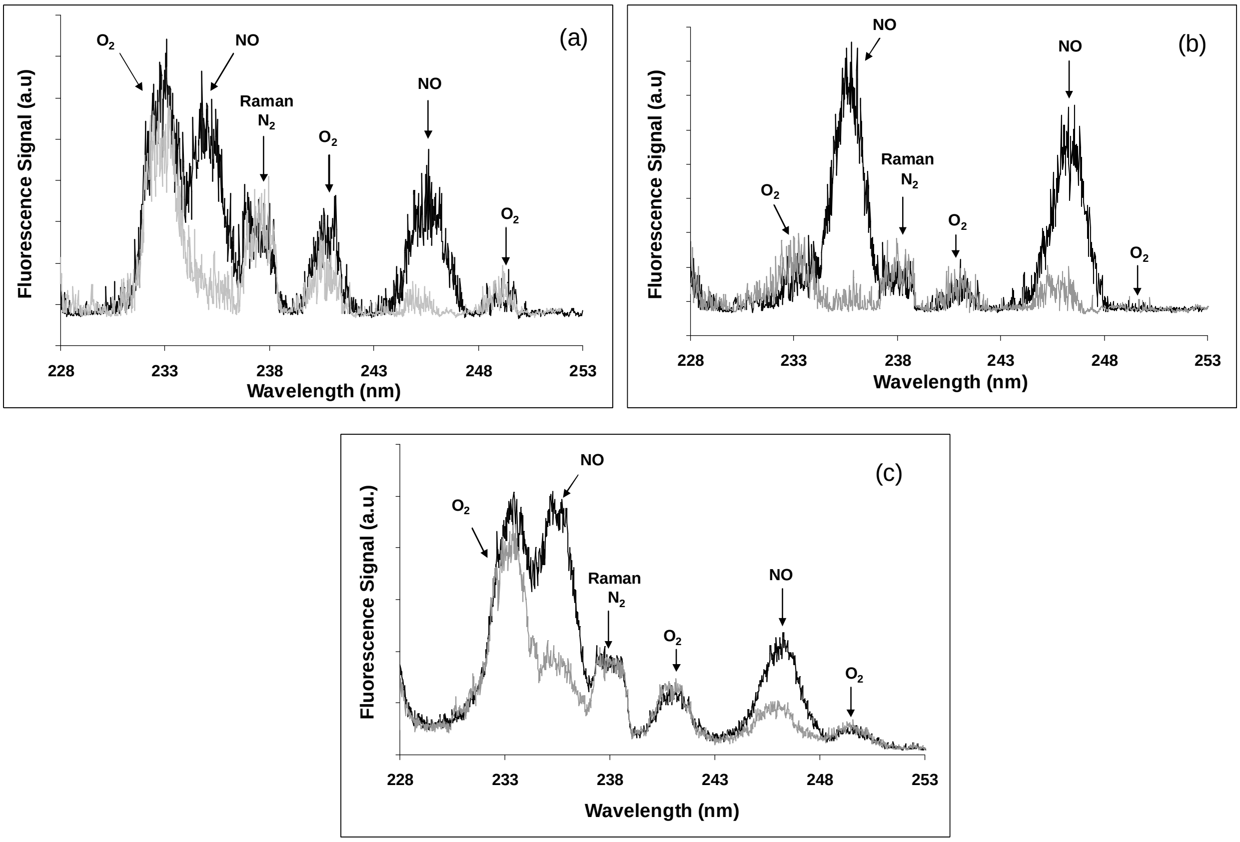

***Figure 33**: Experimental fluorescence spectrum measured in the burnt gases of a lean (ϕ=0.7) CH_4-air counterflow flame: (a) Excitation according to the $Q_2(26.5)$ line on resonance (λ_A, in black) and off resonance (λ_B, in grey) at 0.1 MPa; (b) and (c) Excitation according to the $P_1(23.5)$, $Q_1+P_{21}(14.5)$, $Q_2+R_{12}(20.5)$ line on resonance (λ_A, in black) and off resonance (λ_B, in grey) at 0.1 MPa and 0.7 MPa respectively. Collection bandpass = 1.66 nm.*
[Pillier et al., 2015]

3.2.2.3. Analysis of the NO LIF signal

The LIF signal was analysed with the same procedure as for OH in [Matynia et al., 2012a], we used the proportionality equation between the fluorescence signal S_f and the probed species density population N in the linear fluorescence excitation regime. In the present case, the LIF measurements of NO were performed via the excitation of a set of different neighbouring lines: $P_1(23.5)$, $Q_1+P_{21}(14.5)$, $Q_2+R_{12}(20.5)$ in the A-X(0,0) band, which are not exactly centred at the same wavelength. In this case, the fluorescence signal S_f can be expressed as:

$$\frac{S_f}{E_L} \propto N_{NO} \cdot \left\{ \eta_f \cdot \sum_j \left[g_j \left(Y_L, Y_{NO}, \Delta\lambda_j \right) \cdot F_{b,j}(J", v", T) \cdot B^j_{J'J"} \right] \right\} \qquad \text{Equation 4}$$

where: *j* represents each line of the set;

E_L is the laser energy per pulse;

N_{NO} is the NO density population;

η_f is the fluorescence quantum yield;

$g_j(Y_L, Y_{NO}, \Delta\lambda_j)$ is the spectral overlap function of the laser line with each absorption line, with Y_L the spectral laser line shape, Y_{NO} the absorption line shape, $\Delta\lambda_j$ the spectral shifting between the laser line and each absorption centreline (considering that the laser line is centred at one of the absorption lines of the group);

$F_{b,j}(J", v", T)$ is the Boltzmann fraction of each laser pumped rotational level (J",v") at the temperature T in K;

$B^j_{J'J"}$ is the Einstein absorption coefficient (with J' and J" the upper and lower rotational levels, respectively) for each line j.

The spectral overlap function, fluorescence quantum yield and Boltzmann fraction were calculated as follow.

3.2.2.3.1. Spectral overlap function calculation

The spectral overlap function $g_j(Y_L, Y_{NO}, \Delta\lambda_j)$ was calculated for each line assuming a Gaussian line shape for the laser line Y_L with a Full Width at Half Maximum (FWHM) of 0.06 cm^{-1} (Quantel specifications). The absorption line shape Y_{NO} was calculated from the convolution product of a Lorentzian profile, due to collisional broadening, with a Gaussian profile, due to Doppler broadening. The spectral overlap was determined by calculating the integral of the product of the two line shapes Y_L and Y_{NO} with their areas normalised to unity. The laser line wavelength was centred on the $Q_{1+}P_{21}(14.5)$

line and the corresponding spectral shift $\Delta\lambda_j$ was taken into account for the $P_1(23.5)$ and $Q_2+R_{12}(20.5)$ lines.

3.2.2.3.2. Fluorescence quantum yield calculation

The fluorescence quantum yield $\eta_f = \frac{\sum (A_{J'J''})_{obs}}{A_{eff} + Q_{eff}}$ represents the ability of a molecule to emit fluorescence (i.e. spontaneous emission with Einstein coefficients $A_{J'J''}$) in the experimental observation spectral window compared to the overall de-excitation (radiative and non-radiative) processes. In a multilevel system, these de-excitation processes are characterised by an effective spontaneous emission coefficient A_{eff} and by an effective quenching rate Q_{eff}. According to this definition of the quantum yield, collisional population redistributions in the excited level such as Rotational Energy Transfers (RET) and Vibrational Energy Transfers (VET) must be taken into account. However, the calculations of A_{eff} and Q_{eff} are very complex due to the RET and VET effects and are strongly dependent on the collision rates of NO with neighbouring atoms and molecules.

A few studies have been devoted to the effects of RET and VET on NO fluorescence measurements in atmospheric pressure and high pressure flames. Ravikrishna et al. (1999) performed a comparison between laser-saturated fluorescence and linear LIF measurements of NO in counterflow diffusion flames at 0.1 MPa and showed that both techniques gave nearly identical results, suggesting that RET are small at atmospheric pressure. Driscoll et al. (2002) applied picosecond-LIF to obtain spatial profiles of NO concentrations and effective fluorescence lifetimes in a counterflow, non-premixed CH_4-air flame at atmospheric pressure. Their evaluation of picosecond-LIF signals using a four-level, density-matrix model suggested that RET effects only become important at laser fluences higher than ≈ 100 $mJ.mm^{-2}.pulse^{-1}$. Naik et al. (2004) used a five-level model for NO molecular dynamics to investigate the effects of RET on linear LIF measurements of NO at pressures up to 1.5 MPa. The results indicate that rotational relaxation effects are negligible under high-pressure conditions at low laser fluences, and thus do not need to be accounted for when measuring NO using linear LIF. According to Daily et al. (1999), VET are so slow in the X state that during the 10-ns laser pulse essentially no VET take place.

Based on the above conclusions, the fluorescence quantum yield η_f was quantified assuming a simplified two-level system. In this simplified approach, the de-excitation collision rate $Q_{J'J''}$ (s^{-1}) can be expressed as follows:

$$Q_{J'J''} = N_{tot} \cdot \sum_i \chi_i . \sigma_i . \mathrm{v}_i \qquad \textit{Equation 5}$$

where: *i* is summed among all the collision partners;

N_{tot} is the total density population (molecule.m^{-3});

χ_i is the corresponding mole fraction;

σ_i is the quenching cross section (m^2);

v_i the average relative velocity between NO and the collision partner i (m.s^{-1}).

We calculated the quenching rate by considering that the major colliding partners of NO are CH_4, CO_2, O_2, H_2, CO, H_2O, N_2 and NO itself. Spatial profiles of temperature and mole fractions of those species along the centreline of the counterflow flames were calculated with the OPPDIF code [Lutz et al., 1997] and the GRImech 3.0 mechanism [Smith et al., 1999] in the case of adiabatic flames. The corresponding quenching cross sections were calculated as a function of temperature, based on the models of Paul et al. (1993, 1995) and Settersten et al. (2003) and compared to available experimental values from the literature.

Figure 34 represents the NO mole fraction profile (left-hand side scale) simulated by OPPDIF and the quenching rate profiles (right-hand side scale) calculated with both models [Paul et al., 1993, 1995; Settersten et al., 2003] for the lean CH_4-air flame (ϕ=0.7) at 0.1 MPa and 0.7 MPa. Results show that the quenching rate varies essentially in the NO concentration gradients corresponding to the flamefronts where temperature and flame composition vary significantly. These variations are much weaker in the burnt gases as temperature and gas composition are nearly constant in this area. The quenching rate increases proportionally with pressure. The differences observed between the models of Paul et al. and that of Settersten et al. are within 20%. As the model of Settersten et al. gives quenching cross sections only for CO_2, H_2O and NO colliding species, the following calculations were done using the model of Paul et al.

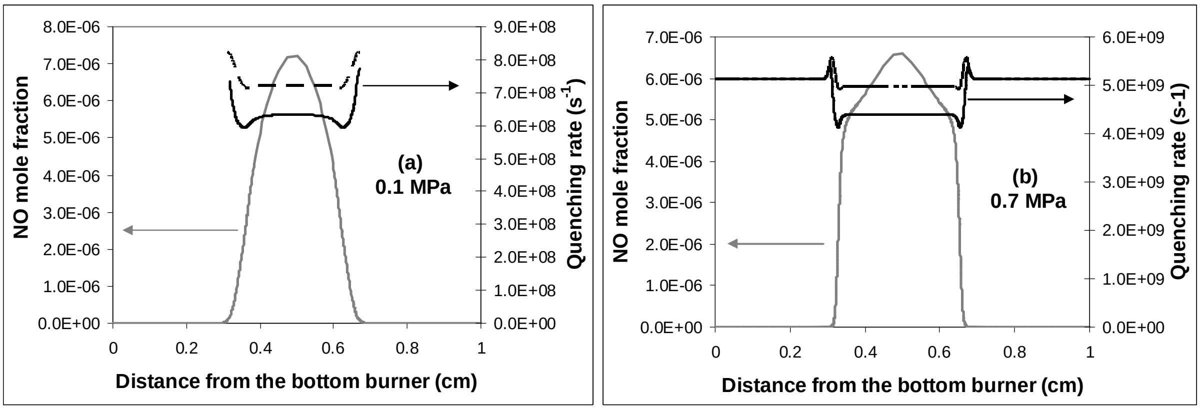

***Figure 34**: NO mole fraction profile (left-hand side scale) simulated by OPPDIF and quenching rate (s^{-1}) profile (right-hand side scale) calculated using the model of [Paul et al., 1993, 1995] (solid line) and [Settersten et al., 2003] (dotted line) in the lean CH_4-air flame (ϕ=0.7) at 0.1 MPa (a) and 0.7 MPa (b)*
[Pillier et al., 2015]

3.2.2.3.3. Boltzmann fraction calculation

The Boltzmann fraction was calculated as a function of temperature using the spectroscopic constants from [Luque et al., 1999; Amiot et al., 1978] for each rotational number J''=23.5; 14.5 and 20.5. The temperature profile was simulated by the OPPDIF code, with the GRImech3.0 mechanism [Smith et al., 1999], with the adiabatic flame assumption.

3.2.2.3.4. Influence on NO LIF signal

In order to evaluate the influence of the spectral overlap, the quantum yield and the Boltzmann fraction on the fluorescence signal profile, we compared both relative spatial profiles of the NO density population N_{NO}, calculated by the OPPDIF code with the GRImech3.0 mechanism with N_{NO} multiplied by $\frac{1}{Q_{J'J''}} \cdot \sum_j \left[g_j\left(Y_L, Y_{NO}, \Delta\lambda_j\right) \cdot F_{b,j}(J'', v'', T) \cdot B^{j}_{J'J''} \right]$, that represents an image of S_f/E_L (see Eq.4). The values of the absorption coefficients $B_{J'J''}$ were taken from the LIFBASE database [Luque et al., 1999].

Our calculations showed that the combined influence of all the three parameters is very weak along the flame axis. These observations lead to the conclusion that, in our conditions, the overall influence of the spectral overlap, quantum yield and Boltzmann fraction variations can be neglected across the flame. Consequently, at a given pressure, the fluorescence signal profile (S_f/E_L) accurately reproduces the N_{NO} population density profile. Hence, in order to determine the absolute concentration of NO, a calibration measurement of the fluorescence signal at only one point in the burnt gases is sufficient. However, this calibration needs to be done for each flame condition (at each pressure). This calibration phase was done by seeding the flame with known quantities of NO and measuring a calibration plot. This procedure is detailed in the next section.

Furthermore, we calculated the sensitivity of the fluorescence signal regarding to the temperature variations in the burnt gases of the lean CH_4-air flame at 0.1 MPa and 0.7 MPa. We found that a variation of ±100 K (T= 1800 K) induces variations of the fluorescence signal of ±4% at 0.1 MPa and ±1% at 0.7 MPa. Then, such uncertainty on the temperature does not have an important impact on the calculated fluorescence signal and consequently on the determined NO concentration. At high pressure, this sensitivity appears to be almost negligible.

3.2.2.4. Calibration of NO LIF signal

The nascent NO mole fraction in the flames was determined using a variable NO seeding (from 0 to 111 ppm of NO in the mixture) method [Thomsen et al., 1997; Schulz et al., 1997]. It was assumed that doped NO does not react in the flame (no NO-reburning). This assumption was supported by computer modelling which indicates that reburning was below 3% for our lean CH_4-air flames. The LIF NO signal was measured at two different excitation wavelengths λ_A and λ_B, which have maximum and minimum NO signal strengths respectively, as illustrated in Figure 35. After measuring the NO LIF signal in the burnt gases of each flame, at the two different wavelengths, for different NO seeding concentrations, the signal was linearly fit as a function of the seeded NO mole fraction in the flame for each excitation wavelength. These two linear fits were extrapolated to their intersection, yielding the nascent NO mole fraction and the value of the baseline signal. This procedure was applied in each individual flame with an uncertainty of ± 10% for NO mole fraction.

The final experimental uncertainty reached ± 20% for all flames. This value takes into account the following uncertainties: i) uncertainties on the calibration procedure (around ± 10%); ii) uncertainties on the mass flow meters (implying uncertainties on the equivalence ratio and dilution ratio) (± 2%); iii) uncertainties on the probe volume position (±2%); iv) uncertainties on the flame temperature (estimated to be equal to the adiabatic flame with an uncertainty of ± 5%); v) the uncertainty on pressure inside the combustion chamber (±1%).

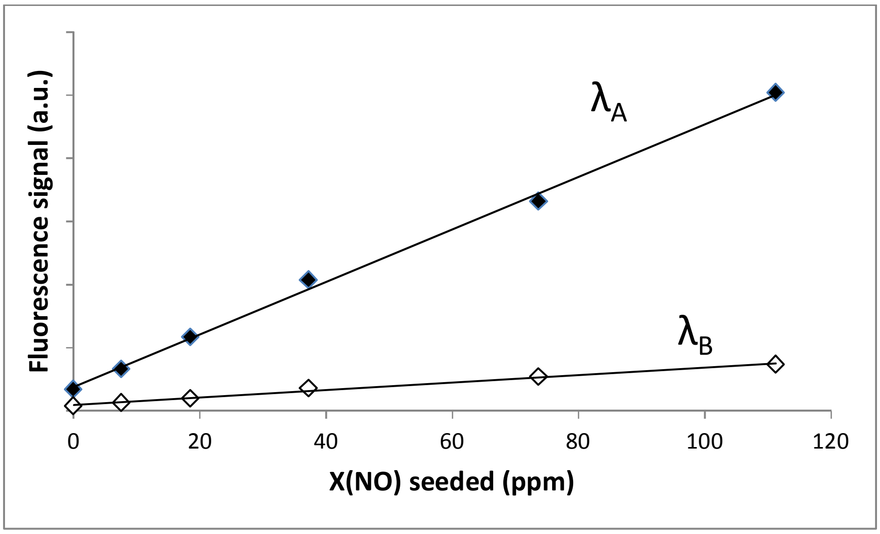

***Figure 35**: Calibration method: LIF NO signal measured in the burnt gases as a function of NO mole fraction seeded in the CH_4-air lean (ϕ= 0.7) flame at 0.1 MPa, at the two wavelengths λ_A and λ_B [Pillier et al., 2015]*

Publication linked to this work:

<u>Pillier L.</u>, Idir I., Molet J., Matynia A., de Persis S., Experimental study and modelling of NOx formation in high pressure counter-flow premixed CH_4/air flames, Fuel 150 (2015) 394-407.

3.3. Main results

3.3.1. CH_4-air flames

3.3.1.1. Flame conditions

The CH_4-air premixed laminar flames conditions are summarised in Table 6. Under certain flame conditions, the gas velocity ratio between the upper and lower burners had to be adjusted to keep the flames well centred between the burners, this ratio is denoted β in Table 6. The flames were stabilised at equivalence ratios of 0.7, 1 and 1.2 and at pressure from 0.1 to 0.7 MPa, depending on flame stability. Note that the stoichiometric flames could not be stabilised at a pressure higher than 0.3 MPa and the rich flame higher than 0.5 MPa because of instabilities.

Equivalence Ratio	**Pressure (MPa)**	**X(CH_4)**	**X(O_2)**	**X(N_2)**	**Total flowrate (L.min^{-1}) (a)**	**Inlet premixed gas Velocity (cm.s^{-1}) (a)**	**β (b)**	**Burner cooled temperature (K)**	**Adiabatic flame temperature (K) (c)**
0.7	0.1	**0.0685**	**0.1952**	**0.7363**	**1.57**	**75.3**	**1.05**	**303**	**1841**
	0.3				**2.50**	**42.0**	**1.05**	**313**	**1849**
	0.5				**2.97**	**30.9**	**1.05**	**323**	**1857**
	0.7				**4.01**	**29.7**	**1.05**	**323**	**1857**
1	0.1	**0.0947**	**0.1896**	**0.7157**	**2.75**	**132.1**	**1**	**303**	**2223**
	0.3				**7.56**	**126.8**	**1**	**313**	**2251**
1.2	0.1	**0.1010**	**0.1835**	**0.7065**	**2.21**	**106.1**	**1.05**	**303**	**2190**
	0.3				**6.07**	**101.8**	**1.05**	**313**	**2205**
	0.5				**7.35**	**76.4**	**1.05**	**323**	**2215**

(a) Experimental conditions for the bottom burner, in standard conditions, i.e. T=273K and P=101325Pa.
(b) β = inlet premixed gas velocity (top burner) / inlet premixed gas velocity (bottom burner)
(c) Flame temperature calculated for a free flame configuration using GDFkin®3.0 associated with NOmecha2.0

Table 6: *CH_4-air counterflow premixed flame conditions*
(X(CH_4) is the mole fraction of methane, X(O_2) is the mole fraction of oxygen and X(N_2) is the mole fraction of nitrogen); Air dilution ratio is used.

3.3.1.2. Modelling

Kinetic modelling was carried out using the OPPDIF code [Lutz et al., 1997]. The NOx submechanism NO-mecha2.0 [Lamoureux et al., 2016] was associated to two detailed mechanisms for methane oxidation: GDFkin®3.0 [El Bakali et al., 2006] and GRImech3.0 [Smith et al., 1999]. GRImech3.0 includes its own NOx chemistry (with the spin forbidden $CH+N_2=HCN+N$ initiation reaction for prompt-NO). In this work, we used it in its original version and in a version associated with NO-mecha2.0 where kinetic and thermodynamic data of the NOx sub-mechanism of GRImech3.0 are substituted by those of NOmecha2.0. For the methane oxidation part, the thermodynamic and transport properties files provided with each mechanism were employed.

3.3.1.3. Results and discussion

Figure 36 compares the experimental and calculated NO mole fraction profiles with the three mechanisms: GDFkin®3.0_NOmecha2.0, GRImech3.0 and GRImech3.0_NOmecha2.0, in the CH_4-air flames at equivalence ratio ϕ=0.7 (Fig. 36a), ϕ=1 (Fig. 36b) and ϕ=1.2 (Fig. 36c), at pressures ranging from 0.1 to 0.7 MPa. In Figure 37, the experimental and calculated maximum NO mole fraction XNO_{max} for the same conditions are reported.

As shown in figure 36, NO profiles calculated with the three mechanisms satisfactorily reproduce the experimental NO profile 'bell' shape for all the equivalences ratio and pressure conditions. Flamefronts positions are in good agreement with experiments for the bottom burner whereas one can note some discrepancies for the upper burner in lean and rich flames at high pressure.

In the lean flames, as shown in Figure 37a, the experimental maximum NO mole fraction is nearly constant when pressure increases, as predicted by GRImech3.0_NOmecha2.0. The unmodified version of GRImech3.0 predicts a slight decrease and GDFkin®3.0_NOmecha2.0 predicts a slight increase of XNO_{max} when pressure increases (within the experimental error bars). In the stoichiometric flames (Figure 37b), an increase of XNO_{max} by a factor of 2 is observed from 0.1 to 0.3MPa, which is correctly predicted by the three mechanisms though with a slight underestimation by GDFkin®3.0_NOmecha2.0. In the rich flames (Figure 37c), GDFkin®3.0_NOmecha2.0 is in excellent agreement with experimental results at 0.1MPa and 0.3MPa, but slightly lower at 0.5MPa. The unmodified GRImech3.0 mechanism overestimates the NO mole fraction at 0.1 and 0.3 MPa (within the error bars at 0.5MPa) and this overestimation is even worse when combining the GRImech3.0 mechanism with NOmecha2.0.

In summary, the three mechanisms are able to predict NO correctly in lean and stoichiometric high pressure flames, whereas in rich flames, GDFkin®3.0_NOmecha2.0 presents the best predictions.

Fig. 36a)

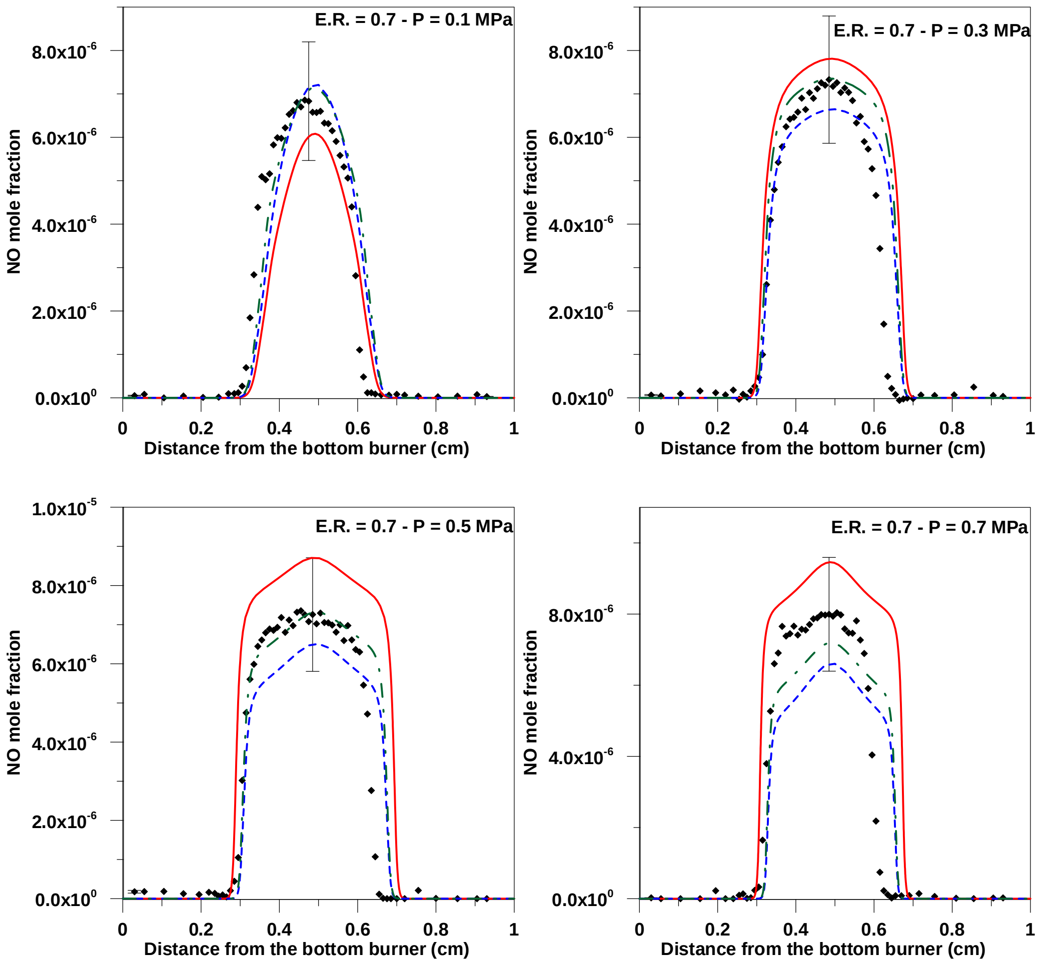

Fig. 36b)

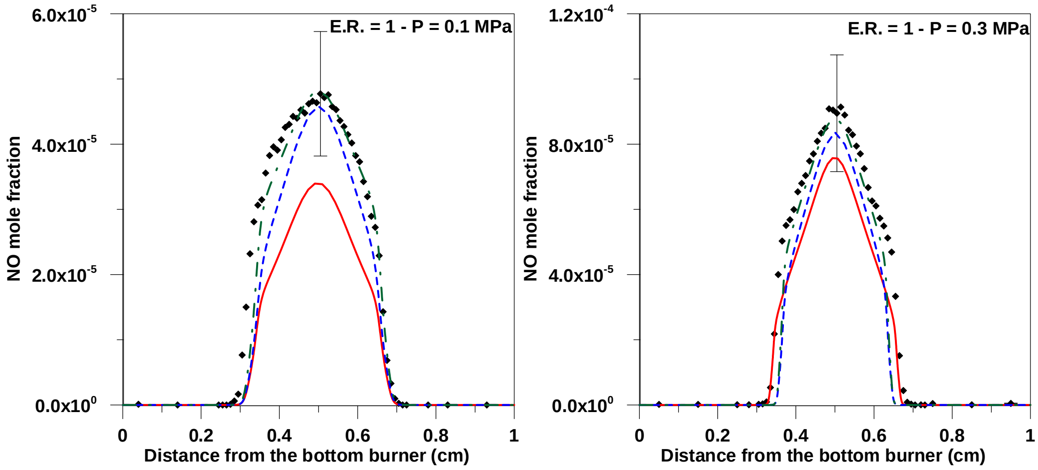

Fig. 36c)

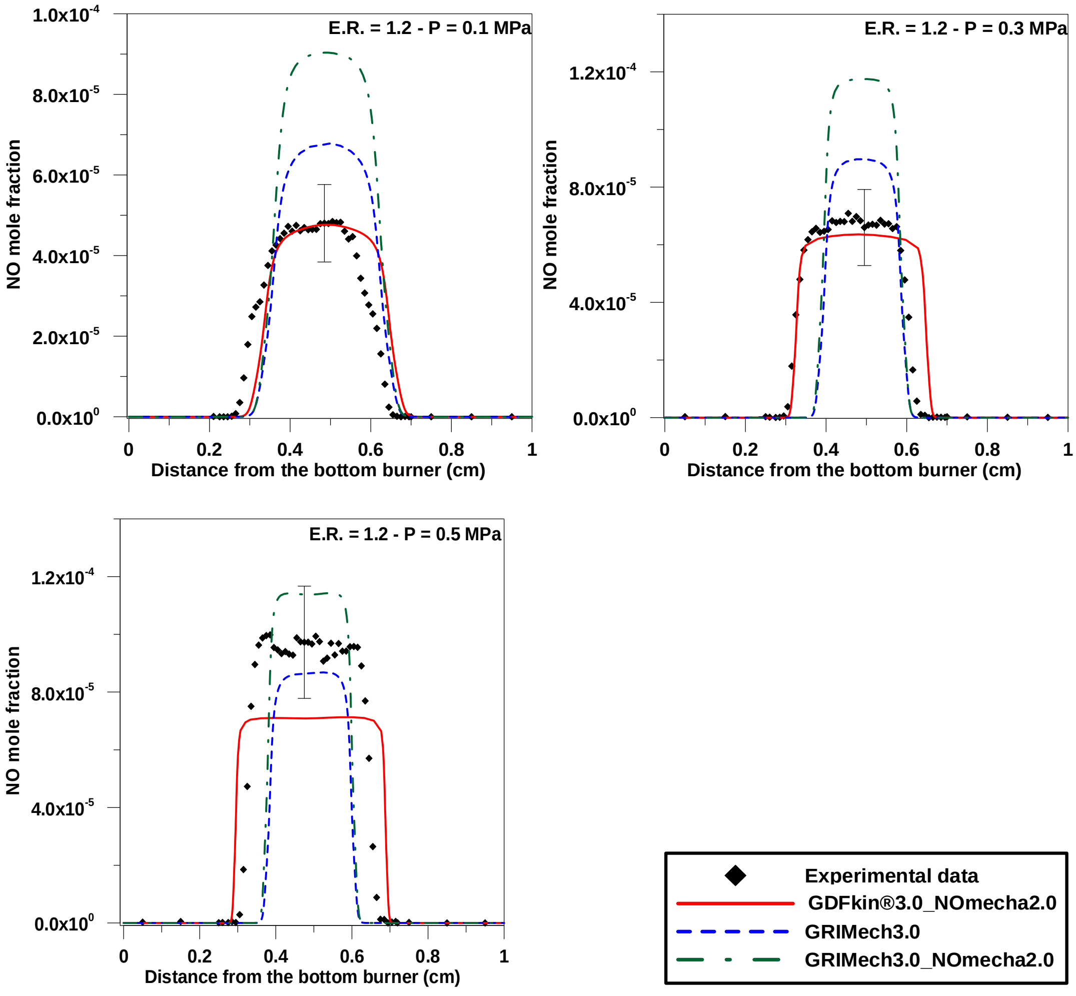

***Figure 36**: Comparison between experimental and calculated NO mole fraction profiles for the CH_4-air flames:*
a) for equivalence ratio =0.7 at pressures from P = 0.1 to 0.7 MPa;
b) for equivalence ratio = 1.0 at pressures from P = 0.1 to 0.3 MPa;
c) for equivalence ratio = 1.2 at pressures from P = 0.1 to 0.5 MPa.
Symbols: experiments; modeling with red solid line: GDFkin®3.0 with NOmecha2.0, blue dotted line: GRImech3.0 and green dotted line: GRImech3.0 with NOmecha2.0.

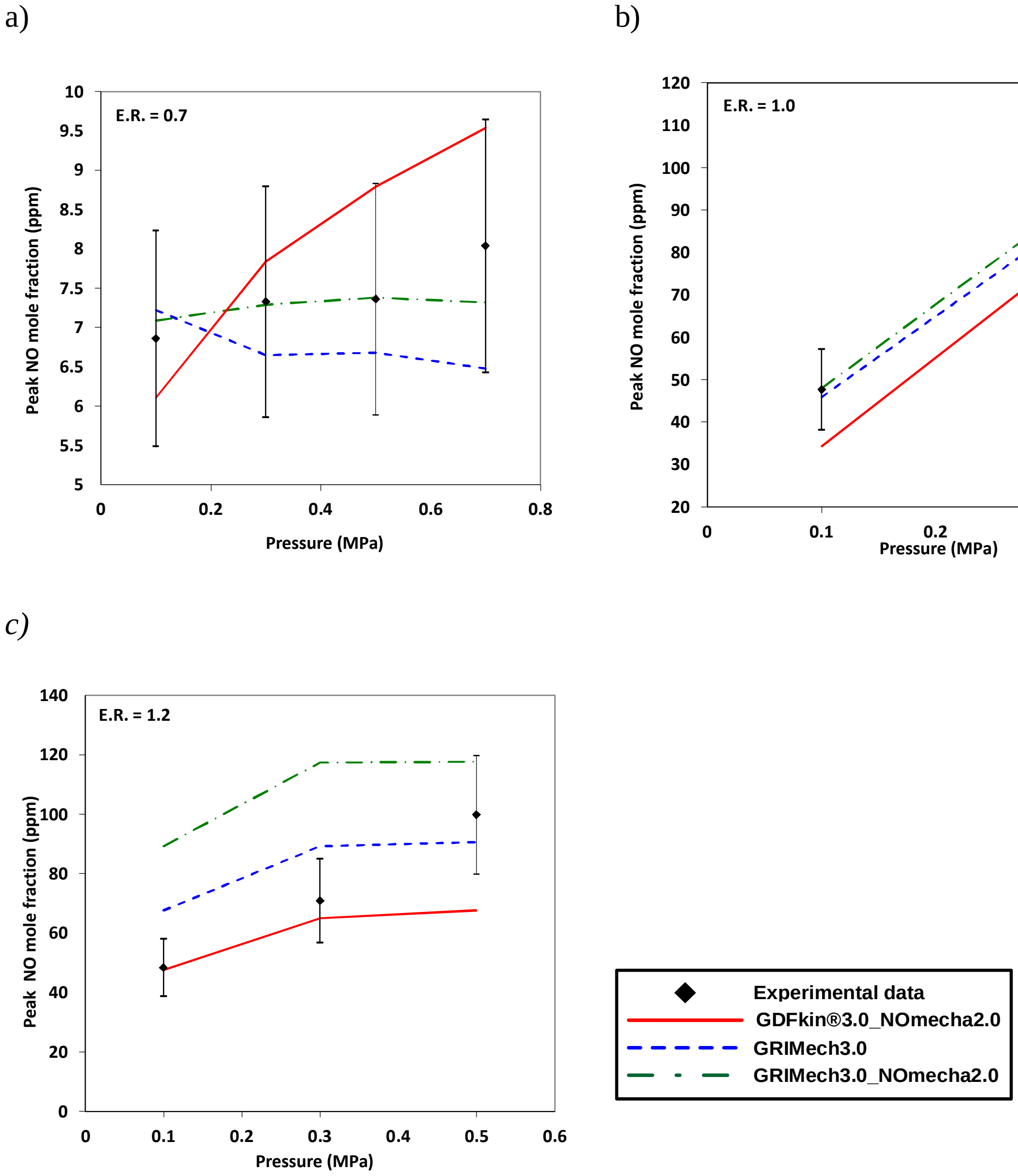

***Figure 37**: Comparison between experimental and calculated peak NO mole fraction XNO_{max} for the CH_4-air flames:*
a) for equivalence ratio =0.7 at pressures from P = 0.1 to 0.7 MPa;
b) for equivalence ratio = 1.0 at pressures from P = 0.1 to 0.3 MPa;
c) for equivalence ratio = 1.2 at pressures from P = 0.1 to 0.5 MPa.
Symbols: experiments; modeling with red solid line: GDFkin®3.0 with NOmecha2.0, blue dotted line: GRImech3.0 and green dotted line: GRImech3.0 with NOmecha2.0.

A kinetic analysis was performed with the GDFkin®3.0_NOmecha2.0 mechanism to evaluate the relative contribution of the four major NO formation pathways (thermal-NO, prompt-NO, N_2O and NNH routes). For that, net rates were considered for all the N-species in the mechanism by summing the Rates Of Consumption (ROC, negative values) and Rates Of Production (ROP, positive values) integrated over the whole flame domain (distance from the bottom burner = 0 to 1 cm). Figure 38 shows the net rates diagram drawn for ϕ=0.7 as a function of the pressure (0.1 to 0.7 MPa). For clarity reasons, net rates are expressed in % and the diagram was simplified by removing negligible pathways (<1%).

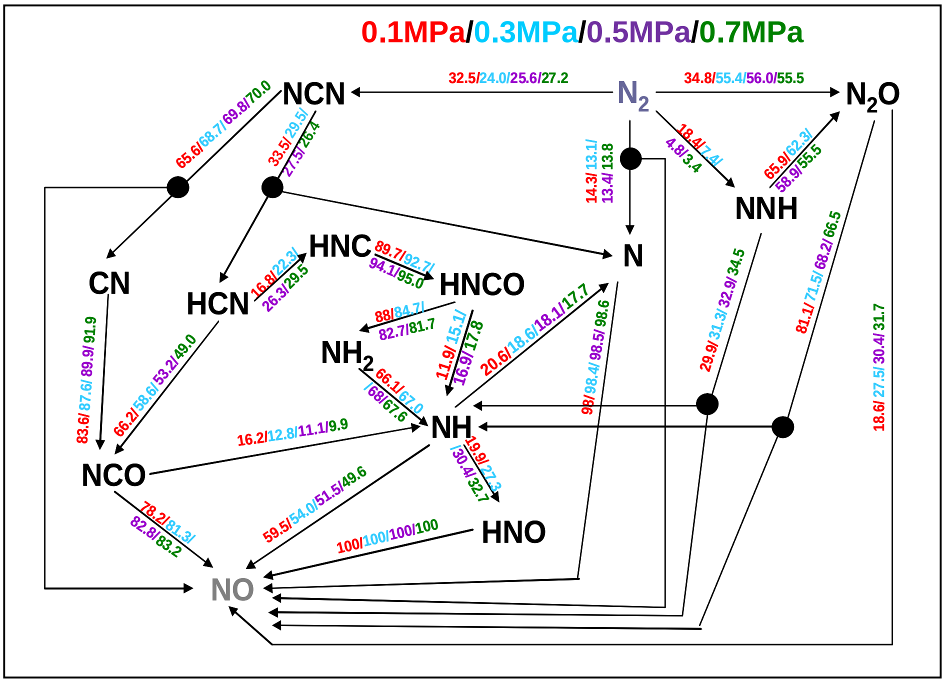

***Figure 38**: Integrated reaction pathways (in %) obtained from net rates in the lean (ϕ=0.7) CH_4-air counterflow flame at four pressures (0.1 to 0.7MPa) for GDFkin®3.0 associated with NOmecha2.0.*

Figure 38 clearly shows the complexity of the chemical structure of the N-species mechanism: it is thus very difficult to obtain directly the contribution to NO formation by only removing each of the four major routes (prompt-NO, thermal-NO, NNH and N_2O) because of crossed pathways. We then compared how the main precursor of NO, that is N_2, decomposes through the four major pathways. Figure 39 shows the net rates of consumption of N_2 (in %) as a function of equivalence ratio and pressure.

a) $\phi = 0.7$

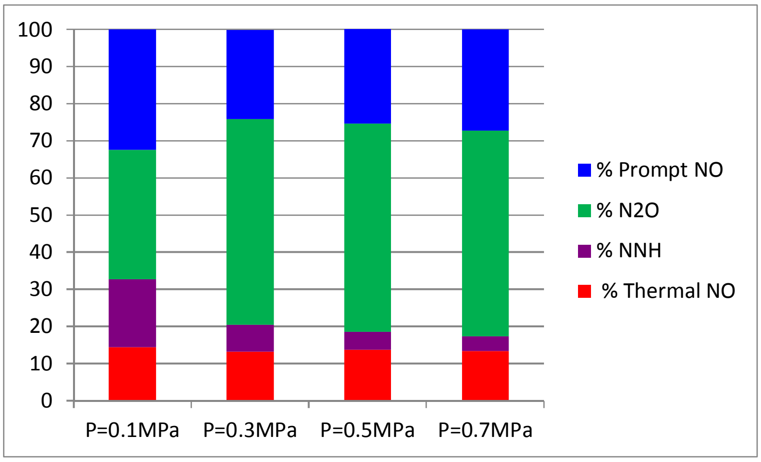

b) $\phi = 1$

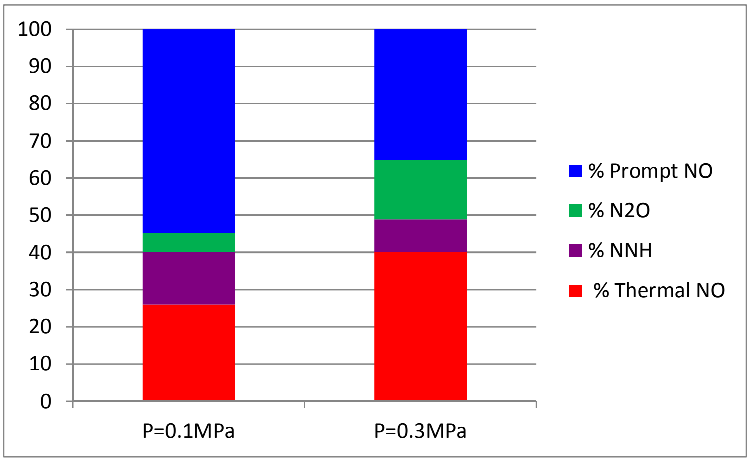

c) $\phi = 1.2$

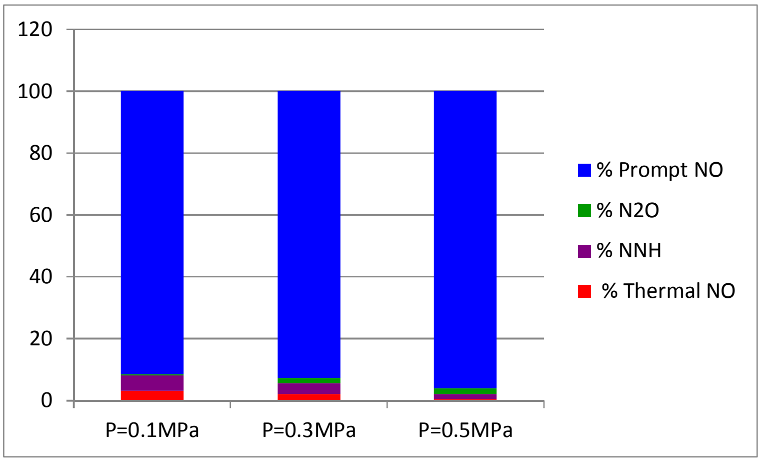

***Figure 39**: Relative contribution of the four NO formation pathways (the thermal-NO in red, the NNH route in purple, the N_2O route in green and the prompt-NO in blue) obtained from N_2 consumption rates: a) for ϕ=0.7; b) for ϕ=1.0 and c) for ϕ=1.2, as a function of pressure in premixed CH_4-air counterflow flames with GDFkin®3.0 associated with NOmecha2.0.*

As shown in figure 39, for lean flames (ϕ=0.7), the contributions of the four major pathways are as follows: 1) the N_2O pathway, 2) the prompt-NO mechanism, 3) the NNH pathway and 4) the thermal-NO pathway. When the pressure increases, the N_2O pathway contribution increases while the NNH pathway decreases, and the thermal-NO pathway remains almost constant. The prompt-NO pathway decreases between 0.1 and 0.3 MPa and then remains almost constant between 0.5 and 0.7 MPa.

For ϕ = 1, the contributions of the four major pathways are as follows: 1) prompt-NO; 2) thermal-NO; 3) NNH and 4) N_2O pathways at atmospheric pressure. When pressure increases, the contributions of the thermal-NO and N_2O pathways increase, and those of the prompt-NO and NNH pathways decrease.

For rich flames (ϕ=1.2) at 0.1MPa, the main pathways are: 1) prompt-NO; 2) NNH; 3) thermal-NO and 4) N_2O. The prompt-NO pathway is clearly dominant is rich flames, increasing slightly when pressure increases.

Concerning the influence of equivalence ratio, the contributions of the NNH and N_2O pathways decrease when ϕ increases. The prompt-NO pathway becomes, as expected, more important in rich flames. Note that the thermal pathway increases from lean to stoichiometric flames and decreases for rich flames.

The same analysis was done with the GRImech3.0_NOmecha2.0 mechanism, showing similar contribution of the four NO formation pathways in lean flames. However, some differences are observed between GDFkin®3.0_NOmecha2.0 and GRImech3.0_NOmecha2.0 for stoichiometric and rich flames. In stoichiometric flames at 0.1 MPa, the relative contributions are the same for both mechanisms (1) prompt-NO, 2) thermal-NO, 3) NNH and 4) N_2O). At 0.3 MPa, the main two pathways are thermal-NO and prompt-NO for both mechanisms, with the thermal-NO pathway dominating for GDFkin®3.0_NOmecha2.0 whereas the prompt pathway dominates for GRImech3.0_NOmecha2.0. For rich flames, the prompt-NO route dominates and the NNH route makes a very small contribution with both mechanisms. The thermal-NO and N_2O routes are negligible for GRIMech3.0_NOmecha2.0 whereas a small contribution of these pathways is observed for GDFkin®3.0_NOmecha2.0.

A sensitivity analysis was also performed for both mechanisms, showing that the most sensitive reactions for NO formation or consumption belong to the hydrocarbon (C-H-O) mechanism, which could explain the differences between the two mechanisms.

A publication has been recently submitted to Combustion and Flame on this work, demonstrating the validation of the NOmecha2.0 mechanism for NO prediction in high pressure flames.

Publications linked to this work:

Lamoureux N., El Merhubi H., Pillier L., de Persis S., Desgroux P., Modeling of NO formation in low pressure premixed flames, Combust. Flame 163 (2016) 557-575.

de Persis S., Pillier L., Idir M., Molet J., Lamoureux N., Desgroux P., NO formation in high pressure premixed flames: experimental results and validation of a new revised reaction mechanism, Combust. Flame, submitted.

3.3.2. CH_4-H_2-air flames

3.3.2.1. Addition of hydrogen in hydrocarbon flames

The addition of hydrogen to a hydrocarbon flame improves the burning stability, the combustion efficiency, and reduces the greenhouse gas and pollutants emissions, such as NO_x, CO_2, CO, unburnt hydrocarbons and soot particles. Blending hydrogen in the fuel allows shortening the ignition delay time [Yu et al., 2013]. As it allows the extension of flammability limits towards fuel-lean conditions [Guo et al., 2005] where the emission of NO_x is significantly reduced, ultra-lean hydrogen-enriched flames can be obtained. An illustration of the interest of hydrogen-enriched combustion is the performance testing of Hythane® fuel (registered trademark for a blend of 20% hydrogen and 80% natural gas by volume) in “test” public transport [Genovese et al., 2011; Riddel et al., 2006; Villante et al., 2012].

Theoretically, the addition of hydrogen to a hydrocarbon fuel may reduce the prompt-NO due to the decrease in hydrocarbon radicals in the flame, assuming a constant temperature. However, the addition of hydrogen may cause a rise in the flame temperature [Boushaki et al., 2012], which would result in an increase in thermal-NO formation. In addition, the NO formation from the NNH mechanism

[Guo et al., 2005] may increase compared to pure hydrocarbon flames. The combined effects of these factors determine the net influence of hydrogen addition on NO_x emission in hydrocarbon flames.

Gauducheau et al. (1998) performed a numerical study, using GRImech2.11 [Bowman et al., 1995], of the effect of including a small amount of hydrogen (20% in fuel) in lean methane-air flames at high pressure (3 MPa). They concluded that the major effect of hydrogen blending is the improved behaviour of the flame in response to strain, which indicates that the flame is able to withstand higher turbulence levels when hydrogen is included.

Rørtveit et al. (2002) reported a comparison of low-NO_x burners for combustion of methane and hydrogen mixtures. The effect of hydrogen addition to natural gas or methane on NOx emissions was found to be significantly dependent on burner type.

Naha et al. (2004) investigated numerically (using GRImech3.0 [Smith et al., 1999]) the effect of hydrogen addition on NO emissions in non premixed methane flames and showed that the observed decrease in the prompt-NO due to hydrogen addition is balanced by the corresponding increase in the thermal-NO, and the total NO is essentially unaffected by hydrogen addition.

Guo et al. (2005) investigated, by numerical simulation using the GRImech3.0 mechanism, the effect of hydrogen addition on flammability limit and NOx emissions in ultra-lean (ϕ=0.4-0.7) counterflow CH_4-air premixed flames at atmospheric pressure. The authors showed that the addition of hydrogen (0-60 % in fuel) increases NO emission in their flame conditions if the equivalence ratio is kept constant. They concluded that this rise in NO formation rate is mainly caused by the rise of the NNH intermediate route, except for the flames with a very low equivalence ratio and at lower hydrogen fraction where the increase in the N_2O intermediate route is more significant.

Coppens et al. (2007a, 2007b) measured NO_x concentrations in CH_4-H_2-O_2-N_2 atmospheric pressure laminar flat flames with varying H_2 content (from 0 to 35%), equivalence ratio (0.7-1.4) and dilution ratio ($D=O_2/(O_2+N_2)$=0.16-0.209). The authors observed that in lean flames, enrichment *by* hydrogen has little effect on NO emissions, while in rich flames the concentration of NO decreases significantly due to a reduction of the prompt-NO formation.

De Ferrieres et al. (2008) investigated, experimentally and numerically (with GDFkin®3.0 mechanism) the effect of hydrogen addition on the flame structure of a natural gas low pressure (8 kPa) premixed flame (stable species measurements with quartz probe sampling and GC/FTIR analyses). Their main conclusions are: i) the C_1 hydrocarbons oxidation sequence initiated by H-abstraction by H, OH and O from methane is favoured when H_2 is added; ii) the C_2 hydrocarbons sequence is consequently disfavoured, which reduces the mole fraction of acetylene, considered as the main PAH and soot precursor. This was also observed by Biet et al. (2007).

Sepman et al. (2008) performed NO measurements by LIF in rich premixed CH_4-H_2-air, C_2H_6-H_2-air and C_3H_8-H_2-air premixed flat flames at atmospheric pressure. They found a modest reduction of NO mole fraction with hydrogen addition (25% in fuel). This decrease in NO is more distinct in methane and propane flames than for ethane flames. Calculations indicate that the decrease in prompt-NO formation with hydrogen addition arises from the concomitant decrease in CH mole fraction.

To our knowledge, no experimental measurements of NO profiles in high pressure counterflow premixed CH_4-H_2-air flames are available in the literature. In this work, we measured NO mole fraction profiles by LIF in laminar high pressure (up to 0.7 MPa) counterflow lean CH_4-H_2-air flames. H_2 content was fixed to 20% in the fuel; i.e. $XH_2/(XH_2+XCH_4) = 0.2$ (with X the mole fraction) and the equivalence ratio was progressively decreased from 0.74 to 0.6. The experimental NO profiles were then compared with modelling using the OPPDIF code [Lutz et al.,1997] and the three detailed kinetic mechanisms: GDFkin®3.0_NCN [Lamoureux et al., 2015], GRImech 2.11 [Bowman et al., 1995] and GRImech 3.0 [Smith et al., 1999]. Calculations with the last version of our mechanism GDFkin®3.0_NOmecha2.0 are currently ongoing. To better understand the effect of hydrogen addition and the effect of reducing the equivalence ratio on NO formation, a kinetic analysis was performed based on rate of production and consumption computations. The relative contribution of each NO formation pathways (thermal-NO, prompt-NO, N_2O and NNH) is discussed hereafter.

3.3.2.2. Flame conditions

Laminar lean premixed CH_4-H_2-air flames were studied in this work, with 20% of H_2 substituted to CH_4 (i.e., $XH_2/(XH_2+XCH_4) = 0.2$, with X the molar fraction). In this case, two expressions of the equivalence ratio can be defined:

. the overall equivalence ratio: $\phi_{CH} = 2 * \left(\frac{XCH_4}{XO_2}\right) + \frac{1}{2} * \left(\frac{XH_2}{XO_2}\right)$

. and the equivalence ratio relative to methane: $\phi_c = 2 * \left(\frac{XCH_4}{XO_2}\right)$

In order to investigate the influence of hydrogen addition, we compared a CH_4-air flame with and without hydrogen addition with the same C/O ratio; i.e. ϕ_C=0.7. As mentioned above, hydrogen addition to CH_4-air flames allows to extend the flammability limits towards very lean conditions, so the equivalence ratio of the CH_4-H_2-air flames was progressively decreased (from ϕ_C=0.7 to 0.57 or ϕ_{CH}=

0.74 to 0.6). Below those values of equivalence ratios, the flames became unstable. As for our previous work [Pillier et al., 2015], the pressure was varied from 0.1 to 0.7 MPa. Flame conditions are summarised in Table 7. Note that the flame with equivalence ratio ϕ_C=0.61 could not be stabilised at 0.7 MPa and the flame with ϕ_C=0.57 was stabilised only at 0.3 MPa.

Equivalence Ratio Φ_{CH}/Φ_C	**Pressure (MPa)**	**X(CH_4)**	**X(H_2)**	**X(O_2)**	**X(N_2)**	**Total flowrate ($L.min^{-1}$) (a)**	**Inlet premixed gas Velocity ($cm.s^{-1}$) (a)**	**Burner cooled temperature (K)**	**Adiabatic flame temperature (K) (b)**
0.74/ 0.7	0.1	**0.0672**	**0.0171**	**0.1922**	**0.7235**	1.86	83.2	303	1907
	0.3					3.71	57.3	313	1917
	0.5					4.29	41.0	323	1918
	0.7					4,96	33.8	323	1919
0.7/ 0.66	0.1	**0.0638**	**0.0159**	**0.1933**	**0.7269**	1.58	70.6	303	1837
	0.3					2.79	43.1	313	1845
	0.5					3.47	33.1	323	1846
	0.7					3.99	27.2	323	1848
0.65/ 0.61	0.1	**0.0592**	**0.0148**	**0.1945**	**0.7315**	1.26	56.4	303	1754
	0.3					2.02	31.1	313	1760
	0.5					2.62	25.0	323	1762
0.6/ 0.57	0.3	**0.0555**	**0.0139**	**0.1952**	**0.7354**	1.51	23.4	313	1673

(a) Experimental conditions for the bottom burner, in standard conditions, i.e. T=273K and P=101325Pa.
(b) Flame temperature calculated for a free flame configuration using GRImech3.0

***Table 7**. CH_4-H_2-air counterflow premixed flame conditions*
Air dilution ratio is used.

3.3.2.3. Results and discussion

Figure 40 compares the experimental and calculated NO mole fraction profiles with the three mechanisms: GDFkin®3.0_NCN [Lamoureux et al., 2015], GRImech 2.11 [Bowman et al., 1995] and GRImech 3.0 [Smith et al., 1999], for all the CH_4-H_2-air flames studied in this work.

Fig. 40a)

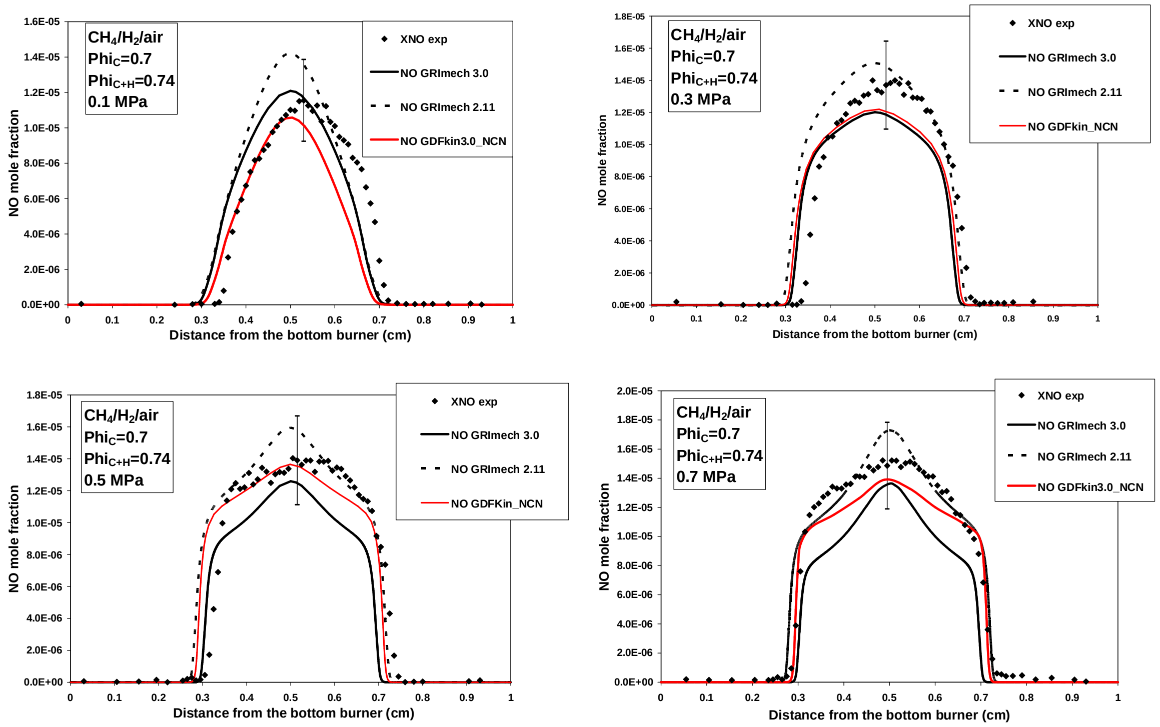

Fig. 40b)

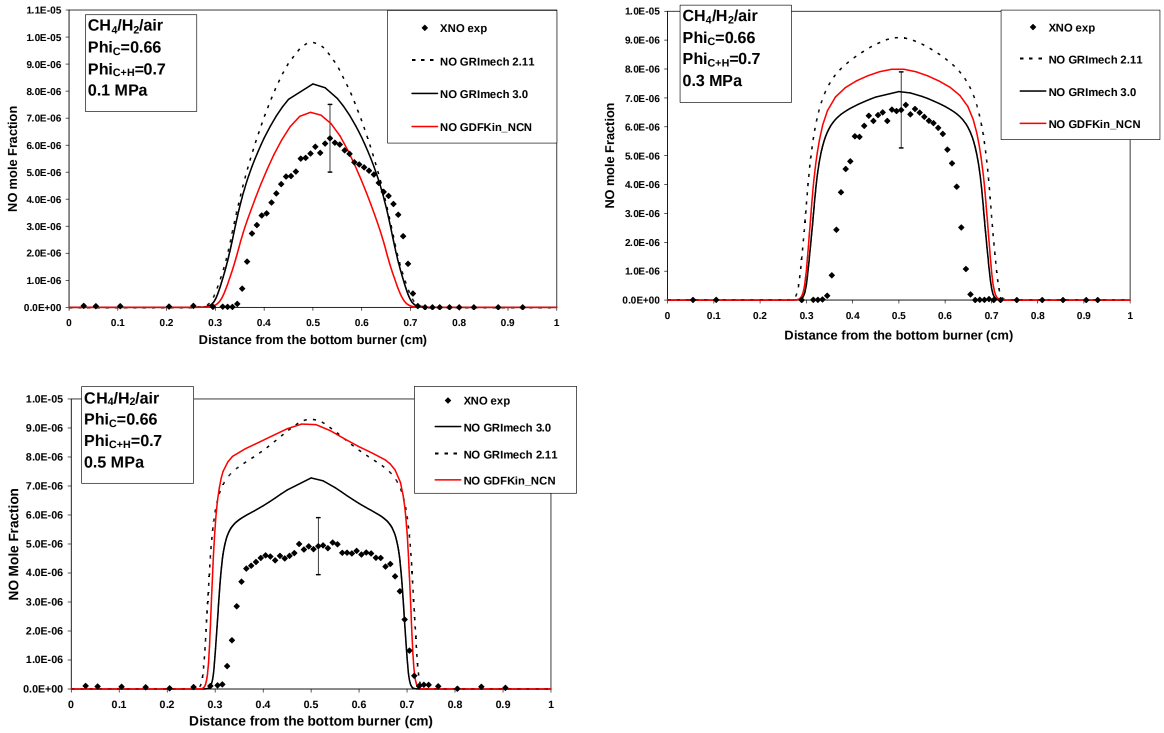

Fig. 40c)

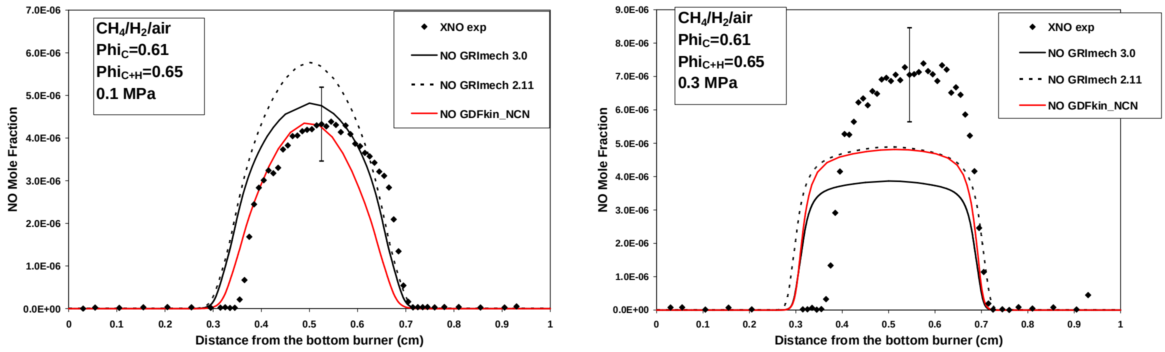

Fig. 40d)

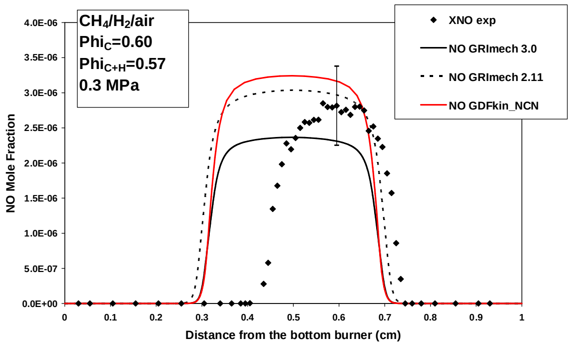

◆Experiments — GDFkin®3.0_NCN — GRImech3.0 ---- GRImech2.11

Figure 40: *Comparison between experimental and calculated NO mole fraction profiles for the CH_4-H_2-air flames:*

a) for ϕ_{CH}=0.74 at pressures from P = 0.1 to 0.7 MPa;

b) for ϕ_{CH}=0.7 at pressures from P = 0.1 to 0.5 MPa;

c) for ϕ_{CH}=0.65 at pressures P = 0.1 and 0.3 MPa;

d) for ϕ_{CH}=0.6 at 0.3 MPa.

Figure 40 shows an overall good agreement between experimental and calculated NO mole fraction profiles in all the lean CH_4-H_2-air flames at atmospheric and high pressures, using the GDFkin®3.0_NCN and the GRImech mechanisms (2.11 and 3.0), except in the flames at ϕ_c=0.66 at 0.5MPa and ϕ_c=0.61 at 0.3MPa. In the flame at ϕ_c=0.60 at 0.3MPa, discrepancies are observed for the flamefront positions. As expected, NO mole fraction decreases with equivalence ratio (almost a factor of 3 between ϕ_c=0.7 and ϕ_c=0.61 at atmospheric pressure).

In Figure 41, we compare maximum NO mole fraction in the CH_4-air flame with and without H_2 addition while keeping the equivalence ratio ϕ_c constant (ϕ_c= 0.7). The experimental results show an increase of about a factor 2 for NO mole fraction when 20% of H_2 is substituted to CH_4. A slight increase of NO mole fraction is observed when pressure increases in the flame with H_2 addition. The three mechanisms reproduce well the evolution of NO mole fraction with pressure and the influence of H_2 addition. A slight overestimation is observed in CH_4-air flames for GDFkin®3.0_NCN at pressures higher than 0.3MPa, and in CH_4-H_2-air flames for GRImech2.11.

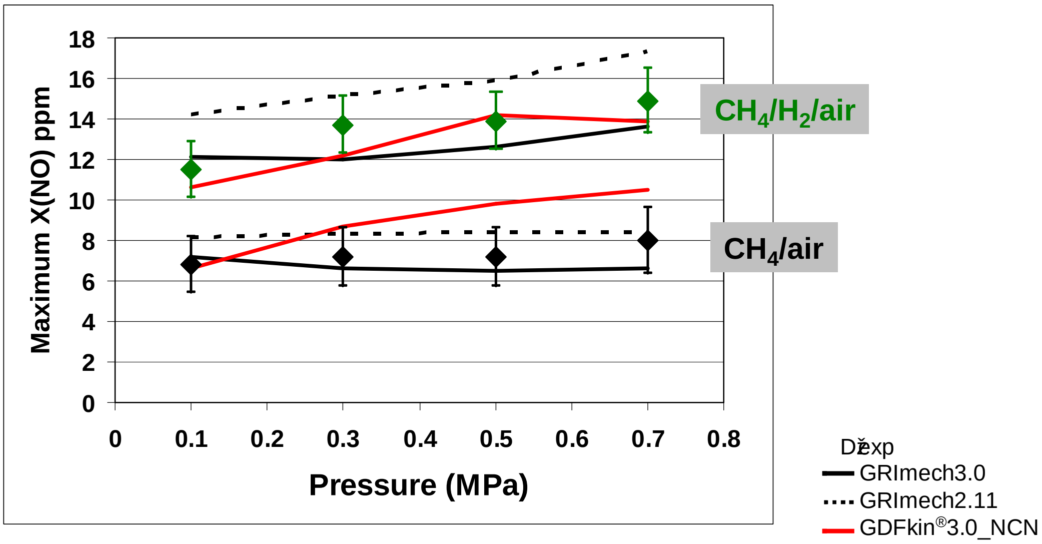

***Figure 41**: Experimental and calculated maximum X(NO) (ppm) as a function of pressure in the CH_4-air flame (ϕ_C=0.7) and the CH_4-H_2-air flame (ϕ_C=0.7; ϕ_{CH}=0.74)*

A kinetic analysis was performed for the lean (ϕ_C=0.7) CH_4-air flame with and without H_2 addition to analyse the influence of H_2 addition on NO formation pathways (prompt-NO, thermal-NO, NNH and N_2O). Rates of consumption of N_2 (NO precursor) integrated over the whole flame domain were calculated. The results are presented (in %) in Figure 42 for GRImech3.0 (Fig. 42a) and GDFkin®3.0_NCN (Fig. 42b).

For both mechanisms, the addition of H_2 leads to:

- an increase of the contribution of the NNH route (more H atoms for the reaction N_2+H = NNH);
- a decrease of the contribution of the N_2O route;
- an increase of the contribution of the thermal-NO route due to temperature increase with H_2 addition.

Concerning the prompt-NO pathway, GDFkin®3.0_NCN predicts an equivalent contribution with and without H_2, whereas GRImech3.0 predicts a slight increase of its contribution.

a)

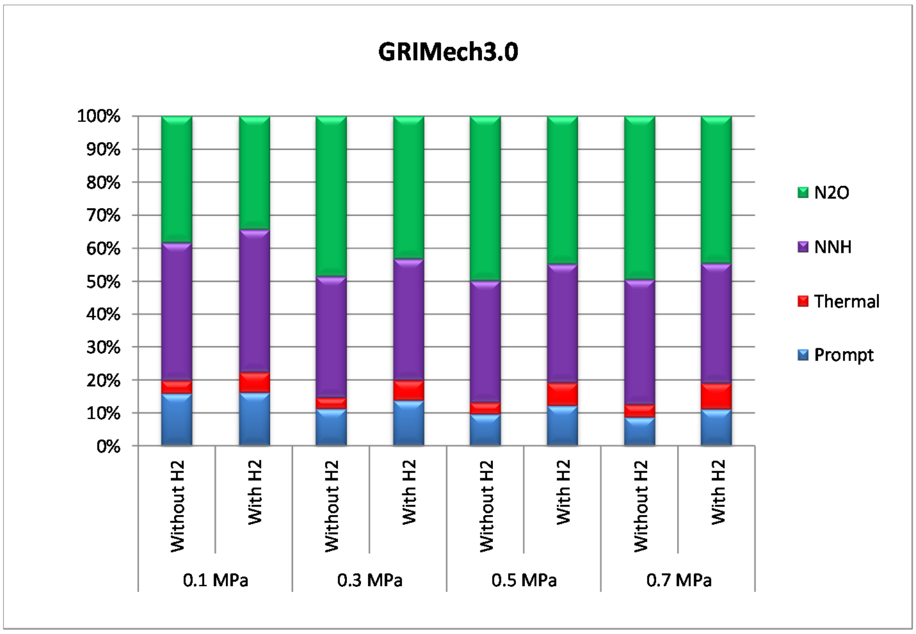

b)

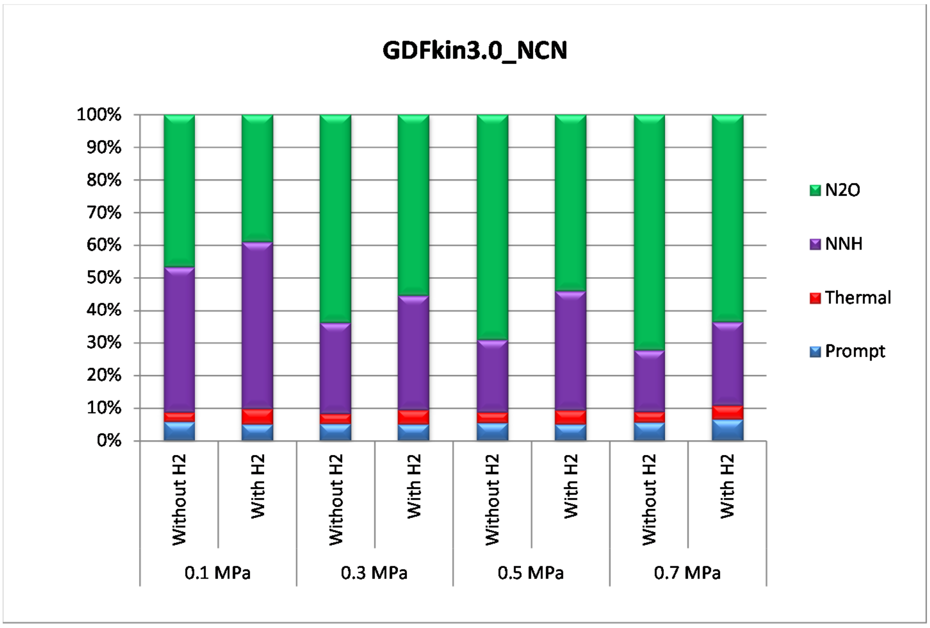

***Figure 42**: Contribution (%) of each NO formation pathways (prompt-NO, thermal-NO, N_2O, NNH) in the CH_4-air flame at ϕ_C=0.7, with and without H_2 addition: a) with GRImech3.0 mechanism and b) with GDFkin®3.0_NCN mechanism*

Part A3: NOx formation in high pressure flames

Publication linked to this work:

de Persis S., Idir M., Molet J., Matynia A., Pillier L., Effect of hydrogen addition on NOx formation in high pressure counterflow premixed CH_4/air flames, in preparation.

A4. Conclusion and perspectives

This part A of the manuscript describes my main research activities in combustion chemistry at ICARE laboratory, which focused on three main topics:

- the development of new combustion modes for cleaner energy production, demonstrating the interest in burning fuel lean mixtures and the potential of oxygen-enrichment in combustion for CO_2 capture;
- the use of biomass fuels for cleaner energy production, an extensive experimental database was obtained on syngas and biogas flames structures at atmospheric and high pressure, the high pressure burner and associated laser diagnostics were developed;
- the study of NO formation in high pressure flames with the validation of the new NOmecha2.0 mechanism at high pressure and the effect of hydrogen addition on NO formation.

My contributions to these studies combined experimental and modelling development.

My activities in combustion research continued after my transfer from ICARE to PC2A in 2013, where I joined the Atmospheric Chemistry Group to develop a project presented in the second part of this manuscript (Part B). The work undertaken during the NO-mecha project is now being finalised with the submission of two papers concerning NO formation in high pressure methane flames and the effect of hydrogen addition.

In parallel, discussions have been initiated with my colleague G. Vanhove from PC2A (lecturer / Combustion Chemistry Group / Rapid Compression Machine team) to develop a research project on plasma assisted Low Temperature Combustion (LTC, T<1000 K) with the development of a new reactor (counterflow cool flame burner).

The growing interest in automotive engines operating in fuel-lean and reduced temperature conditions, such as Partially-Premixed Compression Ignition (PPCI) or Reactivity Controlled Compression Ignition (RCCI), is motivated by a potential significant reduction in soot particles and nitrogen oxides emissions, as well as an improvement in fuel efficiency and substantial reduction in fuel consumption. In such combustion modes, the initiation of combustion is highly dependent on the chemical kinetics associated with the LTC regime, where the peroxy radicals chemistry is predominant and in which complex thermokinetic interactions take place. In the previous ANR project Plasmaflame

(2012-2016), it has been demonstrated that a single nanosecond discharge can induce premixed cool flames at pressures above the atmosphere by stimulating the LTC chemistry through the generation of a pool of radicals. The discharge induces an important reduction of the cool flame induction time, the distribution of stable intermediate products formed by the cool flame being unchanged at the millisecond timescale [Boumedhi et al., 2015; Vanhove et al., 2017]. It is therefore possible to use nanosecond discharges to reduce cool flame induction times, and make them compatible with burner studies. The dynamics of the interactions between nanosecond plasma and LTC kinetics however need some clarification at shorter timescales, and suggest the need for a reactor dedicated to these studies. A burner coupled with a carefully designed electrode system will be of great use to study these interactions in situ and at shorter timescales than those accessible until then. This project therefore focuses on building a counterflow burner designed towards detailed experimental investigation of plasma-assisted cool flames at pressures of the atmosphere and above. In contrast with previous work that was performed using a Rapid Compression Machine (RCM), this permanent regime setup will facilitate implementation of optical diagnostics (LIF) and other advanced sampling techniques, and will constitute a complementary tool to the RCM.

This project has been submitted to the ANR call of projects 2017 (PACCE project: Plasma-Assisted Counterflow Cool flamEs for better engine control, coordinator: G. Vanhove) and is now placed on the top of the complementary list ("Défi 6: Mobilité et Systèmes Urbains Durables", final result: December 2017).

It will benefit from a consortium of renowned specialists. The electrode system will be designed and characterized in the LPP (Laboratoire de Physique des Plasmas, Paris) group. The burner will be built in PC2A, where our expertise on laser diagnostics and sampling of cool flame intermediates will be used to gain quantitative insight on temperature and formation of LTC intermediates. Firstly, this burner will be operated to create ozone-seeded cool flames, which will serve as validation data for a detailed kinetic model. Secondly the burner will be coupled with the electrode developed in LPP to generate plasma-assisted cool flames. Finally, the EM2C (Laboratoire Energétique Moléculaire et Macroscopique, Combustion, Châtenay Malabry) group will develop numerical tools to model the experimental burner configuration by taking into account the physical and chemical processes of the plasma assisted burner.

In this project, I will be involved in the design of the new cool flame burner at PC2A and the development of associated diagnostics (LIF).

Part B - Atmospheric chemical kinetics: Study of the reactivity of radical species in atmospheric chemistry

B1. Context and objectives

Hydroxy OH, hydroperoxy HO_2 and peroxy RO_2 radicals play a key role in atmospheric chemistry through the radical cycle presented in Figure 43, that involves nitrogen oxides (NO and NO_2) and controls the oxidative capacity of the atmosphere, the formation of tropospheric ozone and secondary pollutants (sulfuric and nitric acids, peroxyacyl nitrates, particles, etc…).

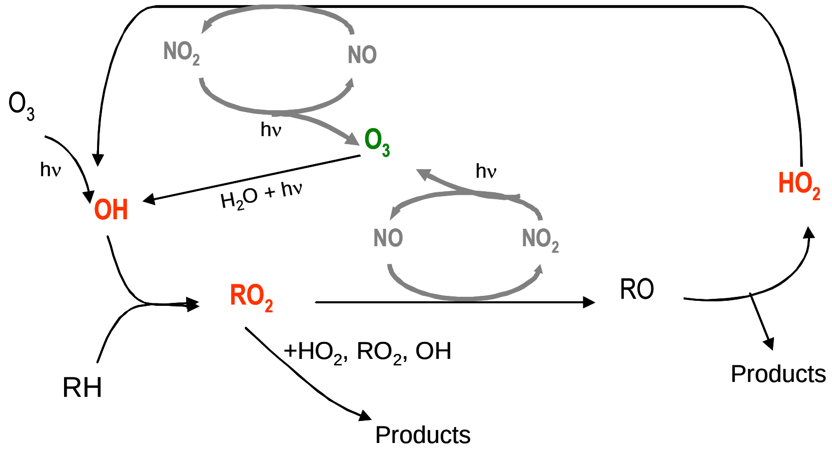

***Figure 43**: Radical reactivity cycle in the atmosphere*

OH radical is the main oxidant in the troposphere (diurnal) and it will oxidize essentially every organic species emitted (Volatile Organic Compounds VOCs from biogenic and anthropogenic sources) through the reaction:

$$RH + OH \rightarrow R + H_2O$$

The alkyl radical R· (RH is a saturated hydrocarbon) will react with oxygen to form peroxy radicals RO_2:

$$R + O_2 + M \rightarrow RO_2 + M$$

The reaction of RO_2 with NO will dominate in regions influenced by anthropogenic NOx emissions, leading to the formation of alkoxy racidals RO along with NO_2 which will be photolyzed to generate ozone O_3:

$$RO_2 + NO \rightarrow RO + NO_2$$

$$NO_2 + h3 \rightarrow NO + O(^3P)$$

$$O(^3P) + O_2 + M \rightarrow O_3 + M$$

Subsequent reactions of the alkoxy radical with O_2 present in the atmosphere leads to the formation of HO_2 and OH (via reaction of HO_2 with NO), thus completing the HOx cycle (Figure 43):

$$RO + O_2 \rightarrow R'CO + HO_2 \qquad (R'= R_{-H})$$

A minor competing reaction can occur in the RO_2/NOx reactions that lead to the formation of organic nitrates and peroxynitrates.

In pristine regions of the atmosphere (i.e., in the marine boundary layer or in remote tropical forests), where NOx concentrations are low (typically NOx < 100 pptv**)**, reactions of RO_2 with HO_2 and with other RO_2 play a larger role and contribute to the radical removal/chain termination process, forming hydroperoxide ROOH:

$$RO_2 + HO_2 \rightarrow ROOH + O_2$$

Because organic hydroperoxides are relatively stable in the atmosphere, this process is considered as a radical sink, reducing the oxidative capacity of the troposphere. However, recent experimental and theoretical studies have shown that radical termination (via reaction with HO_2) may not be the exclusive reaction pathway for certain RO_2. It can lead to three different reaction pathways [Hasson et al., 2012]:

$$\begin{array}{lcll} RO_2 + HO_2 & \rightarrow & ROOH + O_2 & (a) \\ & \rightarrow & ROH + O_3 & (b) \\ & \rightarrow & RO + OH + O_2 & (c) \end{array}$$

The pathway (c) leads to the production of OH, hence radical propagation is occurring.

Research works from the literature agree that, for simple alkylperoxy radicals (R= CH_3, C_2H_5), the reaction between RO_2 and HO_2 generates predominantly/exclusively chain-terminating hydroperoxide species [Wallington and Japar, 1990a, 1990b; Hasson et al., 2004; Raventos-Duran et al., 2007a, 2007b]. However, contradictory results are observed in recent papers, concerning the branching ratios of the three channels in the case of acylperoxy (with a C=O bound), for example in the case of acetylperoxy and propionylperoxy:

- Acetylperoxy $CH_3C(O)O_2$ which has been extensively studied until now [Hasson et al., 2004; Hasson et al., 2005; LeCrâne et al., 2006; Jenkin et al., 2007; Dillon and Crowley, 2008; Groβ et al., 2014 and Winiberg et al., 2016], for which the channel (R1c) forming OH radicals is important (with branching ratio between 5 and 50% depending on publications):

$CH_3C(O)OO + HO_2 \rightarrow CH_3C(O)OOH + O_2$ (R1a)
$\rightarrow CH_3C(O)OH + O_3$ (R1b)
$\rightarrow CH_3C(O)O + OH + O_2$ (R1c) 5-50%

- Propionylperoxy $C_2H_5C(O)O_2$ [Hasson et al., 2012]:

$C_2H_5C(O)OO + HO_2 \rightarrow C_2H_5C(O)OOH + O_2$ (R2a) 35±10%
$\rightarrow C_2H_5C(O)OH + O_3$ (R2b) 25±10%
$\rightarrow C_2H_5C(O)O + OH + O_2$ (R2c) 40±10%

Production of OH also occurs in the reactions of HO_2 with other types of peroxy species - for example, for α-carbonyl peroxy radicals like acetonyl peroxy [Hasson et al., 2004; Dillon and Crowley, 2008; Jenkin et al., 2008]

$CH_3C(O)CH_2OO + HO_2 \rightarrow CH_3C(O)CH_2OOH + O_2$ (R3a)
$\rightarrow CH_3C(O)CH_2OH + O_3$ (R3b)
$\rightarrow CH_3C(O)CH_2O + OH + O_2$ (R3c) 15-67%

Formation of OH in the case of methoxymethyl peroxy has also been confirmed [Jenkin et al., 2010]:

$CH_3OCH_2OO + HO_2 \rightarrow CH_3OCH_2OOH + O_2$ (R4a) 55±8 %
$\rightarrow CH_3OCHO + H_2O + O_2$ (R4b) 26±8 %
$\rightarrow CH_3OCH_2O + OH + O_2$ (R4c) 19±8 %

Theoretical studies [Hasson et al., 2005; Hou et al., 2005] have shown that OH production is generated by decomposition of a singlet tetroxide intermediate ROO…OOH to $RO+O_2+OH$. In the case of simple alkyl peroxy radicals (R= CH_3, C_2H_5), this process is not possible due to higher energy barriers to tetroxide decomposition.

Another important current issue in atmospheric chemistry is the determination of the HOx budget in forested areas, in particular those dominated by emissions of isoprene $CH_2=CHC(CH_3)=CH_2$, the dominant biogenic VOC emitted in the atmosphere. Because of its high reactivity with OH, isoprene influences OH reactivity and subsequent HOx chemistry. Recent effort has been done to understand the chemistry of isoprene derived peroxy radicals [Orlando and Tyndall, 2012; Teng et al., 2017], particularly in pristine regions of the atmosphere, where their fate is controlled mainly by reactions with HO_2 and self- and cross- reactions with other peroxy radicals or unimolecular reactions [Orlando and Tyndall, 2012]. It has been shown [Liu et al., 2013] that reactions of HO_2 with isoprene derived peroxy species can contribute for one half of their fate and generate OH radicals, recycling the HOx process. This chemistry is currently poorly understood.

Very recently, a new reaction pathway has been suggested as possible fate of RO_2 radicals in clean environments: the reaction of RO_2 with OH radicals. Only few studies exist on this class of reactions and to date, they are not included in atmospheric chemistry models.

A modelling study was performed by Archibald et al. (2009) to determine the influence of the reaction RO_2+OH on the trace gas composition in the Marine Boundary Layer. Seven RO_2 were considered (from CH_3O_2 to $C_4H_9O_2$) in their model with rates constants k_{RO2+OH} (between 5.10^{-11} and $1.5.10^{-10}$ $cm^3.molecule^{-1}.s^{-1}$) estimated from previous works [Biggs et al., 1997; Daële and Poulet, 1996]. It was found that the inclusion of such reactions had negligible effect on the mixing ratios of O_3, NOx, OH and other trace gas species. However, an important effect was observed, depending on reaction products, for HCOOH and CH_3OH and a moderate effect on HO_2 formation.

The rate constants have been measured recently for the first time for the reactions of the two simplest peroxy radicals CH_3O_2 and $C_2H_5O_2$ with OH, using a laser photolysis cell by Christa Fittschen's group at PC2A [Bossolasco et al., 2014; Farago et al., 2015; Assaf et al., 2016a, 2017a]. High rate constants were found at 298K: $k_{CH3O2+OH}= (2.8\pm1.4).10^{-10}$ $cm^3.molecule^{-1}.s^{-1}$ [Bossolasco et al., 2014] and $k_{C2H5O2+OH}=(1.2 \pm 0.3).10^{-10}$ $cm^3.molecule^{-1}.s^{-1}$ [Farago et al., 2015]. The rate constant for CH_3O_2 has been later revised to a lower value $k_{CH3O2+OH}= (1.6 \pm 0.4).10^{-10}$ $cm^3.molecule^{-1}.s^{-1}$ [Assaf et al., 2016a]. It was also recently measured by Yan et al. (2016) in a laser photolysis reactor, an even lower value $k_{CH3O2+OH}= (0.84 \pm 0.17).10^{-10} (T/298\ K)^{-0.81}$ $cm^3.molecule^{-1}.s^{-1}$ (292-526 K) has been found. Fittschen et al. (2014) have included this reaction into the Leeds Master Chemical Mechanism (MCM)

[Whalley et al., 2010] using data from a field campaign at Cape Verde Island, representative for the tropical remote ocean, and it was found that this reaction (using the rate constant from [Bossolasco et al., 2014]) represents around 25% of the overall sink for CH_3O_2.

The three possible products channels for the reaction CH_3O_2+OH are:

CH_3O_2 + OH → $CH_2OO + H_2O$ (R5a)
$CH_3O + HO_2$ (R5b)
$CH_3OH + O_2$ (R5c)

This reaction was recently investigated by ab initio calculations [Bian et al., 2015; Müller et al., 2016] and the (R5b) pathway was found to be the major reaction under remote conditions, with possible minor contribution of (R5c), whereas the channel (R5a) producing the Criegee Intermediate CH_2O_2 was found to be negligible. Assaf et al. (2017a) also found that (R5b) forming HO_2 is the major channel with a yield of 80±20 % and an upper limit for (R5a) of 5 % was determined, suggesting a minor yield for methanol formation (R5c).

In conclusion, reactions between RO_2, HO_2 and OH are (or not) included in the chemical mechanisms of atmospheric models and the uncertainties and/or lack of data on reaction rates and branching ratios can lead to important errors on modelling of ozone and radicals concentrations in the atmosphere. New experimental results, with a more detailed characterisation of radicals and products, are then clearly needed.

The aim of this project is the development of a new experimental device to study reactions between RO_2, HO_2 and OH, and to measure the rate constants and branching ratios. The new setup consists of a fast flow tube (several $m.s^{-1}$) coupled to two laser diagnostics: Laser Induced Fluorescence (LIF) for OH radicals measurements, continuous wave-Cavity Ring Down Spectroscopy (cw-CRDS) for HO_2 radicals measurements; and Mass Spectrometry analysis associated with Molecular Beam (MB/MS) sampling for stable species measurements. The coupling between those three techniques with a fast flow reactor is done, as far as we know, for the first time.

This scientific project is part of the Labex CaPPA (Chemical and Physical Properties of the Atmosphere, 2012-2019, WP1 : From gas phase to aerosols: biogenic volatile organic compounds (BVOCs) as precursors for particles) and the CPER project Climibio (Changement climatique, dynamique de l'atmosphère et impacts sur la biodiversité et la santé humaine, 2014-2020, WP1 : Méthodes d'évaluation de la qualité et du changement des milieux). We have obtained a PhD Fellowship (50% Labex CaPPA + 50% Lille 1 University) for F. Kravtchenko (2016-2019) who I co-supervised with C. Fittschen.

B2. Experimental setup development and validation

2.1. Description of the flow reactor and coupling with experimental techniques

2.1.1. Flow reactor

The fast flow reactor technique is known to be well adapted for kinetic studies of elementary reactions, and particularly radical + radical reactions. Rate constants are generally measurable in the range 10^{-14} - 10^{-10} $cm^3.molecule^{-1}.s^{-1}$ in a temperature range usually varying from 200 to 1000 K. This technique is used at low pressure (<1.33 kPa (10 torr), for viscous and laminar flow conditions). The determination of kinetic parameters is usually done using the pseudo-first order approximation where one of the reactant is in excess compared to the other one, its concentration is therefore considered as constant during the reaction.

Our reactor (Figure 44) includes a fixed stainless steel tube (75 cm length and 2.5 cm inner diameter) and an injector (in Pyrex, 83 cm length and 0.8 cm i.d.) which can be moved relative to the main tube allowing the variation of the reaction time between the two reactants. The flow in the reactor is viscous and laminar, comparable to a plug flow reactor, then the reaction time t can be defined by the relation:

$$t = \frac{d}{V} \qquad \textit{Equation 6}$$

where d is the distance between the injector and the end of the fixed tube and V the mean flow velocity in the reactor.

Radicals are generated by microwave discharge (2450 MHz – 200W max, Sairem GMS200W) in both tubes, which are coated with Halocarbon® wax to minimize the heterogeneous loss of radicals on the walls. The pressure in the reactor is maintained between 0 and 1.33 kPa (10 torr) using a rotary vane pump (UNO 120, Pfeiffer) and controlled by a Baratron® pressure gauge. Reactants are highly diluted in Helium.

To control the temperature in the reactor, it is enclosed in a double wall cylinder with a cooling or heating circulation system. The end of the reactor is provided with an optical cell with five optical accesses for LIF and cw-CRDS measurements and a sampling cone for MB/MS measurements.

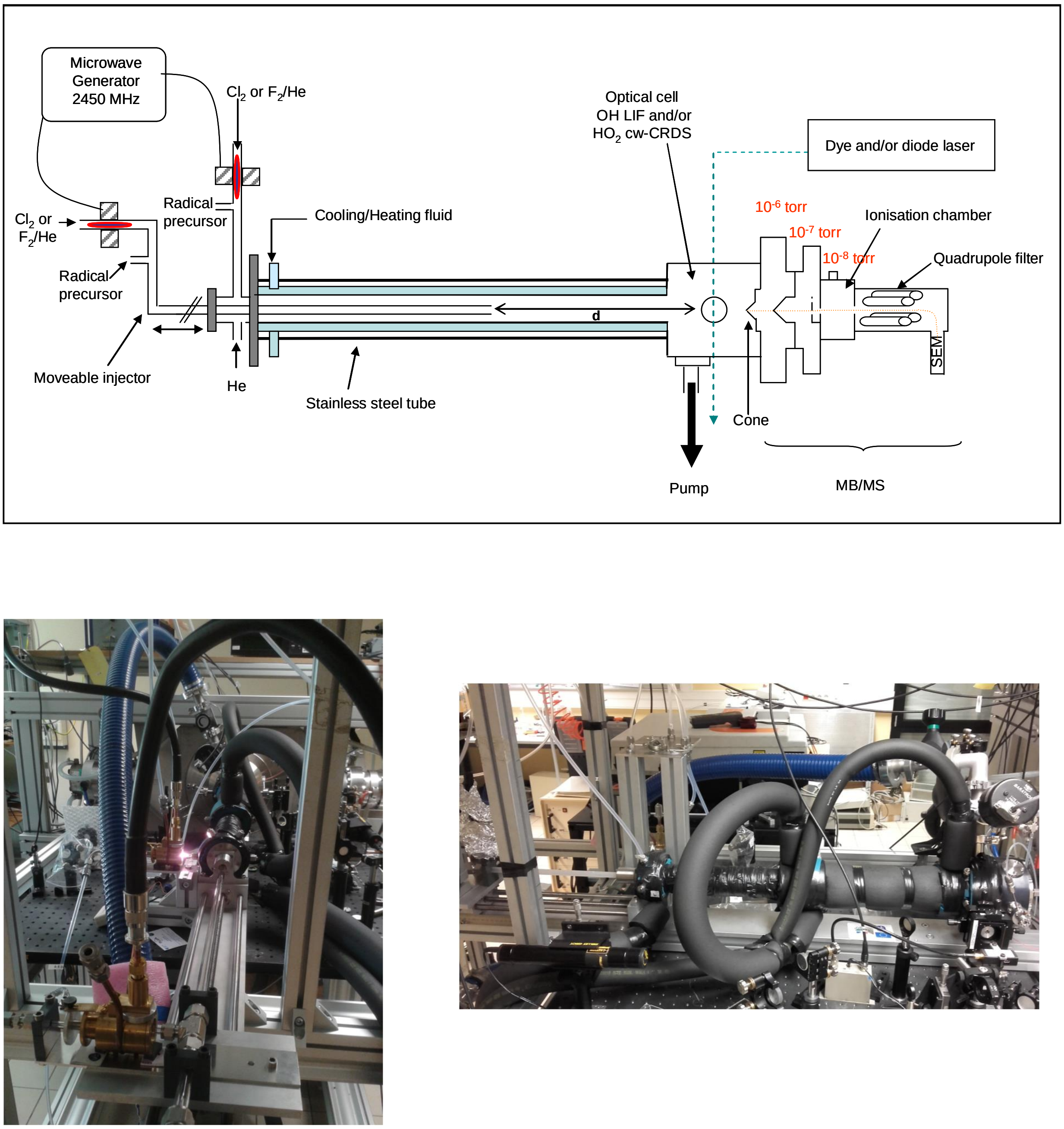

***Figure 44**: Schematic view and pictures of the reactor*

2.1.2. cw-CRDS technique

The Cavity Ring Down Spectroscopy is a multi-paths absorption technique which allows the quantitative measurement of molecular or radical species with high sensitivity. Its principle is based on the trapping of photons from a pulsed or a continuous laser into a resonant optical cavity composed of two mirrors M (with high reflectivity R>99.995%) separated by a distance L (Figure 45).

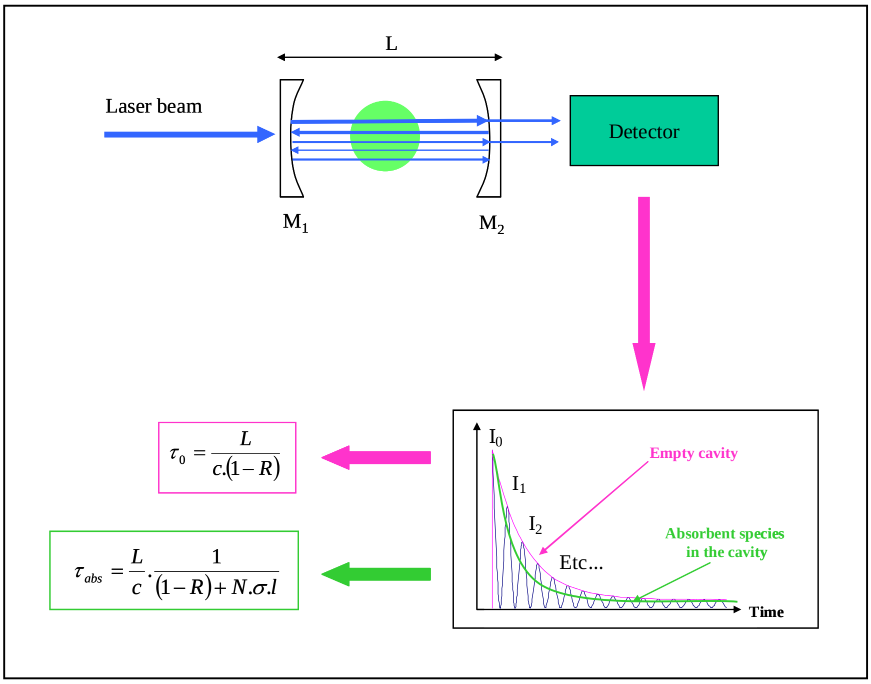

***Figure 45**: Schematic of principle of the CRDS technique*

The incoming laser beam is injected through the front mirror (M_1) and only a small fraction of photons enters inside the cavity, the other part is reflected at the entrance. Then, the beam is reflected on both mirrors and, at each round trip, a part of the light is transmitted through the back mirror (M_2). A detector is placed behind the back mirror to measure the intensity of the transmitted light after each round trip. This intensity decays exponentially over time (because of losses due to mirrors transmission, diffusion and absorbent species present in the cavity):

$$I(t) = I_0.\exp\left(-\frac{t}{\tau}\right) \qquad \textit{Equation 7}$$

With I_0 : intensity transmitted at time t_0

$I(t)$: intensity transmitted over time

τ : ring down time (lifetime of photons in the cavity)

In an empty cavity, the ring-down time τ_0 (in s) is equal to:

$$\tau_0 = \frac{L}{c.(1-R)} \qquad \textit{Equation 8}$$

With L : cavity length (m)

c : celerity ($m.s^{-1}$)

R : mirrors reflectivity coefficient

If absorbent species are present inside the cavity, additional losses induce a faster exponential decay. Considering species with a concentration *N* (in $molecules.cm^{-3}$) and an absorption cross-section σ (in cm^2), the ring-down time τ_{abs} (in s) can be written as:

$$\tau_{abs} = \frac{L}{c}.\frac{1}{(1-R)+N.\sigma.l} \qquad \textit{Equation 9}$$

With l : absorption path length (m)

The absorption coefficient α (in $molecule.cm^{-1}$) is then defined as:

$$\alpha = N.\sigma = \frac{R_l}{c}.\left(\frac{1}{\tau_{abs}} - \frac{1}{\tau_0}\right) \qquad \textit{Equation 10}$$

With R_l : ratio between the cavity length L and the absorption path length *l*.

Knowing the absorption cross-section σ of a given species at a particular wavelength, its absolute concentration can be calculated by measuring τ_{abs} and τ_0.

The cw-CRDS technique is well adapted for the measurement of HO_2 radicals for which absorption cross-sections are very low ($\approx 10^{-19}$ cm^2) in the near-IR region. The laser source used is a Distributed Feed-Back (DFB) laser diode (6629 ± 17 cm^{-1}, 20mW); it is continuous and spectrally very thin (less than one free spectral range of the cavity) compared to pulsed laser sources (Figure 46). The resonance will take place when the laser emission coincides with one mode of the cavity (mono-mode excitation TEM_{00}); this is done by periodic modulation of the cavity length using a piezo-electric transducer (full displacement: 5 µm) glued to the front mirror of the cavity. When resonance occurs, the light builds up inside the cavity and hence the light intensity transmitted through the back mirror increases. An acousto-optic modulator (AOM) is used to interrupt (order 1) very rapidly the light source at a preset threshold value to observe the exponential decay of the light intensity.

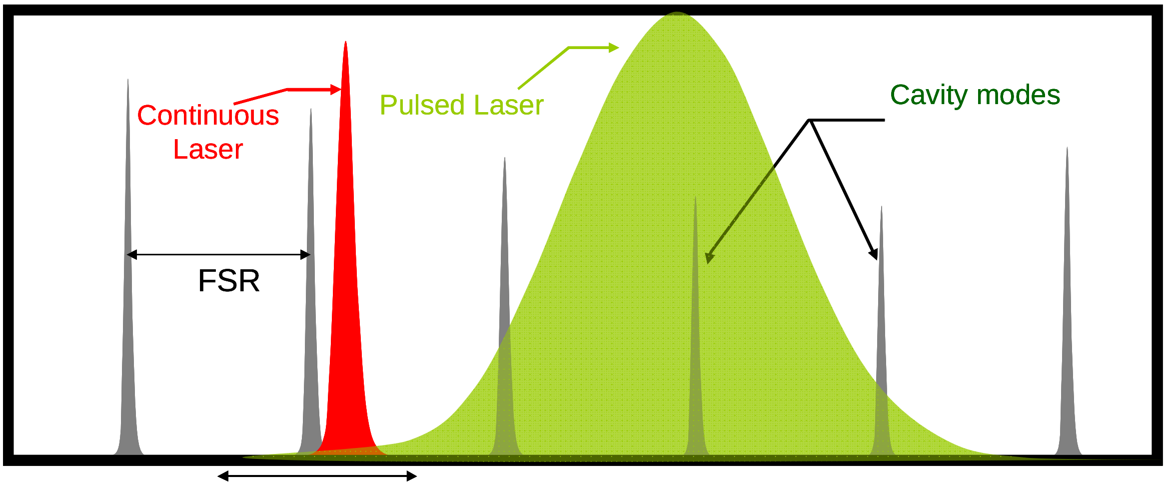

***Figure 46**: Comparison between bandwidths of continuous and pulsed laser and cavity modes [Jain, 2011]*

A simplified schematic view of our experimental setup for cw-CRDS is shown in Figure 47. In order to control the wavelength, 1% of the laser source energy is directed to a wavemeter and 99% to the cavity. The beam passes through a focus lens (f=10 mm) for mode matching (beam waist at the centre of the cavity) and then through the AOM. Two return mirrors are placed between the lens and the cavity to control the propagation of the laser beam. At the exit of the cavity, a lens (f=40 mm) is used to focus the beam on an avalanche photodiode converting the signal into current. A homemade amplifier threshold detector converts the current signal into voltage and triggers the AOM when the cavity comes into resonance and the photodiode signal passes a user-defined threshold. Wedged mirrors are used here in order to avoid interferences from the back surface of the mirrors, the use of such mirrors needs a careful and time consuming procedure of alignment [Assaf, 2017b]. The distance between the cavity mirrors is 23.3 cm. A Helium flow is injected at the mirrors surfaces in order to protect them from deposit and reduce the absorption path length to the flow reactor diameter, i.e. 2.5 cm.

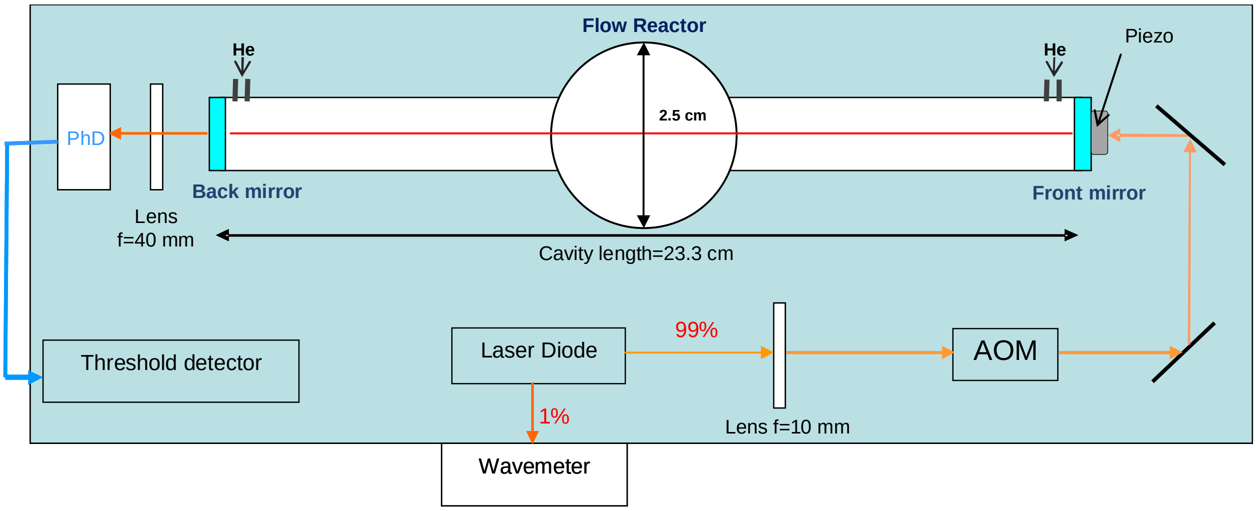

Figure 47*: Schematic view of the cw-CRDS experimental setup*

2.1.3. LIF technique

The LIF technique is well adapted for the measurement of OH radicals (detection limit ≈ 10^7-10^8 molecules.cm^{-3}) in the UV region, for which spectroscopy is well known. As mentioned earlier in this manuscript, LIF gives a signal proportional to OH concentration. A schematic view of our LIF experimental setup is represented in Figure 48. OH is excited through the $A^2\Sigma^+$-$X^2\Pi$ (1,0) vibrational band near 282 nm (Q_1(1) line), using a tuneable dye laser (Quantel TDL50) pumped at 532 nm by a Nd:YAG pulsed laser (Quantel YG981, repetition rate: 10 Hz). The red shifted fluorescence is collected perpendicular to the laser axis near 308 nm using two lenses and an interference filter (308 ± 5 nm) and detected by a photomultiplier (Hamamatsu R928). A part of the laser beam is collected by a fast photodiode in order to monitor the laser beam energy fluctuations.

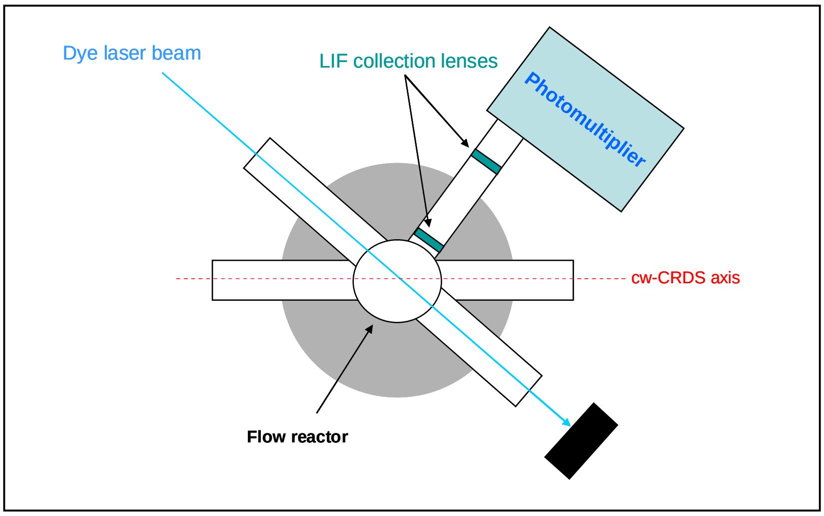

***Figure 48**: Schematic view of the LIF experimental setup*

2.1.4. Molecular beam/Mass spectrometry technique

The Molecular Beam/Mass Spectrometry (MB/MS) technique allows the analysis of both stable and reactive species after sampling and cooling in a molecular jet. The system implemented here was previously used for low pressure flame structure studies at PC2A [Crunelle et al., 1997; Turbiez et al., 1999], it was adapted to the flow reactor geometry (Figure 49).

The gas is sampled through a 45° quartz cone (orifice diameter 600 μm). The molecular beam is formed by a differential pumping between three stages using turbomolecular and diaphragm pumps (with pressure of $10^{-6}/10^{-7}/10^{-8}$ torr in each stage). A stainless steel skimmer (orifice diameter of 800 μm) is placed between the first and the second stage to sample the centre of the beam; it is placed at 1.6 cm from the first sampling cone tip to preserve the free molecular flow regime. A chopper is placed behind the skimmer for modulation of the molecular beam (discrimination between background noise and molecular beam signal) at a 10 Hz frequency. The molecular beam is then collimated through an orifice of 3 mm in the ionisation chamber (third stage). The species present in the molecular beam are analysed by a quadrupole mass spectrometer (Hiden PIC 1000, 512 uma). Ions are produced by electron impact (0-150 eV), extracted, focused, and accelerated by fields up to the quadrupole filter to be separated according to their mass. Ionisation energy can be selected to limit interferences from fragmentation of higher mass species or overlapping of species with the same m/z.

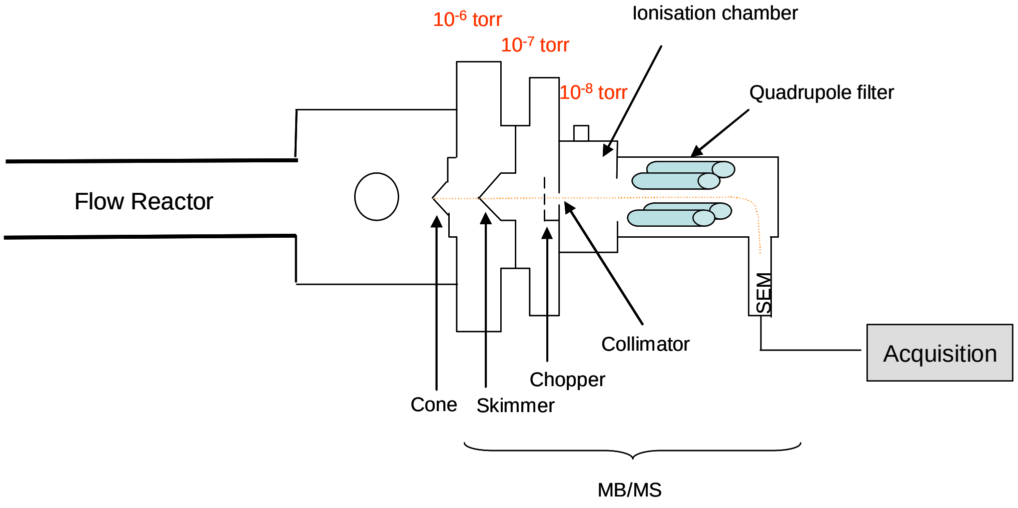

***Figure 49**: Schematic view of the MB/MS experimental setup*

The design of the reactor and coupling with the three techniques was performed with the help of S. Batut (Engineer at PC2A) and O. Hombert (mechanical engineer). This system is complementary to the existing setup at PC2A, combining a photolysis cell to cw-CRDS and LIF techniques. We have started to implement it in 2015. Different tests (not detailed in this manuscript) have then been performed concerning the reactor part itself (pumping limit, leaking tests, temperature homogeneity, implementation of the discharge system for radical generation, etc…) and the coupling with each technique (cw-CRDS, LIF and MB/MS) was undertaken. The cw-CRDS and LIF techniques are now operational, the validation of these techniques are presented below, as well as the first measurements performed with the new mass spectrometer (Hiden). This work was done during the Master II internship and the first year of PhD (2016-2019) of F. Kravtchenko who I co-supervised with C. Fittschen.

2.2. HO_2 radical measurement by cw-CRDS: validation

The cw-CRDS technique was first validated on a stable species, methane, which presents absorption bands in our laser diode wavelength range (6629 ± 17 cm^{-1}). CH_4 cw-CRDS measurements were performed with different known concentrations of CH_4 (in He) in the reactor at a total pressure of 0.27 kPa (2 torr), using the absorption line at 6640.72 cm^{-1} with an absorption cross section $\sigma_{2torr,\ 298K}$= $2.16.10^{-23}$ cm^2 [Frankenberg et al., 2008; Campargue et al., 2010]. As an example, Figure 50 represents a cw-CRDS spectrum (τ versus wavenumber) with (τ_{CH4}) and without (τ_0) methane present in the reactor. The concentration calculated from the measurement of τ_{CH4} and τ_0 (Equation 10) was equivalent to the concentration of CH_4 introduced in the reactor within 5% error.

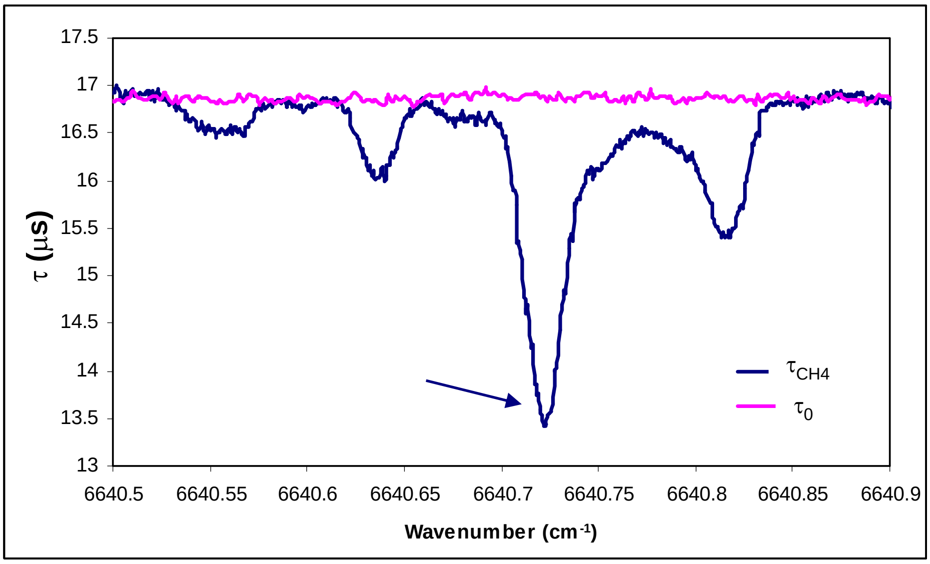

Figure 50: *cw-CRDS spectrum with (τ_{CH4}) and without (τ_0) methane in the reactor*
Total pressure = 0.27 kPa, T=293K

As mentioned earlier, a He flow is injected at the CRDS mirrors surfaces (Figure 47) in order to protect them from deposit and also to control the absorption path length, which is a critical parameter needed to calculate the concentration of a species (Equation 10). We studied the evolution of the absorption path length (at known concentrations of CH_4) as a function of the He flow on the mirrors (Figure 51). Figure 51 shows that the absorption path length decreases as He flow is increased. From a He flow of ≈ 100 sccm, the absorption path length reduces to 2.5 cm which is the reactor inner diameter. Above this value the absorption path length remains constant due to the fast flow in the reactor section (about 1.5 slpm).

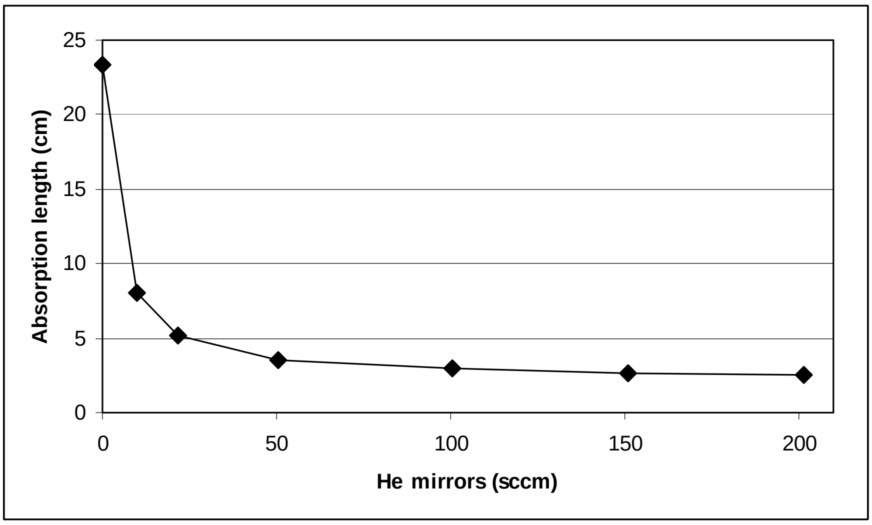

***Figure 51**: Absorption path length versus He flow on the cw-CRDS mirrors*

HO_2 measurements were then performed using the absorption line at 6638.20 cm^{-1} (the most important absorption line in the $2\nu_1$ band of HO_2), which is not perturbed by other absorbing species and for which the absorption cross section is well known [Thiébaud et al., 2007]: $\sigma_{2torr,\ 298K} = 3.09.10^{-19}$ cm^2.

HO_2 radicals can be generated in the reactor in different ways:

- From methanol and chlorine atoms in presence of oxygen:

Cl atoms are produced by passing a 1% Cl_2/He mixture through the microwave discharge

$Cl_2 \rightarrow 2\ Cl$

$CH_3OH + Cl \rightarrow CH_2OH + HCl$ $k_{298K} = 5.5 \times 10^{-11}$ $cm^3.molecule^{-1}.s^{-1}$ [Atkinson et al., 2004]

$CH_2OH + O_2 \rightarrow CH_2O + HO_2$ $k_{298K} = 9.6 \times 10^{-12}$ $cm^3.molecule^{-1}.s^{-1}$ [Atkinson et al., 2004]

- From methanol and fluorine atoms in presence of oxygen:

F atoms are produced by passing a 1% F_2/He mixture through the microwave discharge

$F_2 \rightarrow 2\ F$

$CH_3OH + F \rightarrow CH_2OH + HF$ $k_{298K} = 6.64 \times 10^{-11}$ $cm^3.molecule^{-1}.s^{-1}$ [Atkinson et al., 2004]

$CH_3OH + F \rightarrow CH_3O + HF$ $k_{298K} = 9.96 \times 10^{-11}$ $cm^3.molecule^{-1}.s^{-1}$ [Atkinson et al., 2004]

with a branching ratio 0.4:0.6 for CH_2OH:CH_3O channels [Khatoon and Hoyermann, 1988 ; Dobé et al., 1994].

$CH_2OH + O_2 \rightarrow CH_2O + HO_2$ $k_{298K} = 9.6 \times 10^{-12}$ $cm^3.molecule^{-1}.s^{-1}$ [Atkinson et al., 2004]

$CH_3O + O_2 \rightarrow CH_2O + HO_2$ $k_{298K} = 1.92 \times 10^{-15}$ $cm^3.molecule^{-1}.s^{-1}$ [Atkinson et al., 2004]

- From hydrogen peroxide and fluorine atoms:

$F_2 \rightarrow 2\,F$

$H_2O_2 + F \rightarrow HO_2 + HF$ $k_{298K}=4.98\times10^{-11}$ $cm^3.molecule^{1}.s^{-1}$ [Walther and Wagner, 1983]

To obtain a stable concentration of H_2O_2, we use a solid urea hydrogen peroxide adduct (Aldrich) mixed with sand (SiO_2, Aldrich) to reduce crust formation. The mixture is kept in a flask placed in a temperature-regulated water bath maintained at temperature between 40 and 50 °C. A flow of He is flushed through the flask to carry H_2O_2 into the reactor. The water bath temperature is varied to change the decomposition velocity of the H_2O_2−urea complex and thus change the concentration of H_2O_2 in the gas phase [Ludwig et al., 2006; Hong et al., 2009; Assaf and Fittschen, 2016].

Those different methods to generate HO_2 radicals in our reactor were tested and we found that the one using H_2O_2 urea was the easiest and most stable and reproducible method. As an example, a HO_2 cw-CRDS spectrum is represented in Figure 52, with (τ_{HO2}) and without (τ_0) microwave discharge for a concentration of $HO_2 \approx 2.10^{12}$ $molecule.cm^{-3}$.

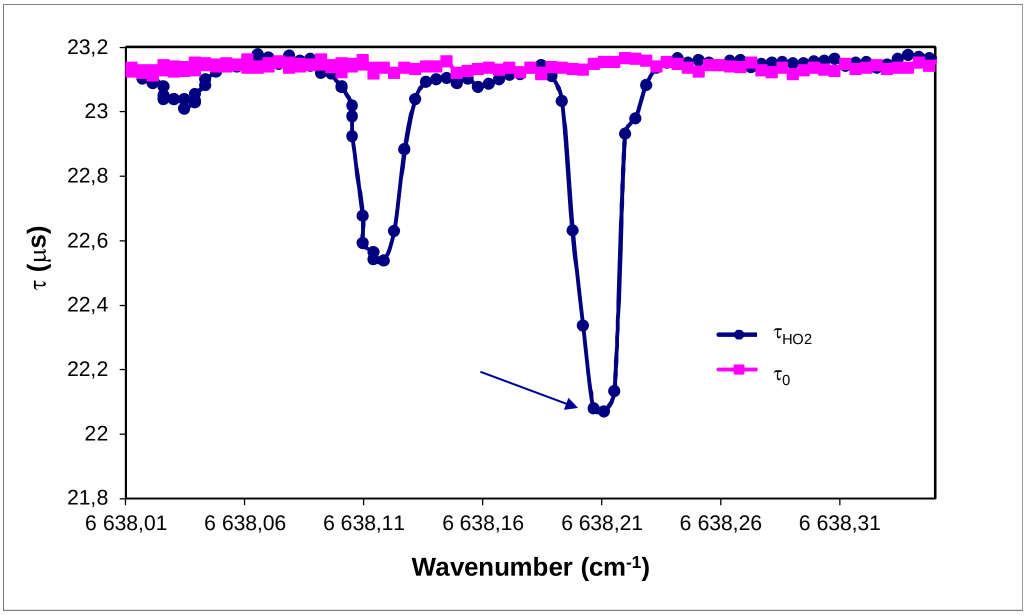

***Figure 52**: HO_2 cw-CRDS spectrum with (τ_{HO2}) and without (τ_0) microwave discharge*
Total pressure = 2 torr, T=293K

As mentioned in section 2.1.1., the walls of the reactor are coated with Halocarbon wax to limit the loss of radicals on the walls. This was checked by measuring the HO_2 concentration at different positions of the injector compared to the optical axis (which is a representation of the contact time between HO_2 radicals, generated in the injector, and walls of the reactor). Results, presented in Figure 53, show only a slight decrease of $[HO_2]$ while increasing the contact time; losses are less than 10%.

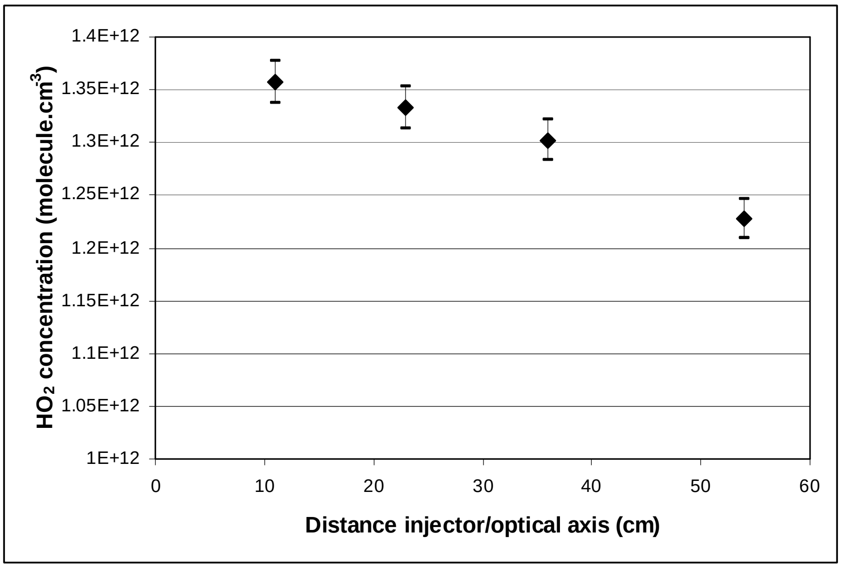

***Figure 53**: HO_2 concentration as a function of the position of the injector compared to the optical axis*

2.3. OH radical measurement by LIF: validation

To generate OH radicals in the reactor, we use H_2O as a precursor with fluorine (1%F_2/He) in the microwave discharge for the production of F atoms:

$F_2 \rightarrow 2\,F$

$H_2O + F \rightarrow OH + HF$ $k_{298K}=1.40\times10^{-11}$ $cm^3.molécule^1.s^{-1}$ [Atkinson et al., 2007]

We first chose to study the reaction of OH radicals with a stable molecule: propane. The reaction rate of the reaction $C_3H_8 + OH \rightarrow C_3H_7 + H_2O$ is well documented in the literature [Baulch et al., 1985; Abbat et al., 1990; Donahue et al., 1998]. To measure the rate constant, OH radicals are produced in the injector (with concentrations of ≈ 1.10^{12} $molecule.cm^{-3}$) and propane is injected in the reactor with a concentration in excess compared to [OH] (from 2.10^{13} to 1.10^{14} molecule.cm^{-3}). OH consumption was followed by LIF (signal proportional to [OH]) as a function of the reaction time, for different concentrations of propane. We also measured OH without propane to determine the first order rate constant for reaction of OH radicals with the walls of the reactor k_w ($\approx$ 6.5 s^{-1}). Figure 54 represents Ln[OH]= f(t) (Ln [OH]= - k't + constant, k' pseudo first order rate constant) for different concentrations of C_3H_8. From these results we can plot the pseudo first order rate constant $k' = k_{C3H8+OH} \times [C_3H_8] + k_w$ as a function of $[C_3H_8]$ to obtain $k_{C3H8+OH}$ (Figure 55). We found a rate constant $k_{C3H8+OH} = 6.6 \times 10^{-13}$ cm^3.molecule^{-1}.s^{-1}, which is lower by about a factor of 2 compared to the results from the literature (see Table 8). The consumption of OH is too slow in our conditions, we suspect a problem of mixing between H_2O and F atoms in the injector for the production of OH radicals and/or contribution of secondary chemistry and OH wall losses inside the injector itself. Different tests are currently performed to solve these problems.

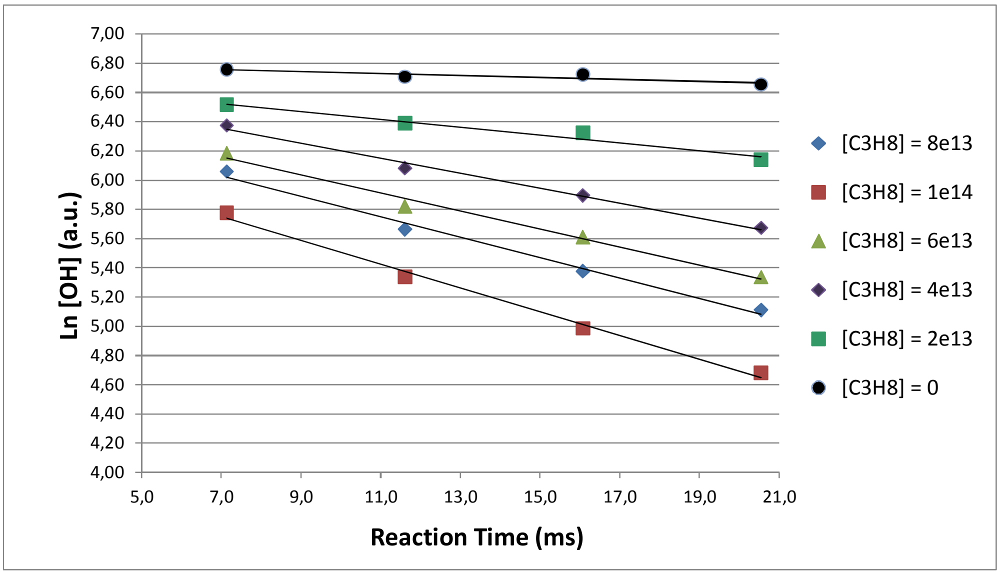

***Figure 54**: Ln[OH] (a.u.) as a function of reaction time (ms) for different concentrations of $[C_3H_8]$ (molecule.cm^{-3})*

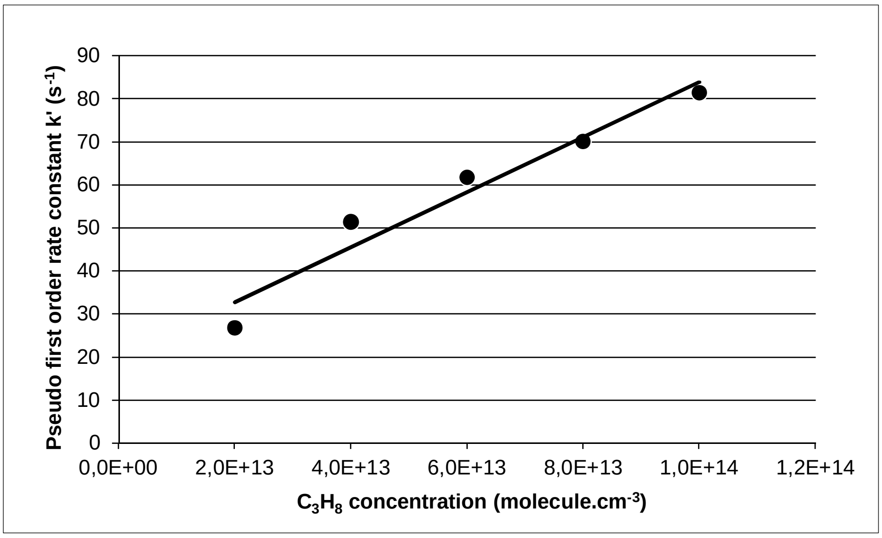

***Figure 55**: Pseudo first order rate constant k' (s^{-1}) as a function of C_3H_8 concentration (molecule.cm^{-3})*

$k_{CH3OH+OH}$ (cm^3.molecule^{-1}.s^{-1})	Temperature (K)	Reference
1.20 (±0.18).10^{-12}	295 ± 2	Baulch et al., 1985
1.21 (±0.10).10^{-12}	297 ± 2	Abbatt et al., 1990
1.09 (±0.03).10^{-12}	300	Donahue et al., 1998

***Table 8**: Rate constants for the reaction C_3H_8+OH from the literature*

(measurements performed in a discharge flow tube)

2.4. First measurements by Molecular Beam/Mass Spectrometry

The new mass spectrometer Hiden (Hiden PIC 1000) was firstly used to determine the dissociation rate of F_2 in the microwave discharge by measuring the signal at m/z=38 with and without discharge, as illustrated in Figure 56. This experiment was performed for different concentrations of F_2 in both microwave discharges (reactor and injector). We measured a dissociation rate of 74(± 10)%; this value is further used to calculate the initial concentrations of radicals in our experiments.

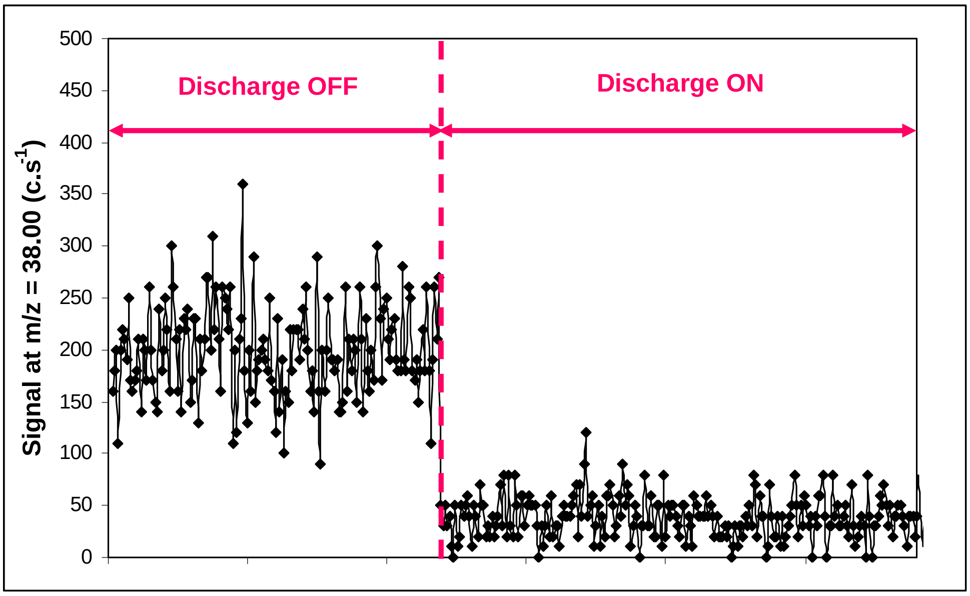

***Figure 56**: Signal at m/z=38 with and without microwave discharge*

As for the validation of the cw-CRDS or LIF techniques, we have tested the response of the mass spectrometer with a stable molecule: CH_4, by studying the reaction:

$CH_4 + F \rightarrow CH_3 + HF$ $k_{300K}= 6.35\times10^{-11}$ $cm^3.molecule^1.s^{-1}$ [Atkinson et al., 2004]

We measured the signals at different m/z = 15 (CH_4), 20 (HF) and 38 (F_2), with and without discharge and with and without CH_4 (in excess), as illustrated in Figure 57. With the discharge ON (production of F atoms) and CH_4, we can clearly see the consumption of CH_4 and formation of HF. The linear response of the mass spectrometer when increasing CH_4 concentration was checked, demonstrating a correct operation of the mass spectrometer. However, the detection limit was found to be between ≈ 5.10^{12} and 1.10^{13} $molecule.cm^{-3}$ depending on species (and m/z); further investigations are needed to improve the sensitivity.

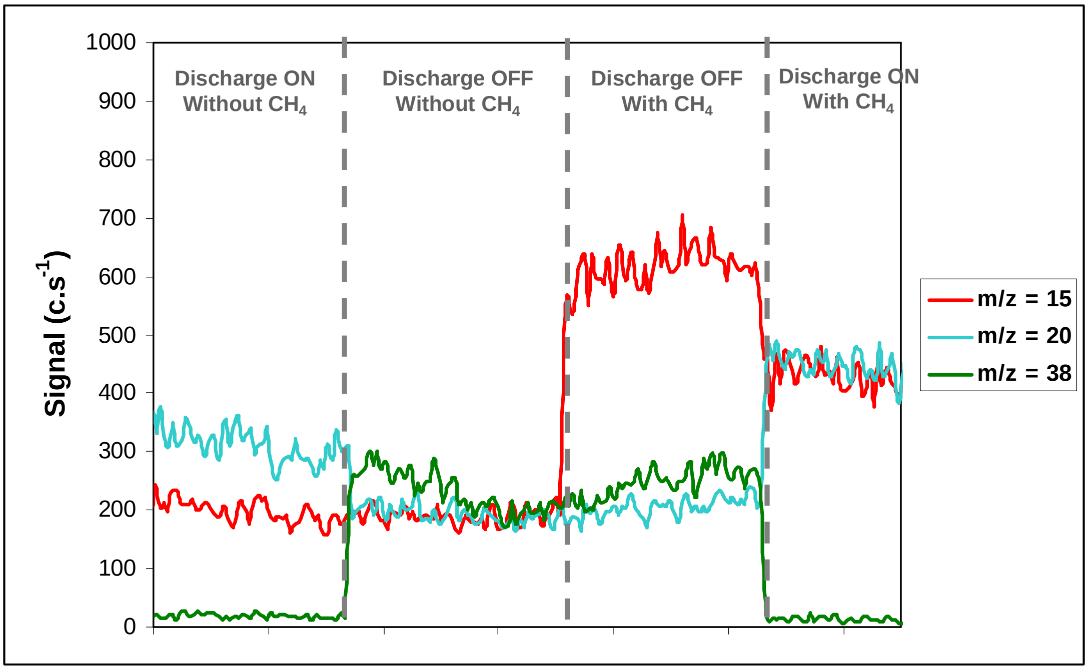

Figure 57*: Signal at m/z = 15 (CH_4), 20 (HF) and 38 (F_2), with and without microwave discharge and with and without CH_4*

B3. Perspectives

We can say that the system is now almost operational. In the near future, we plan to study the reaction between methanol and OH radicals ($CH_3OH + OH \rightarrow CH_2OH + H_2O$ followed by $CH_2OH + O_2 \rightarrow CH_2O + HO_2$) by measuring simultaneously OH and HO_2 radicals and to compare our results with the literature. We will then start to investigate reactions RO_2+OH and RO_2+HO_2 for simple alkylperoxy radicals (R= CH_3, C_2H_5) with the measurements of rate constants and products branching ratios. At a longer term, we will consider reactions of HO_2 with isoprene derived peroxy species with HO_2.

Collaborations are already ongoing in the peroxy chemistry research domain with the group of Hendrik Fuchs (Forschungszentrum Jülich, Germany): PHC Procope - Hydroperoxy radical detection by cavity ring-down spectroscopy in the atmosphere simulation chamber SAPHIR (2017-2018); and Ondřej Votava (J. Heyrovský Institute of Physical Chemistry, Academy of Sciences of the Czech Republic, Praha): PHC Barrande - Hydroperoxy radical detection in ambient atmosphere by cavity ring-down spectroscopy (2014-2018).

As mentioned earlier, on the regional scale, this work is part of the Labex CaPPA and the CPER Climibio program, with, among others, the department SAGE (Science de l'Atmosphère Génie de l'Environnement, IMT Douai) and LPCA (Laboratoire de Physico-Chimie de l'Atmosphère, Université Littoral Côte d'Opale, Dunkerque).

Future international collaborations can be envisaged with different groups, both on experimental or theoretical studies: the group of Dwayne Heard (Atmospheric and Planetary Chemistry group, School of Chemistry, University of Leeds, UK); the group of Geoffrey Tyndall (National Center for Atmospheric research, Atmospheric Chemistry Observations & Modeling Laboratory, Boulder, Colorado, USA) or the group of T. Dillon (Department of chemistry, University of York, UK).

CONCLUSION

This manuscript retraces my 13-year career in research since my PhD and postdoc, with for common theme the development of complex experimental devices, mostly using laser diagnostics, to study the chemical kinetics in reactive gas phase environments (combustion and atmosphere). I have been involved in several collaborative projects with other laboratories and industrial partners, which allow fruitful scientific discussions and the discovery of new enriching fields during interdisciplinary projects (CO_2 capture).

From now, most of my career concerns the study of combustion chemistry in flames, my research activities in this topic focused mainly on the reduction of pollutants emission in energy production systems, either by the development of new combustion modes (lean flames, oxygen enrichment), the use of biomass fuels (biogas, syngas) or a better knowledge of pollutants formation (NOx) in order to reduce it. An important part of my work at ICARE laboratory has been devoted to the development of the high pressure burner, this system has allowed obtaining important experimental results in conditions close to industrial applications (gas turbine, engines). For that, we have faced with difficulties to use the Laser Induced Fluorescence technique at high pressure in terms of spectroscopy (interferences, line broadening, quenching, absorption). My knowledge acquired during my PhD at PC2A in this field was very useful. In parallel, I have been involved in the modelling part of the work (development and validation of detailed chemical mechanisms: GDFkin®3.0, NOmecha2.0) with my colleagues (Abderrahman El Bakali, Christian Vovelle, Stéphanie de Persis, Nathalie Lamoureux, Pascale Desgroux), giving me a dual competence in experiments and modelling.

This scientific background allowed me to start a new research field by joining the ‘Atmospheric Physical Chemistry’ group in PC2A laboratory, where I’m developing a new experimental setup for the study of the reactivity of radical species in atmospheric chemistry. The system, coupling three different techniques (cw-CRDS, LIF and MB/MS) is now operational and we expect that our future studies of the reactions between RO_2 and HO_x will contribute to a better knowledge of the radical species chemistry in the atmosphere and to address the lack of experimental data.

The work of a researcher is also to share his knowledge and train students. During my career, I have co-supervised five PhD students and several other students (Master, Licence, DUT), this important part of the work is for me the most satisfying one.

REFERENCES

-A-

Abbatt J. P. D., Demerjian K. L., Anderson J. G., A new approach to free-radical kinetics: radially and axially resolved high-pressure discharge flow with results for hydroxyl+(ethane, propane, n-butane, n-pentane) products at 297 K, J. Phys. Chem. 94 (1990) 4566-4575.

Amiot C., Bacis R. and Guelachvili G., Infrared study of the $X^2\Pi$ v=0,1,2 levels of $^{14}N^{16}O$. Preliminary results on the v=0,1 levels of $^{14}N^{17}O$, $^{14}N^{18}O$ and $^{15}N^{16}O$, Canadian Journal of Physics 56 (1978) 251-265.

Archibald, A. T., Petit A. S., Percival C. J., Harvey J. N., Shallcross, D. E., On the importance of the reaction between OH and RO2 radicals, Atmos. Sci. Lett. 10 (2009) 102-108.

Assaf E. and Fittschen C., Cross Section of OH Radical Overtone Transition near 7028 cm^{-1} and Measurement of the Rate Constant of the Reaction of OH with HO2 Radicals, J. Phys. Chem. A 120 (2016) 7051-7059.

Assaf E., Sheps L., Whalley L., Heard D.E., Tomas A., Schoemaecker C., and Fittschen C., The Reaction between CH3O2 and OH Radicals: Product Yields and Atmospheric Implications, Environ. Sci. Technol. 51 (2017a) 2170-2177.

Assaf E., Études cinétiques des réactions d'intérêt atmosphériques par la détection simultanée des radicaux OH et RO_X couplée à la photolyse laser, PhD thesis (2017b) University Lille1.

Assaf E., Song B., Tomas A., Schoemaecker C., Fittschen C., Rate Constant of the Reaction between CH3O2 Radicals and OH Radicals revisited, J. Phys. Chem. A 120 (2016a) 8923-8932.

Atkinson R., Baulch D.L., Cox R.A., Crowley J.N., Hampson R.F., Hynes R.G., Jenkin M.E., Rossi M.J., Troe J., Evaluated kinetic and photochemical data for atmospheric chemistry : Volume III - gas phase reactions of inorganic halogens, Atmospheric Chemistry and Physics 7 (2007) 981-1191.

Atkinson R., Baulch D.L., Cox R.A., Crowley J.N., Hampson R.F., Hynes R.G., Jenkin M.E., Rossi J.M., Troe J., Evaluated kinetic and photochemical data for atmospheric chemistry: Volume I - gas phase reactions of Ox, HOx, NOx and SOx species, Atmospheric Chemistry and Physics 4 (2004) 1461-1738.

-B-

Battles B. E. and Hanson R. K., Laser induced fluorescence measurements of NO and OH mole fraction in fuel-lean high pressure (1-10 atm) methane flames: fluorescence modeling and experimental validation, Journal of Quantitative Spectroscopy and Radiative Transfer 54 (1995) 521-537.

Baukal CE, Gebhart B., Oxygen-enhanced/natural gas flame radiation, Int. J. Heat Mass Transfer 40 (1997) 2539-47.

Baulch D. L., Campbell I. M. & Saunders S. M., Rate constants for the reactions of hydroxyl radicals with propane and ethane, J. Chem. Soc., Faraday Transactions 81 (1985) 259-263.

References

Bessler W. G., Schulz C., Lee T., Jeffries J. B. and Hanson R. K., Strategies for laser-induced-fluorescence of nitric oxide in high-pressure flames. I-.A-X(0,0) excitation, Appl. Opt. 41 (2002) 3547-3557.

Bessler W. G., Schulz C., Lee T., Jeffries J. B. and Hanson R. K., Strategies for laser-induced-fluorescence of nitric oxide in high-pressure flames. II. A-X(0,1) excitation, Appl. Opt. 42 (2003a) 2031-2042.

Bessler W. G., Schulz C., Lee T., Jeffries J. B. and Hanson R. K., Strategies for laser-induced-fluorescence of nitric oxide in high-pressure flames. III. Comparison of A-X excitation schemes, Appl. Opt. 42 (2003b) 4922-4936.

Bessler W. G., Schulz C., Sick V. and Daily J. W., A versatile modeling tool for nitric oxide LIF spectra, Proceedings of the Third Joint Meeting of the U.S. Sections of The Combustion Institute, Chicago, paper PI05 (2003c), http://www.lifsim.com.

Bian H., Zhang S., Zhang H., Theoretical Study on the Atmospheric Reaction of CH3O2 with OH, Int. J. Quantum Chem 115 (2015) 1181-1186.

Biet J., Etude expérimentale et numérique de la combustion en mélange pauvre des hydrocarbures légers, PhD thesis (2004), Université d'Orléans, France.

Biet J., Delfau J.L., Pillier L., Vovelle C., Influence of CO2 and H2 on the chemical structure of a premixed, lean methane-air flame, Proc. of the European Combustion Meeting (2007), Chania, Crete.

Biet J., Delfau J.L., Seydi A., Vovelle C., Experimental and modeling study of lean premixed atmospheric-pressure propane/O2/N2 flames, Combust. Flame, 142 (2005) 197-209.

Biggs P., Canosa-Mas C.E., Shallcross D.E., Vipond A., Wayne R.P., Kinetics of the reactions of CF3O2 with OH, HO2 and H, J. Chem. Soc., Faraday Transactions 93 (1997) 2701-2705.

Bisio G, Bosio A, Rubatto G., Thermodynamics applied to oxygen enrichment of combustion air, Energy Conversion Manag. 43 (2002) 2589-600.

Bonne U, Grewer Th., Wagner H.Gg., Messungen in der reaktionzone von wasserstoff - Sauerstoff und methan-sauerstoff flammen, Zeitschrift für Physikalissche Chemie 26 (1960) 93-110.

Bossolasco, A., Farago E. P., Schoemaecker C., Fittschen C., Rate Constant of the Reaction between CH3O2 and OH Radicals, Chem. Phys. Lett. 593 (2014) 7-13.

Boumehdi M. A., Stepanyan S. A., Desgroux P., Vanhove G. & Starikovskaia S.M., Ignition of methane- and nbutane-containing mixtures at high pressures by pulsed nanosecond discharge, Combust. Flame 162 (2015) 1336-1349.

Bounaceur R., Lape N., Roizard D., Vallieres C., Favre E., Membrane processes for post-combustion carbon dioxide capture: A parametric study, Energy 31 (2006) 2256-2570.

Boushaki T., Dhué Y., Selle L., Ferret B., Poinsot T., Effects of hydrogen and steam addition on laminar burning velocity of methane/air premixed flame: Experimental and numerical analysis, Int. J. of Hydrogen Energy 37 (2012) 9412-9422.

Bouvet N., Davidenko D., Chauveau C., Pillier L., Yoon Y., On the simulation of laminar strained flames in stagnation flows: 1D and 2D approaches versus experiments, Combust. Flame 161 (2014) 438-452.

Bouvet N., Experimental and Numerical Studies of the Fundamental Flame Speeds of Methane/Air and Syngas (H2/CO)/Air Mixtures, PhD thesis (2009) Université d'Orléans, France.

Bowman C.T., Hanson R.K., Davidson D.F., Gardiner W.C., Lissianski V., Smith G.P., Golden D.M., Frenklach M. and Goldenberg M., GRI-Mech2.11 Mechanism (1995), http://www.me.berkeley.edu/gri_mech/.

Bozzelli J. W. and Dean A. M., O + NNH: A possible new route for NOx formation in flames, Int. J. Chem. Kin. 27 (1995) 1097-1109.

Brdar R.D., Jones R.M., GE IGCC Technology and Experience with Advanced Gas Turbines, GE Power Systems GER-4207 (2000).

-C-

Cabot G., Calbry M., Xavier P., Vandel A., de Persis S., Belaissaoui B., Favre E., Pillier L., Effect of CO2 Capture on Combined Cycle Gas Turbine Efficiency Using Membrane Separation, EGR and OEA Effects on Combustion Characteristics, Proceedings of ASME Turbo Expo (2014): Turbine Technical Conference and Exposition GT2014, Volume 4A, Paper N° GT2014-25781, Dusseldorf, Germany.

Campargue A., Wang L., Liu A. W., Hu S. M. & Kassi S., Empirical line parameters of methane in the 1.63-1.48 μm transparency window by high sensitivity Cavity Ring Down Spectroscopy, Chemical Physics 373 (2010) 203-210.

Charles EB., Oxygen-Enhanced Combustion, Second Edition: CRC Press (2013).

Coppens F.H.V., De Ruyck J., Konnov A.A., Effects of hydrogen enrichment on adiabatic burning velocity and NO formation in methane+air flames, Exp. Th. And Fluid Sci. 31 (2007a) 437-444.

Coppens F.H.V., De Ruyck J., Konnov A.A., The effects of composition on burning velocity and nitric oxide formation in laminar premixed flames of CH4+H2+O2+N2, Combust. Flame 149 (2007b) 409-417.

Crunelle B., Surdyk D., Pauwels J.F., Sochet L.R., Experimental study of low-pressure premixed methane and ethane flames by molecular beam sampling and mass spectrometry analysis, J. Chim. Phys. 94 (1997) 433-459.

-D-

Daële V., Poulet G., Kinetics and products of the reactions of CH3O2 with Cl and ClO, Journal de Chimie Physique et de PhysicoChimie Biologique 93 (1996) 1081-1099.

Dagaut P. and Nicolle A., Experimental and detailed kinetic modelling study of hydrogen-enriched natural gas blend oxidation over extended temperature and equivalence ratio ranges, Proc. Combust. Inst. 30 (2005) 2631-2638.

References

Daily J.W., Roth E.W., Effect of laser intensity and of lower-state rotational energy transfer upon temperature measurements made with laser-induced fluorescence, Appl. Phys. B 68 (1999) 131-140.

Davidson O., Metz B., de Coninck H., Loos M., Meyer L., IPCC Special Report: Carbon Dioxide Capture and Storage, International Panel on Climate Change (2005) Cambridge University Press, Geneva, Switzerland/Cambridge (UK) http://www.ipcc-wg3.de/specialreports/special-report-on-carbon-dioxide-capture-and-storage.

Davis S.G, Law C.K., Wang H., Propene Pyrolysis and Oxidation Kinetics in a Flow Reactor and Laminar Flames, Combust. Flame 119 (1999) 375-399.

de Ferrières S., El Bakali A., Lefort B., Montero M., Pauwels J.F., Experimental and numerical investigation of low-pressure laminar premixed synthetic natural gas /O2/N2 and natural gas/H2/O2/N2 flames, Combust. Flame 154 (2008) 601-623.

de Persis S., Cabot G., Pillier L., Gökalp I., Boukhalfa A.M., Study of lean premixed methane combustion with CO2 dilution under gas turbine conditions, Energy and Fuels 27 (2) (2013) 1093-1103.

de Persis S., Foucher F., Pillier L., Osorio V., Gökalp I. , Effect of O2 enrichment and CO2 dilution on laminar methane flames, Energy 55 (2013) 1055-1066.

Dechamps P., Pilavachi P. A., Research and Development Actions to Reduce CO2 Emissions within the European Union, Oil Gas Sci. Technol. 59 (3) (2004) 323-330.

Delfau J-L., Biet J., Idir M., Pillier L. and Vovelle C., Experimental and numerical study of premixed, lean ethylene flames, Proc. Combust. Inst. 31 (1) (2007) 357-365.

Dillon T. J. & Crowley J. N., Direct detection of OH formation in the reactions of HO2 with CH3C(O)O2 and other substituted peroxy radicals, Atmospheric Chemistry and Physics 8 (2008) 4877-4889.

Dirrenberger P., Le Gall H., Bounaceur R., Herbinet O., Glaude P-A., Konnov A., Battin-Leclerc F., Measurements of Laminar Flame Velocity for Components of Natural Gas, Energy and Fuels 25 (2011) 3875-84.

Ditaranto M, Oppelt T., Radiative heat flux characteristics of methane flames in oxyfuel atmospheres, Exp. Thermal Fluid Sci. 35 (2011) 1343-50.

Dobé S., Berces T., Temps F., Wagner H.Gg., Ziemer H., Formation of methoxy and hydroxymethyl free radicals in selected elementary reactions, Proc. Combust. Inst. 25 (1994) 775-781.

Donahue N. M., Anderson J. G., Demerjian K. L., New rate constants for ten OH alkane reactions from 300 to 400 K: An assessment of accuracy, J. Phys. Chem. A 102 (1998) 3121-3126.

Driscoll J. J., Sick V., Schrader P. E. and Farrow R. L., Measurements of NO distributions and fluorescence lifetimes in a non-premixed counterflow CH4/air flame using picosecond time-resolved laser-induced fluorescence, Proc. Combust. Inst. 29 (2002) 2719-2726.

Dyakov I.V., Konnov A.A., Ruyck J.D., Bosschaart K.J., Brock E.C.M., De Goey L.P.H., Measurement of adiabatic burning velocity in methane-oxygen-nitrogen-mixtures, Combust. Sci. Technol. 172 (2001) 81-96.

References

-E-

El Bakali A., Pillier L., Desgroux P., Lefort B., Gasnot L., Pauwels J.F. and da Costa I., NO prediction in natural gas flames using GDF-Kin 3.0 mechanism: NCN and HCN contribution to prompt-NO formation, Fuel 85 (2006) 896-909.

-F-

Farago E. P., Schoemaecker C., Viskolcz B., Fittschen C., Experimental Determination of the Rate Constant of the Reaction between C2H5O2 and OH Radicals, Chem. Phys. Lett. 619 (2015) 196-200.

Favre E, Bounaceur R, Roizard D., A hybrid process combining oxygen enriched air combustion and membrane separation for post-combustion carbon dioxide capture, Sep. Purif. Technol 68 (2009) 30-6.

Favre E., Carbon dioxide recovery from post-combustion processes: Can gas permeation membranes compete with absorption?, Journal of Membrane Science 294 (2007) 50-59.

Fenimore C. P., Formation of nitric oxide in premixed hydrocarbon flames, Proc. Combust. Inst. 13 (1971) 373-379.

Figueroa J. D., Fout T., Plasynski S., McIlvried H., Srivastava R. D., Advances in CO2 capture technology-The U.S. Department of Energy's Carbon Sequestration Program, Int. J. Greenhouse Gas Control 2 (2008) 9-20.

Fittschen C., Whalley L. K., Heard, D. E., The Reaction of CH3O2 Radicals with OH Radicals: A Neglected Sink for CH3O2 in the Remote Atmosphere, Environ. Sci. Technol. 118 (2014) 7700-7701.

Frankenberg C., Warneke T., Butz A., Aben I., Hase F., Spietz P. & Brown L.R., Pressure broadening in the $2\nu_3$ band of methane and its implication on atmospheric retrievals, Atmospheric Chemistry and Physics 8 (2008) 5061-5075.

-G-

Gasnot L., Application du couplage de la fluorescence induite par laser et de la chromatographie à l'étude de la formation de NO dans des flammes basse pression méthane/air, PhD thesis (1995), Université Lille1, France.

Gauducheau J.L., Denet B., Searby G., A numerical study of lean CH4/H2/air premixed flames at high pressure, Combust. Sci. and Tech. 137 (1998) 81-99.

Genovese A., Contrisciani N., Ortenzi F., Cazzola V., On road experimental tests of hydrogen/natural gas blends on transit buses, Int. J. Hydrogen Energy 36 (2011) 1775-1783.

Glarborg P. and Bentzen L.L.B. Chemical Effects of a High CO2 Concentration in Oxy-Fuel Combustion of Methane, Energy & Fuels 22 (2008) 291-296.

Goos E., Sickfeld C., Maus F., Seidel L., Ruscic B., Burcat A., Zeuch T., Prompt NO formation in flames: The influence of NCN thermochemistry, Proc. Combust. Inst. 34 (2013) 657-66.

Gore J. P., Lim J., Takeno T. et Zhu X. L., A study of the effects of thermal radiation on the structure of methane/air counter-flow diffusion flames using detailed chemical kinetics, Proceedings of the Fifth ASME/JSME Joint Thermal Engineering Conference, San Diego (1999).

Groß C.B.M., Dillon T.J., Schuster G., Lelieveld J., and Crowley J.N., Direct Kinetic Study of OH and O3 Formation in the Reaction of CH3C(O)O2 with HO2, J. Phys. Chem. A 118 (2014) 974-985.

Grosshandler W.L., RADCAL: A Narrow-Band Model for Radiation Calculations in a Combustion Environment, NIST Technical Note 1402 (1993).

Guo H., Smallwood G.J., Liu F., Ju Y., Gülder O.L., The effect of hydrogen addition on flammability limit and NOx emission in ultra-lean counterflow CH4/air premixed flames, Proc. Combust. Inst. 30 (2005) 303-311.

-H-

Han J.W., Lee C.E., Kum S.M., Hwang Y.S., Study of the improvement of chemical reaction mechanism of methane based on the laminar burning velocities in OEC, Energy and Fuels 21 (2007)3202-7.

Harding L. B., Klippenstein S. J. and Miller J. A., Kinetics of CH + N2 Revisited with Multireference Methods, J. Phys. Chem. A 112 (2008) 522-532.

Hasson A. S., Tyndall G. S. & Orlando J. J., A Product Yield Study of the Reaction of HO2 Radicals with Ethyl Peroxy (C2H5O2), Acetyl Peroxy (CH3C(O)O2), and AcetonylPeroxy (CH3C(O)CH2O2) Radicals, J. Phys. Chem. A 108 (2004) 5979-5989.

Hasson A. S., Kuwata K. T., Arroyo M. C. & Petersen E. B., Theoretical studies of the reaction of hydroperoxy radicals (HO2) with ethyl peroxy (CH3CH2O2), acetyl peroxy (CH3C(O)O2), and acetonylperoxy (CH3C(O)CH2O2) radicals, Journal of Photochemistry and Photobiology A: Chemistry 176 (2005) 218-230.

Hasson A. S., Tyndall G. S., Orlando J .J., Singh S., Hernandez S. Q., Campbell S. & Ibarra Y, Branching Ratios for the Reaction of Selected Carbonyl-Containing Peroxy Radicals with Hydroperoxy Radicals, J. Phys. Chem. A 116 (2012) 6264-6281.

Herzog, H., Peer Reviewed: What Future for Carbon Capture and Sequestration?, Environ. Sci. Technol. 35 (7) (2001) 148-153.

Hong Z., Farooq A., Barbour E.A., Davidson D.F., and Hanson R.K., Hydrogen Peroxide Decomposition Rate: A Shock Tube Study Using Tunable Laser Absorption of H2O near 2.5 μm, J. Phys. Chem. A 113 (2009) 12919-12925.

Hou H., Li J., Song X.L. and Wang B.S., A Systematic Computational Study of the Reactions of HO2 with RO2: The HO2+ C2H5O2 Reaction, J. Phys. Chem. A. 109 (2005) 11206-11212.

References

-J-

Jahn G, Der Zuendvorgang in Gaschemischen. Oldenbourg, (1934) Berlin p.27.

Jain C.D., Laser photolysis coupled to detection by LIF and cw-CRDS: Application to spectroscopic and kinetic studies of OH, HO2 and HONO, PhD thesis (2011) Université Lille1, France.

Jenkin M.E., Hurley M.D. and Wallington T.J., Investigation of the radical product channel of the CH3C(O)O2 +HO2 reaction in the gas phase, Phys. Chem. Chem. Phys. 9 (2007) 3149-3162.

Jenkin M.E., Hurley M.D. and Wallington T.J., Investigation of the Radical Product Channel of the CH3OCH2O2+HO2 Reaction in the Gas Phase, J. Phys. Chem. A 114 (2010) 408-416.

Jenkin M.E., Hurley M.D. and Wallington T.J., Investigation of the radical product channel of the CH3C(O)CH2O2 +HO2 reaction in the gas phase, Phys. Chem. Chem. Phys. 10 (2008) 4274-4280.

-K-

Kaiser E.W., Wallington T.J., Hurley M.D., Platz J., Curran H.J., Pitz W.J., Westbrook C.K., Experimental and modelling study of premixed atmospheric-pressure dimethyl ether - air flames, J. Phys. Chem. A 104 (2000) 8194-8206.

Kee R. J., Grcar J. F., Smooke M. D. and Miller J. A., A fortran program for modelling steady laminar one-dimensional premixed flames, Sandia technical report (1985) SAND85-8240.

Kent J.H., A Noncatalytic Coating for PlatinumRhodium Thermocouples, Combust. Flame 14 (1970) 279-282.

Khatoon T. & Hoyermann K., The Reactions of Fluorine Atoms with Normal and Deuterated Methanols, Berichte der Bunsengesellschaft für Physikalische Chemie 92 (1988) 669-673.

Klassen M. S., Thomsen D. D., Reisel J. R. and Laurendeau N. M., Laser-induced fluorescence measurements of NO formation in high-pressure premixed methane flames, Combust. Sci. Tech. 110-111 (1995) 229-247.

Konnov A.A., Detailed reaction mechanism for small hydrocarbons combustion, Release 0.5. (2000).

Kwak T.H., Maken S., Lee S., Park J.W., Min B., Yoo Y.D., Environmental aspects of gasification of Korean municipal solid waste in pilot plant, Fuel 85 (2006) 2012-2017.

-L-

Lamoureux N., Desgroux P., El bakali A. and Pauwels J. F., Experimental and numerical study of the role of NCN in promt-NO formation in low pressure CH4-O2-N2 and C2H2-O2-N2 flames, Combust. Flame. 157 (2010) 1929-1941.

References

Lamoureux N., El Merhubi H., Gasnot L., Schoemaecker C., Desgroux P., Measurements and modelling of HCN and CN species profiles in laminar CH4/O2/N2 low pressure flames using LIF/CRDS techniques, Proc. Combust. Inst. 35 (2015) 745-752.

Lamoureux N., El Merhubi H., Mercier X., Pauwels J. F. and Desgroux P., HCN quantitative measurement in a laminar low pressure flame at 1036 nm using pulsed CRDS technique, Proc. Combust. Inst. 34 (2013b) 3557-3564.

Lamoureux N., El Merhubi H., Pillier L., de Persis S., Desgroux P., Modeling of NO formation in low pressure premixed flames, Combust. Flame 163 (2016) 557-575.

Lamoureux N., Mercier X., Pauwels J. F. and Desgroux P., NCO quantitative measurement in premixed low pressure flames by combining LIF and CRDS techniques, J. Phys. Chem. A. 115 (2011) 5346-5353.

Lamoureux N., Mercier X., Western C., Pauwels J. F. and Desgroux P., NCN quantitative measurement in a laminar low pressure flame, Proc. Combust. Inst. 32 (2009) 937-944.

Lamoureux N., Western C. M., Mercier X. and Desgroux P., Reinvestigation of the spectroscopy of the $A^3\Pi_u$-$X^3\sum_g$ transition of the NCN radical at high temperature: application to quantitative NCN measurement in flames, Combust. Flame. 160 (2013a) 755-765.

Le Crâne J.-P., Rayez M.-T., Rayez J.-C. & Villenave E., A reinvestigation of the kinetics and the mechanism of the CH3C(O)O2 + HO2 reaction using both experimental and theoretical approaches, Phys. Chem. Chem. Phys. 8 (2006) 2163-2171.

Lee J.G., Kim J.H., Lee H.J., Park T.J., Kim S.D., Characteristics of entrained flow coal gasification in a drop tube reactor, Fuel 75 (9) (1996) 1035-1042.

Li J., Zhao Z., Kazakov A., Chaos M., Dryer F.L., Scire J.J., A comprehensive kinetic mechanism for CO, CH2O, and CH3OH combustion, Int. J. Chem. Kin. 39 (2007) 109-136.

Liu F., Guo H., Smallwood G. J., The chemical effect of CO2 replacement of N2 in air on the burning velocity of CH4 and H2 premixed Flames, Combust. Flame 133 (4) (2003) 495-497.

Liu Y. J., Herdlinger-Blatt I., McKinney K.A., and Martin S.T., Production of methyl vinyl ketone and methacrolein via the hydroperoxyl pathway of isoprene oxidation, Atmos. Chem. Phys. 13 (2013) 5715-5730.

Ludwig W., Brandt B., Friedrichs G., and Temps F., Kinetics of the Reaction C2H5 + HO2 by Time-Resolved Mass Spectrometry, J. Phys. Chem. A 110 (2006) 3330-3337.

Luque J. and Crosley D. R., LIFBASE: Database and spectral simulation program (version 1.5), SRI International Report MP 99-009 (1999).

Lutz A.E., Kee R.J., Grcar J.F., Rupley F.M., OPPDIF: A Fortran Program for Computing Opposed-flow Diffusion Flames, Report No. SAND96-8243 (1997) Sandia National Laboratories.

References

-M-

Malte P. C. and Pratt D. T., The role of energy-releasing kinetics in NOx formation: fuel-lean, jet-stirred CO-Air combustion, Combust. Sci. Tech. 9 (1974) 221-231.

Matynia A., Delfau J.L., Pillier L., Vovelle C., Comparative study of the influence of CO2 and H2O on the chemical structure of lean and rich methane/air flames at atmospheric pressure, Combustion, Explosion and Shock Waves 45 (6) (2009) 635-645.

Matynia A., Idir M., Molet J., Roche C., de Persis S. and Pillier L., Absolute OH concentration profiles measurements in high pressure counterflow flames by coupling LIF, PLIF and absorption techniques, Appl. Phys. B 108 (2012a) 393-405 .

Matynia A., Molet J., Roche C., Idir M., de Persis S. and Pillier L., Measurement of OH concentration profiles by laser diagnostics and modelling in high pressure counterflow premixed methane-air and biogas-air flames, Combust. Flame 159 (2012b) 3300-3311.

Mazas AN. Study of oxygen-enriched premixed flames: effects of water and carbon dioxide addition. PhD thesis (2010) Ecole Centrale de Paris, France.

Merlo N., Boushaki T., Chauveau C., de Persis S., Pillier L., Sarh B., Gökalp I., Experimental study of oxygen enrichment effects on turbulent non-premixed swirling flames, Energy and Fuels 27 (10) (2013) 6191-6197.

Merlo N., Boushaki T., Chauveau C., de Persis S., Pillier L., Sarh B., Gökalp I., Combustion Characteristics of Methane-oxygen Enhanced Air Turbulent Nonpremixed Swirling Flames, Experimental Thermal and Fluid Science 56 (2014) 53-60.

Moskaleva L.V. and Lin M.C., The Spin-Conserved Reaction CH + N2 = H + NCN: A Major Pathway to Prompt NO Studied by Quantum/Statistical Theory Calculations and Kinetic Modeling of Rate Constant, Proc. Combust. Inst. 28 (2000) 2393-2401.

Müller J.-F., Liu Z., Nguyen V. S., Stavrakou T., Harvey J. N., Peeters J., The Reaction of Methyl Peroxy and Hydroxyl Radicals as a Major Source of Atmospheric Methanol, Nat. Commun. 7 (2016) 13213.

-N-

Naha S., Aggarwal S.K., Fuel effects on NOx emissions in partially premixed flames, Combust. Flame 139 (2004) 90-105.

Naïk S. V. and Laurendeau N. M., Spectroscopic, calibration and RET issues for linear laser-induced fluorescence measurements of NO in high-pressure diffusion flames, Appl. Phys. B. 79 (2004) 641-651.

References

-O-

Oh J. and Noh D., Laminar burning velocity of oxy-methane flames in atmospheric condition, Energy 45 (2012) 669-75.

Orlando J.J. and Tyndall G.S, Laboratory studies of organic peroxy radical chemistry: an overview with emphasis on recent issues of atmospheric significance, Chem. Soc. Rev. 41 (2012) 6294-6317.

-P-

Paul P. H., Carter C. D., Gray J. A., Durant J. L., Thoman J. W. and Furlanetto M. R., Corrections for the NO $A^2\Sigma^+$ (v'=0) electronic quenching cross-section, Sandia Report (1995) SAND94-8237.

Paul P. H., Gray J. A., Durant J. L. and Thoman J. W., A model for temperature-dependent collisional quenching of NO $A^2\Sigma^+$, Appl. Phys. B 57 (1993) 249-259.

Pillier L., de Persis S., Cabot G., Bounaceur R., Liu Y., Boukhalfa A., Most J-M., Gökalp I. and Favre E., Coupling of oxygen-enriched combustion and CO2 capture by membrane processes, 4th European Combustion Meeting (ECM2009) (2009) Vienna, Austria.

Pillier L., Idir I., Molet J., Matynia A., de Persis S., Experimental study and modelling of NOx formation in high pressure counter-flow premixed CH4/air flames, Fuel 150 (2015) 394-407.

-R-

Rasi S., Veijanen A., Rintala J., Trace compounds of biogas from different biogas production plants, Energy 32 (8) (2007) 1375-1380.

Raventós-Duran M. T., Percival C.J., McGillen M.R., Hamer P.D. & Shallcross D.E., Kinetics and branching ratio studies of the reaction of C2H5O2 + HO2 using chemical ionisation mass spectrometry, Phys. Chem. Chem. Phys. 9 (2007a) 4338-4348.

Raventós-Duran M. T., McGillen M.R., Percival C. J., Hamer P. D. & Shallcross D. E., Kinetics of the CH3O2 + HO2 reaction: A temperature and pressure dependence study using chemical ionization mass spectrometry, Int. J. Chem. Kin. 39 (2007b) 571-579.

Ravikrishna R.V., Cooper C.S., and Laurendeau N.M., Comparison of Saturated and Linear Laser-Induced Fluorescence Measurements of Nitric Oxide in Counterflow Diffusion Flames, Combust. Flame 117 (1999) 810-820.

Richards G.A., Casleton K.H. and Weiland N.T., Syngas Utilization, in Synthesis Gas Combustion Fundamentals and Application, Edited by Lieuwen T., Yang V. and Yetter R., CRC Press Taylor and Francis Group (2009).

Riddel B., Bro C., Malmö hydrogen and CNG/Hydrogen filling station and Hythane bus project, WHEC 16 (2006), Lyon France.

References

Rolon J.C., PhD thesis (1988) Ecole Centrale Paris, France.

Rortveit G.J., Zepter K., Skreiberg O., Fossum M., Hustad J.E., A comparison of low-NOx burners for combustion of methane and hydrogen mixtures, Proc. Comb. Inst. 29 (2002)1123-1129.

-S-

Schulz C., Sick V., Heinze J. and Stricker W., Laser-induced-fluorescence detection of nitric oxide in high-pressure flames with A-X(0,2) excitation, Appl. Opt. 36 (1997) 3227-3232.

Sepman A.V., van Essen V.M., Mokhov. A.V., Levinsky H.B., The effects of hydrogen addition on Fenimore NO formation in low-pressure, fuel-rich premixed, burner stabilized CH4/O2/N2 flames, Int. J. Hydrogen Energy 33 (2008) 5850-5857.

Settersten T. B., Patterson B. and Gray J. A., Temperature-dependent cross sections for quenching of NO LIF by NO, H2O, and CO2, Proceedings of the Third Joint Meeting of the U.S. Sections of The Combustion Institute (2003).

Smith G.P., D.M. Golden, M. Frenklach, N.W. Moriarty, B. Eiteneer, M. Goldenberg, C.T. Bowman, R.K. Hanson, S. Song, W.C. Gardiner, V.V. Lissianski, Z. Qin, GRImech3.0 Mechanism (1999), http://www.me.berkeley.edu/gri_mech/

-T-

Teng A.P., Crounse J.D., Wennberg P.O., Isoprene Peroxy Radical Dynamics, J. Am. Chem .Soc. 139 (2017) 5367-5377.

Thiébaud J., Crunaire S. & Fittschen C., Measurements of Line Strengths in the $2\nu_1$ Band of the HO2 Radical Using Laser photolysis/Continuous Wave Cavity Ring-Down Spectroscopy (cw-CRDS), J. Chem. Phys. A 111 (2007) 6959-6966.

Thomsen D. D., Kuligowski F. F. and Laurendeau N. M., Background corrections for laser-induced-fluorescence measurements of nitric oxide in lean, high-pressure, premixed methane flames, Appl. Opt. 36 (1997) 3244-3252.

Turbiez A., Devynck P., Desgroux P., and Pauwels J.F., Coupling of gas chromatography and molecular beam/mass spectrometry analytical techniques: Application to flame structure study, Review of Scientific Instruments 70 (1999) 2828-2835.

-V-

Vanhove G., Boumehdi M.A., Shcherbanev S., Fenard Y., Desgroux P., Starikovskaia S.M., A comparative experimental kinetic study of spontaneous and plasma-assisted cool flames in a rapid compression machine, Proc. Combust. Inst. 36 (2017) 4137-4143.

Vasudevan V., Hanson, R.K., Bowman C.T., Golden D.M. and Davidson D.F., Shock tube study of the reaction of CH with N2: overall rate and product branching, J. Phys. Chem. A 111 (2007) 11818-11830.

Villante C., Genovese A., Hydromethane: A bridge towards the hydrogen economy or an unsustainable promise?, Int. J. Hydrogen Energy 37 (2012) 11541-11548.

-W-

Wall, T. F., Combustion processes for carbon capture, Proc. Combust. Inst. 31 (2007) 31-47.

Wallington T.J. and Japar S.M., FTIR product study of the reaction C2H5O2+HO2 in air at 295K, Chem. Phys. Lett. 166 (1990a) 495-499.

Wallington T.J. and Japar S.M., Reaction of CH3O2+HO2 in air at 295K: A product study, Chem. Phys. Lett. 167 (1990b) 513-518.

Walther C.D. and Wagner H.G., Uber die Reaktionen von F-atomen mit H2O, H2O2 und NH3, Berichte der Bunsen-Gesellschaft für Physikalische Chemie 87 (1983).

Whalley L. K., Furneaux K. L., Goddard A., Lee J. D., Mahajan A., Oetjen H., Read K. A., Kaaden N., Carpenter L. J., Lewis A. C., Plane J. M. C., Saltzman E. S., Wiedensohler A., Heard D. E., The Chemistry of OH and HO2 Radicals in the Boundary Layer over the Tropical Atlantic Ocean, Atmos. Chem. Phys. 10 (2010) 1555-1576.

Winiberg F.A.F., Dillon T.J., Orr S.C., Groß C.B.M., Bejan I., Brumby C.A., Evans M.J., Smith S.C., Heard D.E., and Seakins P.W., Direct measurements of OH and other product yields from the HO2+CH3C(O)O2 reaction, Atmos. Chem. Phys. 16 (2016) 4023-4042.

Wu K-K, Chang Y-C, Chen C-H, Chen Y-D., High-efficiency combustion of natural gas with 21-30% oxygen-enriched air, Fuel 89 (2010) 2455-62.

-Y-

Yan C., Kocevska S., Krasnoperov L.N., Kinetics of the Reaction of CH3O2 Radicals With OH Studied Over the 292-526 K, J. Phys. Chem. A 120 (2016) 6111-6121.

Yu Y., Vanhove G., Griffiths J.F., de Ferrieres S., Pauwels J.F., Influence of EGR and Syngas Components on the Autoignition of Natural Gas in a Rapid Compression Machine: A Detailed Experimental Study, Energy Fuels 27 (2013), 3988-3996.

-Z-

Zeldovich Y. B., The oxidation of nitrogen in combustion and explosions, Acta Physicochimica 21 (1946) 577-628.

Zhang W., Chen Z., Li W., Shu G., Xu B., Shen Y., Influence of EGR and oxygen enriched air on diesel engine NO-Smoke emission and combustion characteristic, Applied Energy 107 (2013) 304-314.